



THE HONG KONG  
POLYTECHNIC UNIVERSITY

香港理工大學

Pao Yue-kong Library

包玉剛圖書館

---

## Copyright Undertaking

This thesis is protected by copyright, with all rights reserved.

**By reading and using the thesis, the reader understands and agrees to the following terms:**

1. The reader will abide by the rules and legal ordinances governing copyright regarding the use of the thesis.
2. The reader will use the thesis for the purpose of research or private study only and not for distribution or further reproduction or any other purpose.
3. The reader agrees to indemnify and hold the University harmless from and against any loss, damage, cost, liability or expenses arising from copyright infringement or unauthorized usage.

### IMPORTANT

If you have reasons to believe that any materials in this thesis are deemed not suitable to be distributed in this form, or a copyright owner having difficulty with the material being included in our database, please contact [lbsys@polyu.edu.hk](mailto:lbsys@polyu.edu.hk) providing details. The Library will look into your claim and consider taking remedial action upon receipt of the written requests.

**THE CONTROL OF AIRFLOW  
AND ACOUSTIC ENERGY FOR  
VENTILATION SYSTEM IN  
SUSTAINABLE BUILDING**

**WANG ZHIHONG**

**Ph.D**

**The Hong Kong  
Polytechnic University**

**2014**

**THE HONG KONG POLYTECHNIC UNIVERSITY  
DEPARTMENT OF CIVIL AND ENVIRONMENTAL  
ENGINEERING**

**THE CONTROL OF AIRFLOW AND  
ACOUSTIC ENERGY FOR VENTILATION  
SYSTEM IN SUSTAINABLE BUILDING**

**WANG ZHIHONG**

**A THESIS SUBMITTED IN PARTIAL FULFILLMENT OF  
THE REQUIREMENT FOR THE  
DEGREE OF PHILOSOPHY  
DECEMBER 2013**

## **CERTIFICATE OF ORIGINALITY**

**I hereby declare that this thesis is my own work and that, to the best of my knowledge and belief, it reproduces no material previously published or written, nor material that has been accepted for the award of any other degree or diploma, except where due acknowledgement has been made in the text.**

\_\_\_\_\_ (Signed)

WANG ZHIHONG (Name of student)

## ABSTRACT

Noise and air pollution problems become significant in a crowded city such as Hong Kong since buildings are usually close to the heavy traffic lines. Conventional window cannot fulfill all the functions of noise reduction, lighting and natural ventilation. New ventilated system, which combines the multiple quarter-wave resonators (silencer) with the new wing wall is designed to balance between acoustic and ventilation performances.

Wind-driven natural ventilation is an effective way to preserve the safe and healthy indoor environment. The single-sided ventilation incorporated with wing walls could benefit from the dual flow ventilation mechanism and significantly increase the interior air circulation.

Noise attenuation of the new ventilated window design improves significantly by combining flexible absorber and quarter-wave resonator effects. 10 dB to 22 dB transmission loss can be achieved in the frequency range between 500 Hz and 2 kHz band. The best ventilation performance of the wing wall is at an incident

angle of 45 °. Outlet air flow rate of ventilated window design is double of that of "the openable window".

Rounded-inlet ventilated duct has effective performance in noise attenuation at any incident angle of the noise source. Even without combining with any acoustic absorptive materials, the noise reduction of ventilated duct can still much better than the conventional window. The ventilated duct has the acoustic effects similar to a standard expansion chamber with the extended inlet and outlet expansion chamber. The value of such a design is that part of the chamber between the extended pipe and the sidewall acts as a side branch resonator, therefore, improving the transmission loss.

Computational simulation (CFD) and flow visualization technique in this research are verified by the results. The new design has effective acoustic and ventilation performance. The new natural ventilation design is an effective way in maintaining the comfort and health of the indoor environment.

## **PUBLICATIONS ARISING FROM THE THESIS**

Michelle Wang, Catherine Hui & Chuang Fai NG (2012). The acoustic and ventilation performance of new ventilated window design. *Journal of the Acoustical Society of America*, 131 (4), 3509.

Zhihong Wang, C. F. NG & Edith Ngai (2012). Ventilated window design with multiple resonators and panel absorbers. The 41st International Congress and Exposition on Noise Control Engineering. August 19th -22nd, 2012. New York City, USA, The Marriott Marquis at Manhattan.

Z.H Wang, C.K. Hui & C.F. Ng (2014) The acoustic performance of ventilated window with quarter-wave resonators and membrane absorber. *Applied Acoustics*, 78, 1-6.

## ACKNOWLEDGEMENT

I would like to express my deepest gratitude to my supervisor, Dr C. F. NG, for his excellent guidance, patience, caring, supporting and providing me with an excellent atmosphere for doing research during the last three years. I would like to thank Dr K.S. Lam, who also supported my research and support my thesis writing and submission. I would like to all the members in this group. My research would not have been possible without their helps.

I would like to thank Ms. Emily Fung, who always willing to help and give her best suggestion in the laboratory for helping me to finish experimental measurements from this field.

I would also like to thank my parents. They were always supporting me and encouraging me with their best wishes.

Finally, I would like to thank my husband, Mr. Yang Chen. Thanks for his understanding caring and love through the happy times and bad.



# TABLE OF CONTENTS

<b>CERTIFICATE OF ORIGINALITY.....</b>	<b>I</b>
<b>ABSTRACT .....</b>	<b>II</b>
<b>PUBLICATIONS ARISING FROM THE THESIS.....</b>	<b>IV</b>
<b>ACKNOWLEDGEMENT .....</b>	<b>V</b>
<b>LIST OF FIGURES .....</b>	<b>XIII</b>
<b>LIST OF TABLES .....</b>	<b>XXVI</b>
<b>LIST OF ABBREVIATIONS .....</b>	<b>XXVIII</b>
<b>CHAPTER 1 .....</b>	<b>1</b>
<b>INTRODUCTION.....</b>	<b>1</b>
1.1 BACKGROUND INFORMATION .....	1
1.2 PROBLEM STATEMENT .....	3
1.3 RESEARCH OBJECTIVES.....	5
1.4 RESEARCH SIGNIFICANCE .....	6
1.5 DISSERTATION ORGANIZATION .....	8
<b>CHAPTER 2 .....</b>	<b>11</b>

<b>LITERATURE REVIEW.....</b>	<b>11</b>
2.1 DRIVING FORCES OF NATURAL VENTILATION.....	11
2.2 NATURAL VENTILATION STRATEGIES .....	13
2.3 CRITICAL ISSUES IN NATURAL VENTILATION.....	15
2.4 REVIEW OF GREEN FEATURES IN SUSTAINABLE BUILDING DESIGN IN HONG KONG .....	16
2.4.1 <i>Balcony</i> .....	16
2.4.2 <i>Glass curtain wall</i> .....	19
2.4.3 <i>Double skin fa çade (DSF)</i> .....	21
2.4.4 <i>New ventilation windows</i> .....	25
2.5 ACOUSTICS IN NATURAL VENTILATED BUILDING.....	28
2.6 THE CONCEPT OF WING WALL .....	29
2.7 APPLICATIONS OF NATURAL VENTILATION AND WING WALL DESIGN .....	34
2.7.1 <i>UMNO Tower</i> .....	34
2.7.2 <i>Post Tower</i> .....	37
<b>CHAPTER 3 .....</b>	<b>40</b>
<b>RESEARCH METHODOLOGY .....</b>	<b>40</b>
3.1 INTRODUCTION.....	40

3.2 RESEARCH GAPS .....	41
3.3 OVERVIEW OF THE APPROACH .....	43
3.3.1 <i>Small-scale experimental and Full-scale direct techniques for predicting ventilation</i> .....	44
3.3.2 <i>Sound transmission loss Measurement</i> .....	46
3.3.3 <i>CFD simulation</i> .....	47
3.3.4 <i>Flow visualization techniques</i> .....	49
3.4 SUMMARY .....	51
<b>CHAPTER 4 .....</b>	<b>53</b>
<b>NOISE CONTROL AND AIR VENTILATION PERFORMANCE OF CONVENTIONAL WING WALL .....</b>	<b>53</b>
4.1 THE CONCEPT OF WING WALL .....	53
4.2 MODEL EXPERIMENTS IN LABORATORY .....	55
4.2.1 <i>Acoustic experiments</i> .....	55
4.2.2 <i>Small-scale ventilation experiments</i> .....	58
4.2.3 <i>Ventilation test for different types of dual-flow ventilated windows</i> ...	63
4.2.4 <i>Single ventilation and cross ventilation performance in a wing wall design</i> .....	67
4.3 SUMMARY .....	68

<b>CHAPTER 5 .....</b>	<b>72</b>
<b>NOISE CONTROL OF MULTIPLE QUARTER-WAVE RESONATORS</b>	<b>72</b>
5.1 INTRODUCTION .....	72
5.2 MODIFIED DESIGN OF VENTILATED WINDOW .....	73
5.3 THE TRANSMISSION LOSS OF QUARTER-WAVE RESONATORS .	75
5.4 ACOUSTIC PERFORMANCE OF SILENCER FOR VENTILATED WINDOW MEASURED IN DUCT.....	85
5.4.1 <i>Formula of flexible absorber</i> .....	85
5.4.2 <i>Specimen and measurement setup</i> .....	86
5.4.3 <i>Transmission loss results measured in duct</i> .....	89
5.4.4 <i>Acoustic performance of ventilated silencer in a room</i> .....	91
5.5 FULL-SCALE MOCKUP EXPERIMENTS IN FO TAN .....	93
5.6 TESTING IN AN ANECHOIC SOURCE ROOM.....	101
5.7 SUMMARY .....	102
<b>CHAPTER 6 .....</b>	<b>106</b>
<b>VENTILATION AND ACOUSTICS PERFOARMENCE OF NEW VENTILATED WINDOW DESIGN .....</b>	<b>106</b>
6.1 INTRODUCTION .....	106

6.2 ACOUSTICS PERFORMANCE OF THE NEW ROUNDED-INLET CYLINDRICAL VENTILATED DUCT DESIGN.....	107
6.2.1 <i>Rounded-inlet cylindrical ventilated duct</i> .....	107
6.2.2 <i>Acoustics test with absorber in the rounded-inlet cylindrical ventilated duct</i> .....	111
6.2.3 <i>Calculations of the Transmission loss of the round inlet duct</i> .....	113
6.2.4 <i>Comparing the noise reduction between straight-inlet rectangular duct and rounded-inlet cylindrical duct</i> .....	118
6.3 VENTILATION TEST FOR ROUNDED-INLET CYLINDRICAL VENTILATED DUCT .....	121
6.4 SUMMARY .....	124
<b>CHAPTER 7 .....</b>	<b>126</b>
<b>COMPUTATIONAL SIMULATION .....</b>	<b>126</b>
7.1 INTRODUCTION.....	126
7.2 K-EPSILON (K-E) TURBULENCE MODEL .....	128
7.3 COMPUTATIONAL SIMULATION OF CONVENTIONAL WINDOW .....	130
7.4 COMPUTATIONAL SIMULATION OF WING WALL.....	133
7.4.1 <i>Conventional wing wall</i> .....	133

7.5 COMPUTATIONAL OF WING WALL WITH BARRIERS ON EACH	
SIDE.....	136
7.5.1 <i>Conventional wing wall with two barriers</i> .....	137
7.5.2 <i>Ventilated window with wing wall at 45 °</i> .....	141
7.6 ROUNDED-INLET WING WALL AT 0 °, 45 °AND 90 °.....	147
7.7 DISCUSSION .....	151
7.8 SUMMARY .....	153
<b>CHAPTER 8 .....</b>	<b>155</b>
<b>FLOW VISUALIZATION .....</b>	<b>155</b>
8.1 INTRODUCTION.....	155
8.1.1 <i>Water Table Apparatus</i> .....	156
8.1.2 <i>Reynolds number</i> .....	158
8.2 FLOW VISUALIZATION .....	159
8.2.1 <i>Conventional window</i> .....	159
8.2.2 <i>Conventional wing wall</i> .....	161
8.2.3 <i>Rounded-inlet wing wall at 0 °, 45 °and 90 °</i> .....	162
8.3 SUMMARY .....	165
<b>CHAPTER 9 .....</b>	<b>167</b>

<b>DISCUSSION .....</b>	<b>167</b>
9.1 INTRODUCTION .....	167
9.2 SUMMARY OF MAJOR FINDINGS.....	167
9.3 IMPLICATION OF THE DESIGN .....	171
<b>CHAPTER 10 .....</b>	<b>178</b>
<b>CONCLUSION.....</b>	<b>178</b>
10.1 INNOVATION OF THE DESIGN.....	178
10.2 CONCLUSION .....	180
<b>APPENDIX I .....</b>	<b>184</b>
<b>APPENDIX II.....</b>	<b>189</b>
<b>LIST OF BIBLIOGRAPHY .....</b>	<b>195</b>

# LIST OF FIGURES

FIGURE 1- 1 HIGH-RISE BUILDINGS IN HONG KONG. ....	1
FIGURE 1- 2 TYPICAL WING WALLS IN HONG KONG. ....	4
FIGURE 1- 3 MULTIPLE QUARTER-WAVE RESONATORS. ....	7
FIGURE 1- 4 VENTILATED WINDOW WITH SILENCER (TOP VIEW). ....	8
FIGURE 1- 5 ROUNDED-INLET VENTILATED DUCTS. ....	8
FIGURE 2- 1 WIND-DRIVEN VENTILATION. ....	12
FIGURE 2- 2 STACK VENTILATION. ....	12
FIGURE 2- 3 DIFFERENT TYPES OF RECTANGULAR BALCONY. ....	17
FIGURE 2- 4 LEVELS OF BALCONY ACOUSTIC TREATMENT AND THEIR GENERALIZED POTENTIAL NOISE ATTENUATION. ....	18
FIGURE 2- 5 GLASS CURTAIN WALLS OF THE INTERNATIONAL COMMERCE CENTRE (ICC) BUILDING. ....	20
FIGURE 2- 6 PRINCIPLES OF AIRFLOW IN THE CAVITY OF DOUBLE-SKIN FAÇADE. ..	22
FIGURE 2- 7 DSF OF NO.1 PEKING ROAD. ....	23
FIGURE 2- 8 DSF IN SCIENCE PARK. ....	24
FIGURE 2- 9 DOUBLE-SKIN FAÇADE IN HONG KONG SCIENCE PARK. ....	24



FIGURE 2- 10 SINGLE-SIDED GLAZED VENTILATED WINDOW.....	27
FIGURE 2- 11 AIRFLOW OF SINGLE-SIDED GLAZED VENTILATED WINDOW.....	27
FIGURE 2- 12 THE CONCEPT OF WING WALL (KALOGIROU, 2009). ....	31
FIGURE 2- 13 VENTILATION STRATEGIES BY THE ARRANGEMENT OF OPENINGS (GIVONI, 1976). ....	33
FIGURE 2- 14 UMNO TOWER BY KEN YEANG 1 (TYE, 2006). ....	35
FIGURE 2- 15 WING WALLS ON THE SOUTHEAST OF UMNO TOWER. ....	35
FIGURE 2- 16 OFFICE FLOOR PLANS (TOP). ....	36
FIGURE 2- 17 OFFICE FLOOR PLANS (BOTTOM). ....	36
FIGURE 2- 18 CFD SIMULATION OF AIR PRESSURE CONTOURS AROUND THE BUILDING (PLAN VIEW) (WOOD & SALIB, 2012). ....	37
FIGURE 2- 19 EXTENDED DSF CREATES “WING WALL EFFECT” IN POST TOWER (KING, 2012). ....	37
FIGURE 2- 20 POST TOWER, GERMANY (KING, 2012). ....	38
FIGURE 2- 21 CFD STUDIES OF THE PRESSURE DIFFERENCE FOR THE WING WALL IN POST TOWER, GERMANY (WOOD & SALIB, 2012). ....	38
FIGURE 3- 1 THE USE OF CFD FOR NATURAL VENTILATION PERFORMANCE AT THE INITIAL DESIGN STAGE.....	48

FIGURE 4- 1 TYPICAL USE OF WING WALLS IN HONG KONG. ....	54
FIGURE 4- 2 WOOD BOARD WING WALL MODELS. ....	56
FIGURE 4- 3 PHYSICAL CONFIGURATIONS AND PLAN OF THE EXPERIMENTAL SET-UP OF THE EXPERIMENT. ....	56
FIGURE 4- 4 MEMBRANE ABSORBER.....	57
FIGURE 4- 5 NOISE REDUCTION BETWEEN MEMBRANE ABSORBER AND CONTROL IN SOURCE AND RECEIVING ROOM.   —•— CONTROL TESTS IN TWO ROOMS;   —■— TESTS WITH MEMBRANE ABSORBERS IN TWO ROOMS.....	57
FIGURE 4- 6 EXPERIMENTAL SETUPS FOR AIRFLOW MEASUREMENTS. ....	59
FIGURE 4- 7 FLOOR PLANS AND LAYOUT CONFIGURATIONS OF THE AIRFLOW MEASUREMENTS.....	59
FIGURE 4- 8 A) AIR FLOW DIRECTIONS IN WOOD BOARD WING WALL MOCKUP, AT 0 °, B) AIR FLOW DIRECTION IN WOOD BOARD WING WALL MOCKUP, AT 30 °, 45 °, 60 ° AND 90 °.....	59
FIGURE 4- 9 GRADE 1 WIND AT THE DUCT WITH WING WALL OF DESIGNS.....	60
FIGURE 4- 10 GRADE 1 WIND AT THE DUCT WITHOUT WING WALL OF DESIGNS. ....	60
FIGURE 4- 11 GRADE 3 WIND AT THE DUCT WITH WING WALL OF DESIGNS.....	61
FIGURE 4- 12 GRADE 3 WIND AT THE DUCT WITHOUT WING WALL OF DESIGNS. ....	62

FIGURE 4- 13 FOUR DIFFERENT TYPES OF DUAL-FLOW VENTILATED WINDOWS. A) WITH A PARALLEL WING WALL; B) WITH A 90 °WING WALL (LEFT SIDE); C) WITHOUT WING WALL; AND D) WITH A 45 °WING WALL (RIGHT-SIDE). .....	64
FIGURE 4- 14 AIRFLOW SPEED FOR DIFFERENT ANGLES IN THE FOUR CASES.....	66
FIGURE 4- 15 AIR VELOCITIES IN A SINGLE-VENTILATED/ CROSS-VENTILATED ROOM;	
■ AIR VELOCITY IN THE SINGLE-VENTILATED ROOM; ■ AIR VELOCITY IN THE CROSS-VENTILATED ROOM. ....	68
FIGURE 5- 1 3D-VIEW AND TOP-VIEW OF THE MULTIPLE QUARTER-WAVE RESONATORS. ....	74
FIGURE 5- 2 POLYESTER PANEL ABSORBER. ....	76
FIGURE 5- 3 MEMBRANE ABSORBER WITH QUARTER-WAVE RESONATORS. ....	76
FIGURE 5- 4 MEMBRANE ABSORBER.....	76
FIGURE 5- 5 A) BACK SIDE OF THE DUCT; B) FRONT VIEW OF THE TRANSPARENT DUCT; C) DUCT WITH MQWRs.....	77
FIGURE 5- 6 NOISE MEASUREMENTS A) IN THE DUCT AND; B) NOISE MEASUREMENT IN THE ROOM. ....	78

FIGURE 5- 7 TESTS CARRIED IN TWO ROOMS: DUCT ONLY AND DUCT WITH  
QUARTER-WAVE RESONATORS; —♦— DUCT ONLY- TEST IN TWO ROOMS; —■—  
DUCT & QUARTER- TEST IN TWO ROOMS..... 79

FIGURE 5- 8 EXPERIMENTAL RESULTS OF DUCT ONLY TEST IN ROOMS AND DUCT  
ONLY TEST IN THE TUBE; —♦— DUCT ONLY- TEST IN TWO ROOMS; —■— DUCT  
ONLY- TEST IN TUBE. .... 80

FIGURE 5- 9 EXPERIMENTAL COMPARISONS BETWEEN DUCT ONLY TEST AND DUCT  
WITH QUARTER-WAVE RESONATORS IN THE TUBE; —♦— DUCT ONLY- TEST IN  
TUBE; —■— DUCT & QUARTER- TEST IN THE TUBE. .... 81

FIGURE 5- 10 EXPERIMENTAL COMPARISONS BETWEEN DUCT ONLY TEST AND DUCT  
WITH QUARTER-WAVE RESONATORS IN THE TUBE; —♦— DUCT & QUARTER-  
TEST IN TWO ROOMS; —■— DUCT & QUARTER- TEST IN TUBE..... 82

FIGURE 5- 11 EXPERIMENTAL COMPARISONS BETWEEN DUCT WITH QUARTER-WAVE  
RESONATORS TEST IN TUBE BOTH IN THE EXPERIMENT AND IN THEORY; —■—  
DUCT & QUARTER- TEST IN TUBE EXPERIMENT; —♦— DUCT & QUARTER-  
TEST IN TUBE THEORY. .... 84

FIGURE 5- 12 EXPERIMENTAL COMPARISONS BETWEEN DUCT ONLY TEST IN BOTH  
OF THE EXPERIMENT AND THEORY; —♦— DUCT ONLY- TEST IN TUBE  
EXPERIMENT; —■— DUCT ONLY- TEST IN TUBE THEORY..... 85







FIGURE 5-13 MULTIPLE QUARTER-WAVE RESONATORS INSTALLED INSIDE THE DUCT (WANG ET AL, 2014).....	87
FIGURE 5- 14 TRANSMISSION LOSS MEASUREMENT SETUP ON SILENCER (FOR VENTILATED WINDOW) IN TUBE (ALL DIMENSIONS IN MM) (WANG ET AL, 2014).. ..	88
FIGURE 5-15 TRANSMISSION LOSS MEASUREMENT RESULTS MEASURED IN DUCT FOR THREE TYPES OF SILENCER (FOR VENTILATED WINDOW);  TUBE WITH CAVITY OPEN - FILLED WITH ABSORPTION MATERIAL;  TUBE WITH CAVITY OPEN - WITH MULTIPLE QUARTER-WAVE RESONATORS;  TUBE WITH CAVITY CLOSED WITH MEMBRANE. ....	89
FIGURE 5-16 NOISE MEASUREMENT SETUP ON VENTILATED SILENCER IN ROOM. ..	92
FIGURE 5-17 TRANSMISSION LOSS MEASUREMENT RESULTS MEASURED IN TWO ROOMS FOR THREE TYPES OF SILENCER (FOR VENTILATED WINDOW);  TUBE WITH CAVITY OPEN - FILLED WITH ABSORPTION MATERIAL;  TUBE WITH CAVITY OPEN - WITH MULTIPLE QUARTER-WAVE RESONATORS;  TUBE WITH CAVITY CLOSED WITH MEMBRANE. ....	93
FIGURE 5- 18 PHYSICAL CONFIGURATIONS OF THE ACOUSTIC TEST; RECEIVING ROOM: 3M (W) X 5M (L) X 5M (H).....	94
FIGURE 5- 19 CONFIGURATION OF VENTILATED WINDOW. ....	94






FIGURE 5- 20 A) BACK SIDE VIEW OF THE DESIGN; B) FRONT SIDE VIEW OF THE DESIGN; C) VENTILATED DUCT OF THE WING WALL DESIGN AND THE MEMBRANE ABSORBERS IN THE VENTILATED DUCT. ....	96
FIGURE 5- 21 TRANSMISSION LOSS IN THE FULL-SCALE MOCKUP EXPERIMENT;  QUARTER AND MEMBRANE;  MEMBRANE;  POLYESTER;  QUARTER-WAVE. ....	97
FIGURE 5- 22 TRANSMISSION LOSS OF THE PANEL ABSORBER;  DUCT ONLY- TEST IN TUBE. ....	100
FIGURE 5- 23 A) TRADITIONAL EXPERIMENTAL MOCKUP ROOM; B) REVISED ANECHOIC EXPERIMENT MOCKUP ROOM. ....	102
FIGURE 6- 1 ROUNDED-INLET CYLINDRICAL VENTILATED DUCT; A) FRONT VIEW OF THE DUCT; AND B) BACK VIEW OF THE DUCT. ....	108
FIGURE 6- 2 PHOTOS OF THE EXPERIMENTAL SET-UP; A) NOISE SOURCE; B) POSITIONS OF THE MICROPHONE AT THE SOURCE SIDE. ....	108
FIGURE 6- 3 INCIDENT ANGLES OF MEASUREMENTS IN THE EXPERIMENT. ....	109
FIGURE 6- 4 LAYOUT OF SCALED MOCK UP MEASUREMENTS IN THE ROOM. ....	110

FIGURE 6- 5 TRANSMISSION LOSS OF ROUND INLET VENTILATED DUCT IN THE ROOM;

—◆— 90 °IN THE ROOM; —✕— 60 °IN THE ROOM; —\*— 45 °IN THE ROOM;  
—●— 30 °IN THE ROOM; —+— 0 °IN THE ROOM. .... 111

FIGURE 6- 6 ACOUSTICS TESTS (WITH ABSORBER IN THE VENTILATED DUCT) WHEN

THE MICROPHONE PUT IN THE ROOM..... 112

FIGURE 6- 7 NOISE ATTENUATION OF ABSORBER AT 0 °IN THE ROUNDED-INLET

VENTILATED DUCT; —◆— 0 °WITH ABSORBER IN THE ROOM; —■— 0 °IN THE  
ROOM. .... 112

FIGURE 6- 8 NOISE ATTENUATION OF ABSORBER AT 90 °IN THE ROUNDED-INLET

VENTILATED DUCT; —◆— 90 °WITH ABSORBER IN THE ROOM; —■— 90 °IN  
THE ROOM. .... 113

FIGURE 6- 9 TWO ROOMS LINKED WITH A DUCT- MUFFLER EFFECT. .... 115

FIGURE 6- 10 THEORETICAL PREDICTIONS OF TRANSMISSION LOSS OF SIDE BRANCH

RESONATOR..... 116

FIGURE 6-11 TRANSMISSION LOSS BY USING ROUNDED-INLET VENTILATED

DUCT-EXPERIMENTAL; —◆— TRANSMISSION LOSS. .... 117

FIGURE 6- 12 INCIDENT ANGLES OF MEASUREMENTS IN THE EXPERIMENT. .... 119

FIGURE 6- 13 LAYOUT OF SCALED MOCK UP MEASUREMENTS..... 119







FIGURE 6- 14 ADDITIONAL INSERTION LOSS IN THE ROUNDED-INLET CYLINDRICAL VENTILATED DUCT  0 °.....	120
FIGURE 6- 16 ADDITIONAL INSERTION LOSS IN THE ROUNDED-INLET CYLINDRICAL VENTILATED DUCT  90 °.....	121
FIGURE 6- 17 INCIDENT ANGLES TO THE WALL OF VENTILATION MEASUREMENTS FOR STRAIGHT-INLET RECTANGULAR DUCT.....	122
FIGURE 6- 18 INCIDENT ANGLES TO THE WALL OF VENTILATION MEASUREMENTS FOR ROUNDED-INLET CYLINDRICAL DUCT. ....	122
FIGURE 6-19 VENTILATION MEASUREMENTS COMPARISONS BETWEEN STRAIGHT-INLET RECTANGULAR DUCT AND ROUNDED-INLET CYLINDRICAL DUCT AT INCIDENT ANGLES TO THE OPENING;  INLET (STRAIGHT-INLET RECTANGULAR DUCT);  INLET (ROUNDED-INLET CYLINDRICAL DUCT);  OUTLET (STRAIGHT-INLET RECTANGULAR DUCT);  OUTLET (ROUNDED-INLET CYLINDRICAL DUCT). ....	123
FIGURE 7- 1 COMPUTATIONAL SIMULATION WORK FLOWCHART.....	128
FIGURE 7-2 PHYSICAL CONFIGURATIONS OF CONVENTIONAL WINDOW.....	131
FIGURE 7- 3 GRIDS OF THE SIMULATION MODEL.....	132



FIGURE 7- 4 PLAN VIEWS OF THE VECTOR DIAGRAM FOR A CONVENTIONAL WINDOW AT THE WIND ANGLE OF 45 °AND WIND SPEED OF 0.06M/S.....	132
FIGURE 7- 5 PHYSICAL CONFIGURATIONS OF CONVENTIONAL WING WALL.....	134
FIGURE 7- 6 GRIDS OF THE SIMULATION MODEL.....	135
FIGURE 7- 7 PLAN VIEWS OF THE VECTOR DIAGRAM FOR A CONVENTIONAL WING WALL AT WIND ANGLE OF 45 °AND WIND SPEED OF 0.06M/S.....	136
FIGURE 7- 8 PHYSICAL CONFIGURATIONS OF CONVENTIONAL WING WALL WITH TWO BARRIERS. ....	137
FIGURE 7- 9 GRIDS OF THE SIMULATION MODEL.....	139
FIGURE 7- 10 PLAN VIEWS OF THE VECTOR DIAGRAM FOR A CONVENTIONAL WING WALL WITH TWO BARRIERS TO WIND ANGLE OF 45 °AND WIND SPEED OF 0.06M/S.....	139
FIGURE 7- 11 3D VIEWS OF THE VECTOR DIAGRAM FOR A CONVENTIONAL WING WALL WITH TWO BARRIERS TO WIND ANGLE OF 45 °AND WIND SPEED OF 0.06M/S.....	140
FIGURE 7- 12 CONFIGURATION OF VENTILATED WINDOW WITH WING WALL AT 45 °.....	141
FIGURE 7- 13 STREAMLINES WHEN THE MODEL PLACES AT 45 °AT WATER SUPPLY VELOCITY OF 1MM/S.....	143

FIGURE 7- 14 FLOW PATHS WHEN THE MODEL PLACES AT 45 ° AT WATER SUPPLY	
VELOCITY OF 1MM/S.....	144
FIGURE 7- 15 STREAMLINES WHEN THE MODEL PLACES AT 45 ° AT WATER SUPPLY	
VELOCITY OF 5MM/S.....	145
FIGURE 7- 16 FLOW PATH WHEN THE MODEL PLACES AT 45 ° AT WATER SUPPLY	
VELOCITY OF 5MM/S.....	145
FIGURE 7- 17 STREAMLINES WHEN THE MODEL PLACES AT 45 ° AT WATER SUPPLY	
VELOCITY OF 10MM/S.....	146
FIGURE 7- 18 FLOW PATH WHEN THE MODEL PLACES AT 45 ° AT WATER SUPPLY	
VELOCITY OF 10MM/S.....	146
FIGURE 7- 19 CONFIGURATION OF VENTILATED WINDOW WITH WING WALL AT 45 °	
.....	147
FIGURE 7- 20 VENTILATED WINDOW WITH WING WALL AND ROUNDED-INLET	
CYLINDRICAL VENTILATED DUCT IN WIND DIRECTION OF 0 °.....	149
FIGURE 7- 21 ROUNDED-INLET WING WALL AT WIND DIRECTION OF 45 °.....	150
FIGURE 7- 22 ROUNDED-INLET WING WALL IN WIND DIRECTION OF 90 °.....	151
FIGURE 7- 23 PERCENTAGE OF AIR SPEED TO WIND SPEED BY CFD AT INCIDENT	
ANGLE OF 45 ° FOR DIFFERENT CONFIGURATIONS; —●— INLET VELOCITY;	
—■— OUTLET VELOCITY.....	152


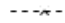


FIGURE 7- 24 PERCENTAGE OF AIR SPEED TO WIND SPEED BY CFD AND BY  
EXPERIMENTAL AT INCIDENT ANGLE OF 90 °, 45 °AND 0 °FOR ROUNDED-INLET  
WING WALL;  OUTLET VELOCITY-CFD;  INLET VELOCITY-CFD;  
 OUTLET VELOCITY- EXPERIMENTAL;  INLET VELOCITY-  
EXPERIMENTAL. .... 153

FIGURE 8- 1 PHYSICAL DIMENSION AND PLAN VIEW OF THE WATER TABLE FOR  
VENTILATION TEST. .... 157

FIGURE 8- 2 FLOW VISUALIZATION FOR CONVENTIONAL WINDOW. .... 160

FIGURE 8- 3 CONVENTIONAL WING WALL. .... 161

FIGURE 8- 4 PHYSICAL CONFIGURATION OF ROUNDED-INLET WING WALL. .... 162

FIGURE 8- 5 FLOW PATTERNS OF ROUNDED-INLET WING WALL. .... 163

FIGURE 9- 1 TOP VIEWS OF A DUAL-FLOW VENTILATED WINDOW WITH WING WALL.  
..... 168

FIGURE 9- 2 FLOW DIRECTIONS OF DUAL-FLOW VENTILATED WINDOW WITH WING  
WALL IN A SINGLE-VENTILATED ROOM. .... 168

FIGURE 9- 3 ROUNDED-INLET CYLINDRICAL DUCTS WITH WING WALL DESIGN. .. 169

FIGURE 9- 4 OVERLAPPING FUNCTIONS OF A CONVENTIONAL WINDOW..... 172

FIGURE 9- 5 CONVENTIONAL WINDOWS AT DAYTIME (TOP VIEW). .....	172
FIGURE 9- 6 CONVENTIONAL WINDOWS AT NIGHT TIME/ SUN SHADING MODE (TOP VIEW). .....	173
FIGURE 9- 7 FUNCTIONS OF VENTILATED WINDOW DESIGN AT SUN SHADING MODE. .....	173
FIGURE 9- 8 FUNCTIONS OF THE WING WALL DESIGN. ....	174
FIGURE 9- 9 VIEW OF THE WING WALL DESIGN.....	175
FIGURE 9- 10 FUNCTIONS OF VENTILATED WINDOW WITH WING WALL DESIGN AT DAYTIME. ....	176
FIGURE 9- 11 FUNCTIONS OF VENTILATED WINDOW WITH WING WALL DESIGN AT NIGHT TIME OR SUN SHADING MODE. ....	176
FIGURE 9- 12 FUNCTIONS OF ROUNDED-INLET CYLINDRICAL DUCT.....	177
FIGURE 10- 1 FUNCTIONS OF ROUNDED-INLET CYLINDRICAL DUCT.....	178
FIGURE 10- 2 EXPANSION CHAMBER WITH EXTENDED INLET AND OUTLET.....	180

# LIST OF TABLES

TABLE 2- 1 TYPES OF NATURAL VENTILATION. ....	13
TABLE 2- 2 ADVANTAGES AND DISADVANTAGES OF NATURAL VENTILATION. ....	15
TABLE 3- 1 RESEARCH OBJECTIVES VS. RESEARCH METHODOLOGY.....	43
TABLE 3- 2 ADVANTAGES OF DIFFERENT MODELS.....	51
TABLE 6-1 VENTILATION MEASUREMENTS FOR ROUNDED INLET DUCT AND STRAIGHT-INLET RECTANGULAR DUCT.....	123
TABLE 7-1 ADVANTAGES AND LIMITATIONS OF K-E TURBULENCE MODEL.....	129
TABLE 7- 2 GEOMETRY OF CONVENTIONAL WINDOW IN COMPUTATIONAL SIMULATION.....	130
TABLE 7- 3 GEOMETRY OF CONVENTIONAL WING WALL IN COMPUTATIONAL SIMULATION.....	133
TABLE 7- 4 GEOMETRY OF CONVENTIONAL WING WALL WITH TWO BARRIERS IN COMPUTATIONAL SIMULATION.....	137

TABLE 7- 5 FLOW STATISTICS OF 2D VENTILATED WINDOW WITH WING WALL AT 45 °

AT DIFFERENT WATER SUPPLY VELOCITY. .... 143

TABLE 7- 6 AIRFLOW STATISTICS AT 0 °, 45 ° AND 90 ° AT A WATER SUPPLY

VELOCITY OF 5MM/S..... 149

## LIST OF ABBREVIATIONS

MQWR Multiple Quarter-wave Resonator

CFD Computational Fluid Dynamics

TL Transmission Loss

NR Noise Reduction

DSF Double Skin Façade

M Microphone

# CHAPTER 1

## INTRODUCTION

### 1.1 BACKGROUND INFORMATION

Hong Kong geographically belongs to subtropical climate regions, which induce in a hot and humid climate for most of the time annually. Hong Kong becomes a “vertical city” because of the limited buildable area (Figure 1-1). A large number of residential and non-residential buildings in Hong Kong are close to heavy traffic lines due to the little buildable area. As a result, both the noise and air pollution problems become serious. Many of residential buildings in Hong Kong expose directly to the sun makes people cannot fulfill their requirement in natural ventilation. Therefore, they have to depend on air conditioning most of the day in hot and humid seasons.



Figure 1- 1 High-rise buildings in Hong Kong.



Some problems on energy efficiency also arise from the current building regulations, government's approaches and practices. The height or bulk of a building, especially the continuing trend of building super-tall buildings in Hong Kong might bring about adverse environmental impacts. Buildings account for the huge amount of the electricity consumption in Hong Kong; therefore reducing building energy use is a key component of people's response to the global challenge of climate change. Electricity generation also affects the air quality. On this point alone, the importance of energy efficiency is a matter of significant public interest.

Noise pollution seems even more severely in city Hong Kong; windows so have to be secured closed most of the time due to its high noise level. Consequently, windows have to be securely closed to prevent any unexpected noise pollution in most of the day in particular in spring and autumn seasons, accordingly, residents cannot fully enjoy the fresh air induced by natural ventilation.

Now mitigation measures of noise and air pollution are in tremendous demand. However, in designing a natural ventilation system, there is always a conflict between ventilation and acoustic requirements. Larger openings are indeed in

enhancing the effectiveness of natural ventilation; conversely. At the same time, large openings may also produce higher noise levels.

## **1.2 PROBLEM STATEMENT**

Residential buildings regularly need much more holding and thermal comfort compare with non-residential property because they are the real private spaces.

The importance of natural ventilation should be addressed in order to maximize this demand. The design of naturally ventilated buildings must arrive at the beginning of each process. However, few residential buildings in Hong Kong at present require the use of natural ventilation design. Large opening allows better natural ventilation, but the sound insulation effect would be unacceptable at this circumstance. The conflict between the balance of natural ventilation and noise pollution still exists.

In hot summer times, air conditioning cannot be entirely removed because of the sub-tropical climates providing Hong Kong a tropical climate. However, we still believe a certain amount of fresh air could be induced into the indoor

environment in spring and autumn times if there is a potentially valuable natural ventilation system.

The use of wing wall creates difference between high pressure and low pressure zones. Therefore, it is termed as “alternation to create effective natural ventilation” (Mak, 2007) and is shown in Figure 1-2.



Figure 1- 2 Typical wing walls in Hong Kong.

The aim of this study is to work out noise management techniques which maintain both the acoustical and airflow performance of ventilation inlets and outlets. In practice, there is a requirement of intention to fulfill natural ventilation performance and sound isolation. There is also a need for a regular

decision-support framework for designers who are considering the use of natural ventilation in residential building construction.

### **1.3 RESEARCH OBJECTIVES**

This research is to determine the effectiveness of the control of airflow and acoustic energy for ventilation system in sustainable building design. Different ventilated window designs carry out by steps, and their performances have tested in each stage. The following objectives will carry out:

1. To determine systematic relationship between openings and airflow;
2. To investigate and assess the impact of noise attenuation of multiple quarter-wave resonators system;
3. To investigate and assess the development of ventilated window design from using straight duct to rounded-inlet duct;
4. To evaluate the effectiveness of ventilated window in acoustic energy and ventilation energy.

#### **1.4 RESEARCH SIGNIFICANCE**

According to literature reviews, the performance of the wing wall in some extent has a successful operation of enhancing the effectiveness of natural ventilation, usually at exceptional opening conditions (Kalogirou, 2009; Givoni, 1976; Mak et al., 2007). However, external wind speed in Hong Kong is inconsistent distributed all year round especially in summer days when sometimes there is no breath at all whereas sometimes typhoons performance with extreme high wind velocity. The air quality is out of expectation in most of the time although wing wall widely used in public housing in Hong Kong for decades. Nevertheless, based on the recent studies, wing wall is a single functional tool as it can only produce fresh air but has extremely limited studies concerning its use in noise reduction.

Wing wall reduces the noise pollution by combining with sound absorptive foams. However, foams also cause some negative impacts primarily to human health; as it is one of the sources of dust and requires replacement and maintenance of ordinary. Quarter-wave resonators could be a voluntary choice as it requires less maintenance, allow air goes smoothing without harming human

health but also with exceptional sound screening effects. Most of the studies in recent years pay attention to its application in industry (i.e. mufflers in engines) despite the fact that extremely few studies discuss its importance in the construction environment.

This research stands for the enhancement of ventilated window design. The basic objective starts to investigate the feasibility of applying ventilated window with wing wall construction in buildings, which can provide effective natural ventilation and at the same time guarantee successful noise reduction capabilities.

The research significance of the modified design of ventilated window consists of two parts: 1) MQWR systems made of plexi-glass plastic film (Figure 1-3), and 2) wing wall connects with ventilated window (Figure 1-4). The combination of ventilated window with wing wall is the new concept contrasting with traditional open windows or wing wall. The goal of this design would be to get a balance between the positive relationship between acoustic energy and ventilation energy.



Figure 1- 3 Multiple quarter-wave resonators.

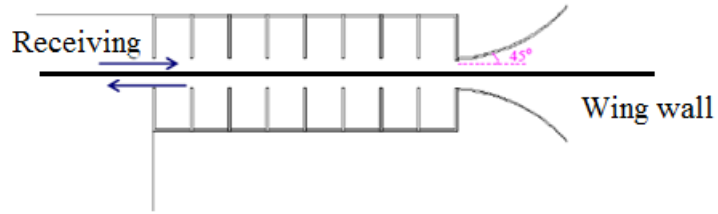


Figure 1- 4 Ventilated window with silencer (top view).

Examinations are also carried out without using any absorbers by changing the angles of opening orientation and also by changing the shapes of the ventilated duct. For example, use the rounded-inlet ventilated duct to replace the straight-inlet rectangular duct (Figure 1-5).

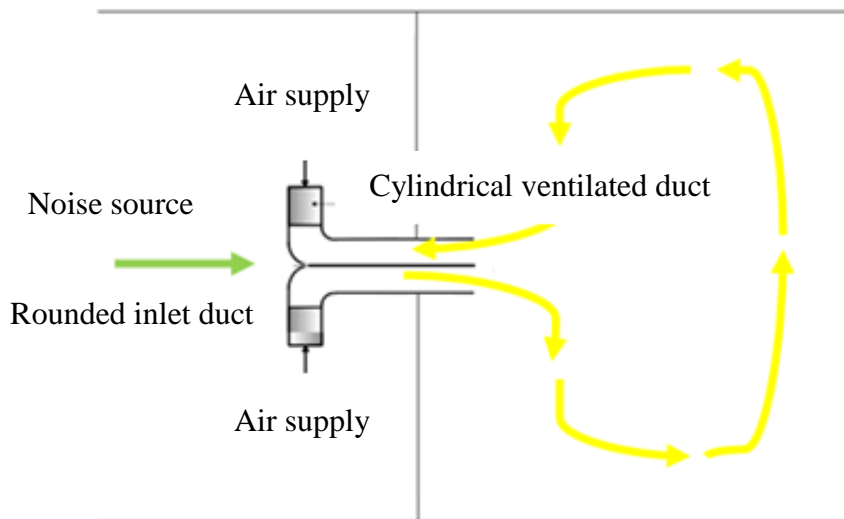


Figure 1- 5 Rounded-inlet ventilated ducts.

## 1.5 DISSERTATION ORGANIZATION

The thesis has ten chapters and the organization presents in the following way:

**Chapter 1- Introduction:** Presents brief background information, research objectives and research significance and also explains the structures of the thesis.

**Chapter 2- Literature review:** Reviews the driving forces of natural ventilation; green features in Hong Kong in the recent years; review the acoustics in natural ventilation buildings natural ventilation and wing wall design.

**Chapter 3- Research methodology:** Outlines the methodology used in this thesis, including small-scale experimental and full-scale experimental measurements, computational simulations and flow visualization simulations.

**Chapter 4- Noise control and air ventilation performance of conventional wing wall:** Carries out the design and analysis of conventional wing wall, experimental measurements for acoustic performance and ventilation performance.

**Chapter 5- Noise control of multiple quarter wave resonators:** Carries out the design and assessment of MQWR, experimental measurements for the acoustic



performance (different combinations: i.e. panel absorber, with membrane absorber, etc.).

**Chapter 6- Ventilation performance of new ventilated window design:**

Analyzes mockup experimental measurements at different wind direction (i.e. 0°, 45°, 60° and 90°) for counter flow ventilated window and rounded-inlet cylindrical duct ventilated window.

**Chapter 7- Computational Simulation:** Analyze the airflow patterns of different ventilated window design. Prove the test results.

**Chapter 8- Flow Visualization:** Analyze and validate the test results of the airflow patterns by using flow visualization technique.

**Chapter 9- Discussion**

**Chapter 10- Conclusion**

## **CHAPTER 2**

### **LITERATURE REVIEW**

#### **2.1 DRIVING FORCES OF NATURAL VENTILATION**

The wind-driven ventilation is an increasingly prominent issue in building performance in order to reduce the building energy consumption. The weather in Hong Kong is hot and humid weather conditions that require turning on the air conditioning in almost half a year time. However, it has been pointed out that natural ventilation limited to a certain climate. (Levermore et al., 2000). There are two main types of natural ventilation: single-sided ventilation and cross ventilation. The focus is on single-sided ventilation, which is also acceptable in urban city such as Hong Kong where a large number of people and limited space has.

The driving forces for natural ventilation are wind-driven ventilation and stack ventilation. Figure 2-1 illustrates the basic principle of wind-driven ventilation, and Figure 2-2 shows the basic principle of stack ventilation. Wind-driven ventilation occurs when the pressure difference results in air movements from

high pressure to low pressure; while the stack ventilation happens at the vast difference increasing the airflow rate between warm air (rises because of its lighter density) and cold air (falls due to its heavier density) (Table 2-1).

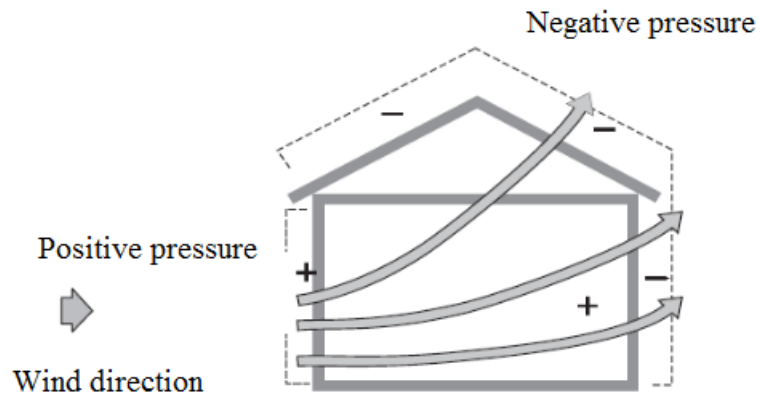


Figure 2- 1 Wind-driven ventilation.

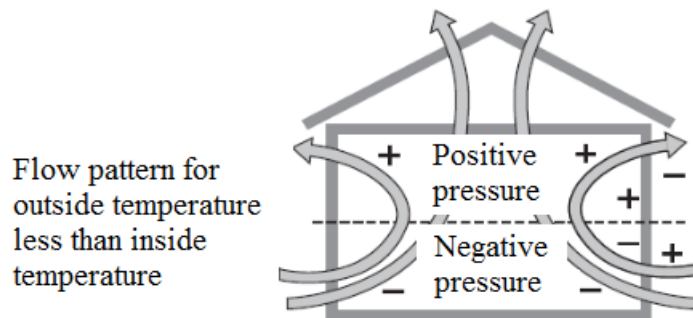


Figure 2- 2 Stack ventilation.

Wind-driven ventilation	Stack ventilation
1. By pressure	1. By buoyancy

---

2. Pressure difference makes air movements	2. Warm air rises (lighter), cold air falls (heavier)
3. Air flows from high pressure to low pressure	3. Chimney always uses to create a large difference to increase the air flow rate

---

Table 2- 1 Types of natural ventilation.

## 2.2 NATURAL VENTILATION STRATEGIES

Recently, architectures and building designers have been more concerned about the green issue. They would like to adopt green concept in designing a new building as a multi-functional building which can improve the living standard, achieve energy saving and produce less damage to the environment.

In this research, we focus on wind-driven ventilation. It is a passive strategy of using wind to dampen down or freshen the air. With wind being a critical driving force for ventilation, building orientation becomes a critical issue. In the summer, wind provides same much fresh air in summer and winter. An expression for the volume of airflow induced by wind as (Walker, 2010):

$$Q_{\text{wind}} = C \times A \times V \quad (2-1)$$

Where,

$Q_{\text{wind}}$  is the volume of airflow ( $\text{m}^3/\text{h}$ )

A is the area of opening ( $\text{m}^2$ )

V is the outdoor wind speed ( $\text{m/h}$ )

C is the coefficient of effectiveness

Wind-driven natural ventilation is “an effective way to maintain the comfortable and healthy indoor environment. The most widely used method to calculate the volumetric flow rate of wind-driven ventilation” (Chu & Wang, 2010). Q through opening is the equation:

$$Q = \Delta P \cdot C_p \quad (2-2)$$

Where,

$\Delta P$  presents the difference of static pressure of two rooms

$C_p$  is the discharge coefficient

Tan et al. (2005) suggested  $C_p = 0.70$  for vents and windows and  $C_p = 0.95$  for internal small openings. Larger the static pressure difference between the

rooms larger the volumetric flow rate if discharge coefficient used as a constant in this equation.

### 2.3 CRITICAL ISSUES IN NATURAL VENTILATION

Zhao's (2007) studies had focused on the diagnostic performances contained energy saving, thermal comfort, acoustic control, indoor air quality and cost in non-residential building. He concluded that a "decision-support framework" should be highly recommended at the beginning of the design stage in the partnership with architectural and engineering concerns to achieve natural ventilation performance of the whole design. The advantages and disadvantages of natural ventilation implement in Table 2-2.

<b>Advantages</b>	<b>Disadvantages</b>
Low energy consumption	Orientations need to be carefully controlled
Low cost	Requires surrounded free space
Low maintenance	Rain/sunlight enters the room

Table 2- 2 Advantages and disadvantages of natural ventilation.

## **2.4 REVIEW OF GREEN FEATURES IN SUSTAINABLE BUILDING DESIGN IN HONG KONG**

Within the increasingly concerns about the natural ventilation strategies, architects and engineers have begun to use different types of screens and shading devices to achieve the overall acoustic comfort and thermal comfort. In Hong Kong, there are a number of forms of external shading devices and designs widely use in buildings.

### **2.4.1 Balcony**

Buratti (2006) also argued that indoor noise typically caused by road and railway traffic especially in summer times when windows always fully open. Hosaam et al. (2005) had investigated the “impact of balcony depth and parapet form on the acoustical performance of building facades close to roadways. The protection obtains by various parapet depths ranges between 4 dB(A) and 8 dB(A) while an additional protection of between 0.5 dB(A) and 4 dB(A) can be obtained by inclining the parapets”. Naish (2012) examined a variety of balconies’ effectiveness in sound attenuation performance, and he found the parapets could

produce the largest improvement combined with absorptive materials on the ceiling.

The traffic noise easily leaks from the sidewall of the balcony; noise reduction of a balcony is not that impressive. Different forms of rectangular balcony widely used in Hong Kong and many other cities around the world show in Figure 2-3 (Tang, 2005).

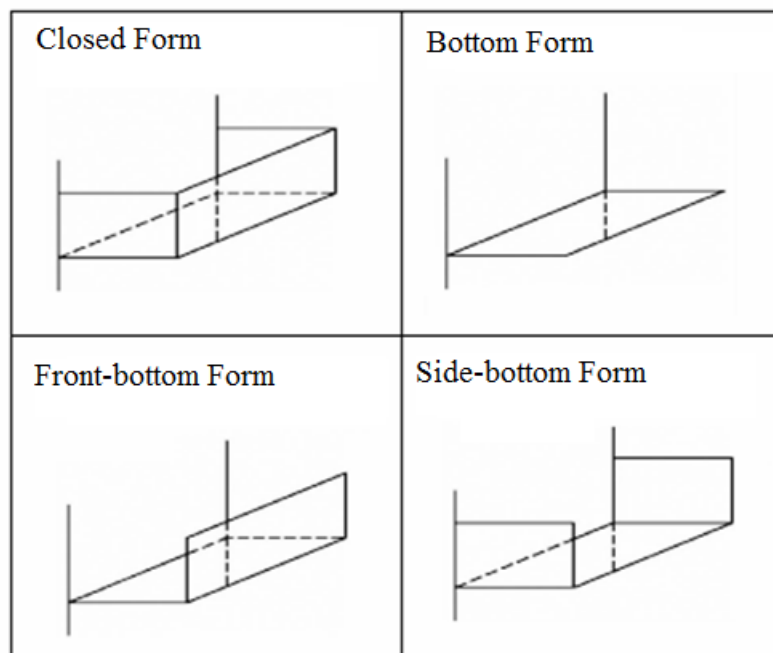


Figure 2- 3 Different types of rectangular balcony.

There is significant noise amplification due to reflection from the upper balcony of low frequency at such source distances. Sound amplification observes near the



upper balcony floor for all balcony forms. The elevation angle of the balcony correlates remarkably well with the A-weighted insertion loss produced by the balcony in the lack of top reflections. Ishizuka and his colleague (2012) had designed “a balcony with ceiling-mounted reflectors” on high-rise building in Japan. Their findings illustrated “a balcony equipped with reflectors could reduce road traffic noise by 7 dB(A) to 10 dB(A) comparing with conventional balcony”. The design was strictly depending on the incident angles between the noise source and reflectors and the efficiency is equivalent to a balcony with absorptive ceiling. Figure 2-4 clearly exemplified “the levels of balcony acoustic treatment and their generalized potential noise attenuation” (Naish et al., 2013).

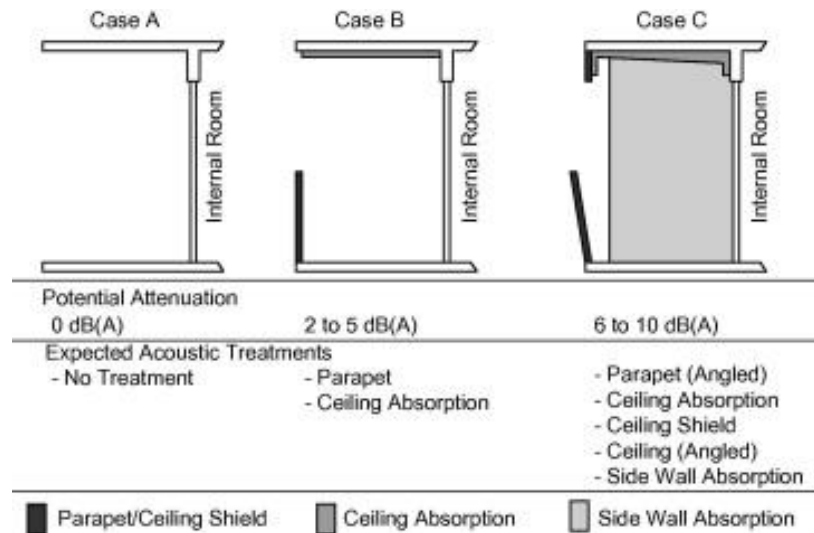


Figure 2- 4 Levels of balcony acoustic treatment and their generalized potential noise attenuation.

More and more engineers and scientists have begun to doubt about the effectiveness of the balcony in terms of reducing environmental issues such as reducing noise and air pollution. Most noise can enter the balcony through its anterior opening, such as the sidewalls, and side parapets. The lighting level and natural air ventilation at the facade raise when balconies with larger open space; hence new balcony design can effectively improve the acoustic environment for residential buildings without affecting the ventilation and lighting. Nevertheless, the noise contributions from sidewall reflections can cause degradation of the balcony effective in shielding against the noise, as well (Gratia et al., 2003).

#### **2.4.2 Glass curtain wall**

In Hong Kong, a variety of building designs use glasses. One named full-height curtain wall. Glass recognized as a favorable material attributable to its transparency. Broad use of glass can be regarded as a green feature in the green building movements these days. There are many advantages using transparent materials such as improving visual views, suitable for day lighting and reduction in energy consumption in terms of energy costs; and also beneficial for commercial investments if the building designed in such a modern and

innovation trend (Gratia et al., 2003). Curtain wall merely keeps out the weather due to it is an outer covering of a building. Glass curtain wall has become tremendously popular especially in commercial building over a century.



Figure 2- 5 Glass curtain walls of the International Commerce Centre (ICC) building.

Curtain wall takes into consideration design requirements such as “thermal expansion and contraction; building sway and movement; water diversion, and thermal efficiency for cost-effective heating, cooling and lighting in the building” (Shield et al, 2001). An example of glazed curtain wall showed in Figure 2-5 is the International Commerce Centre (ICC) building.

However, literatures showed that the glass might be a vulnerable-building material, when it exposed to high heat conditions. As one of the benefits of glass curtain wall is it is suitable for daily lighting, it is highly likely that the energy bills of using air conditioners to settle down the hot air may be higher than the bills pay for lighting. Excessive thermal stress on the glass surface and air pressure inside well-sealed offices as in curtain walled building would break the glass (Shield et al., 2001). From the safety aspect, Chow (2003) also argued that the breaking of the window might provide adequate intake air flow rate to burn up all the combustibles to produce a mass fire.

#### **2.4.3 Double skin façade (DSF)**

Locally at Hong Kong, air conditioning occupies the largest energy consumption (approximate 40%) (Chan et al., 2001). Double-glazing can achieve exceptional acoustic comforts and thermal insulation. Matthias and his colleagues conducted simulations in evaluating the effectiveness of different types of DSFs and the outcomes showed significant energy consumption saving (up to 9.18%) is possible among all the simulation results (Haase et al., 2007).

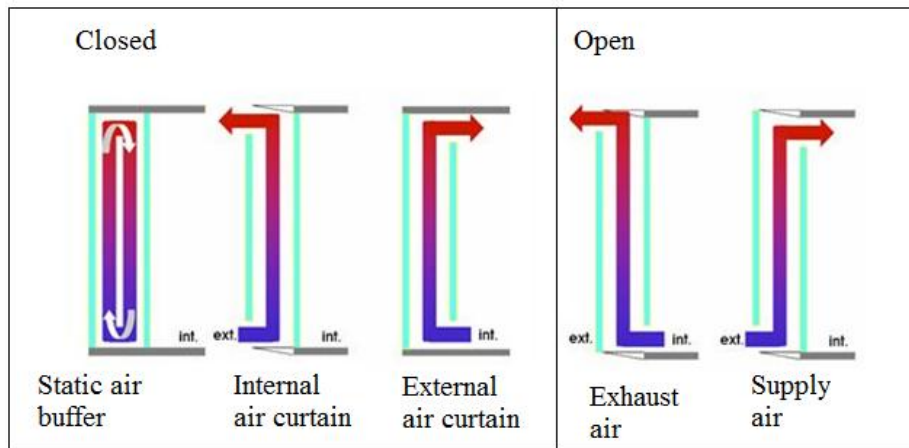


Figure 2- 6 Principles of airflow in the cavity of double-skin faade.

Figure 2-6 shows the different airflow concepts that can be applied to DSF. At the present time, DSF has developed that act as “climate responsive elements with hybrid ventilation (natural and mechanical) concepts with an option to change the airflow concept due to unusual weather conditions in different seasons” (Heiselberg, 2007; Gosselin & Chen, 2008). An example of DSF is at No.1 Peking Road in Figure 2-7 (Haase et al., 2006). Chan et al. (2009) did a computational simulation and also an experiment on the energy performance of the DSF.



Figure 2- 7 DSF of No.1 Peking Road.

On the other side, however, the DSF has received opposing voices at the same time. The energy savings depends on the weather condition and the design, which involving numerous factors for instance glass selection, shading, day lighting, wind loads, ventilation strategies, and maintenance and so on. Currently there is little work has done on the effectiveness of DSF in hot and humid weather conditions. Chan and his colleagues have also conducted a study to evaluate the energy performance of DSF, and there is 26% of annual savings can be achieved in cooling loads in a building (Chan et al., 2009) and its effectiveness is more visible contrasting with single façade. However, the payback period is too long makes the DSF is economical invisible. There are full of green features in the Science Park in Hong Kong and some examples of DSF

show in Figure 2-8 and Figure 2-9.



Figure 2- 8 DSF in Science Park.



Figure 2- 9 Double-skin façade in Hong Kong Science Park.

There are still relatively few buildings understanding the operation of curtain wall (Gratia et al., 2004). To maintain ease and reduce cooling loads, it is

necessary to apply natural cooling strategies. “Counteraction between wind and heat is one of the reasons of poor ventilation and should obtain sufficient awareness. Wind velocity increases the upper limit comfortable temperature and humidity does reversely” (Zhou et al., 2009; Yin et al., 2010).

Gratia and Herde (2004) also examined the effectiveness of natural ventilation in relation to building orientation and wind velocity. The result showed to implement the strategy of daily natural ventilation is difficult when the sun is shining or the building inserted with a southern double skin. Gratia and Herde also validated “in a building with northern double-skin, cross-ventilation will be less difficult since the temperatures in the double-skin would be closer to the outside temperatures, and so the air flow direction will be less significant. The cross-ventilation is less effective than single-sided ventilation for the constant ventilation rate” (Gratia & Herde, 2004).

#### **2.4.4 New ventilation windows**

Full-scale model experiments have carried out in public housing flats to investigate the sound attenuation performance for ventilation windows (Wong et



al., 2012). Ventilation windows built in the flat just next to heavy traffic lines, where the noise level outside exceeded 80 dB(A). The measurement results explained the insertion loss could achieve 6.6 dB for the ventilation windows, compared to the conventional window. However, ventilation performance was not considered in this research.

Huang et al. (2012) also performed a study on the performance of ventilated soundproof windows with fans. The sound attenuation performance was satisfactory. Sound insulation had not been changed by changing the glass thickness. They tried to use a fan to improve the overall ventilation performance, but the fan at the same time made noise; which will not be considered a green factor to achieve natural ventilation and will not be counted in this research.

Another new ventilation window designed and installed in the PolyU Homantin New halls, in Hong Kong. A site visit carried out to the new PolyU Homantin Hall in 2012; details have showed in Appendix I. Airflow measurement and noise measurement conducted for noise and ventilation measurement of the new double glaze window in the new PolyU Homantin Hall. The double-glazed window shown in Figure 2-10 in student rooms consists of two panes of glass

that aimed at providing the soundproofing while maintaining proper ventilation.

Figure 2-11 shows the airflow of single-sided glazed ventilated window. Site measurement conducted to determine the noise reduction and natural ventilation performance of the double-glazed window.



Figure 2- 10 Single-sided glazed ventilated window.

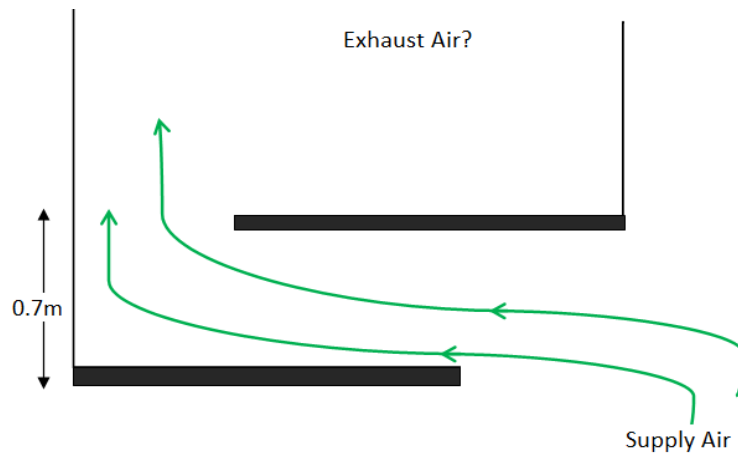


Figure 2- 11 Airflow of single-sided glazed ventilated window.

The acoustic reduction performances of the double-glazed window in PolyU Homantin Hall are between 10.4 dB(A) to 16.9 dB(A) and have insufficient

natural ventilation performance. It seems that the new design single sided glazed ventilated window does not improve the noise reduction and the natural ventilation significantly.

## **2.5 ACOUSTICS IN NATURAL VENTILATED BUILDING**

In designing a natural ventilation system, there is always a conflict between ventilation and acoustic requirements. Larger openings always involved in enhancing the effectiveness of natural ventilation; however, at the same time large openings may also generate higher noise levels. There is a lack of international standards to govern the acceptable noise level.

On the acoustics aspects, foams or fiber layers use most in attenuating the noise intrusion. However, foams also cause some negative impacts primarily to human health; as it is one of the sources of dust and requires replacement and maintenance of anticipated. Quarter-wave resonators could replace traditional sound absorption material as it requires little maintenance, and they allows air to pass straightly without harming human health but also with real considerable noise screening effects. Most of the studies in recent years pay attention to its

function in the industry (i.e. mufflers in engines) despite the fact that few studies discuss its importance in the building environment.

## **2.6 THE CONCEPT OF WING WALL**

Silencers come in many shapes and sizes, and almost all of them can be classified into four types: reactive, dissipative, absorptive, and dispersive or diffusive. Reactive silencers do not use sound absorbing materials but instead employ geometric design principles. Absorptive silencers utilize conventional sound absorbing materials. Dissipative silencer utilizes flow resistance to reduce flow velocity. Dispersive or diffusive silencers reduces noise by preventing its generation.

Field and Fricke (1997) had investigated the use of MQWR system in noise attenuation; the effectiveness of the noise attenuation of the multiple resonator system is feasible. 7 dB and 6 dB attenuation achieved at the frequency level of 1.25 kHz and 3.15 kHz respectively. It also examined that lined duct inlet with less than 1m can provide valuable natural ventilation airflow. Their experiments showed out lower costs compared to sound insulation and minimal maintenance

requirements. However, the efficiency of an in-duct active noise control system employed to prevent an external sound source is unknown. Salis et al (2002) reviewed a few noise control techniques and assessed the variation of airflow characteristics with sound insulation to road traffic noise of facades incorporating ventilation openings. They found that natural ventilation openings offer minimal resistance to the noise passage, and incur high flow constraints.

Field (2008) proposed acceptable indoor noise level criteria for office buildings achieving minimum natural ventilation standards in sustainable buildings. They argued the current global noise standard was impossible to meet natural ventilation efficiency. As a result, they suggested the acceptable level of external noise could be set higher than for sealed and mechanically ventilated building.

Most of the current conventional treatments (e.g. louvers, screening) are effective at high frequencies but are not effective at low frequencies. Low frequency treatment needs to be complemented. The benefits can be obtained from their practical application is limit.

In naturally ventilated spaces, the key reasons influences the ventilation rate was

the opening conditions (Figure 2-12).

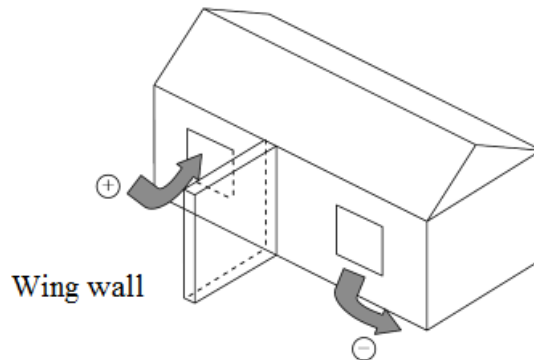


Figure 2- 12 The concept of wing wall (Kalogirou, 2009).

The arrangement of openings in the building elevation is also the determining factor for effective natural ventilation. The most effective arrangement is placing the openings in opposing walls to ensure cross ventilation. However, in case while only one wall can have a window opening, the pressure gradient across the openings is extremely small. It described wing wall could be used to promote natural ventilation when the windows located on the same side of the wall. Orientations of wind direction are crucial in affecting the natural ventilation. The location of the outlet window is not as noticeable as the location of the inlet window.

Prof. Mak has explained “wing walls project outward adjacent to a window so that even a slight breeze against the wall creates a high-pressure zone on one side

and low on the other. The pressure differential draws outside air in through one open window and out the adjacent one. Wing walls are extremely useful on sites with low outdoor air velocity and variable wind directions” (Mak et al., 2007)

Air movement is caused by the difference of pressure distribution moving from high pressure to areas of low pressure (Kalogirous, 2009). The more spread out of the building is the irregular its shape is the expected is for natural ventilation. A spread out configuration has a larger area of exterior walls for a given floor area. There are opportunities to take openings which can catch the wind from different directions. An asymmetrical shape can have a higher opportunity of developing areas of high and low pressures.

Both experimental and CFD prediction have conducted in the evaluation of the planning and design phase of development in order to assess the effectiveness of the wing wall. The first experiment investigated the effectiveness of the airflow by wing wall firstly carried out by Givoni (1976). He conducted to investigate airflow through room models with and without wing walls in a wind tunnel. The results show that single-sided ventilation incorporated with wing walls can significantly increase wind velocity.

The arrangement of the openings in the building elevation is the determining factor for effective natural ventilation. The most effective arrangement is placing the openings in opposite walls to ensure cross ventilation. However, in case only one wall can have windows. The pressure gradient across the openings is extraordinarily small. Under this circumstance, a projection placed downwind of the window creates a high pressure, and a projection placed upwind of a window creates a gentle pressure. Thus, it is possible to create a steeper pressure gradient across the openings and thus increase the indoor air velocity (Figure 2-13).

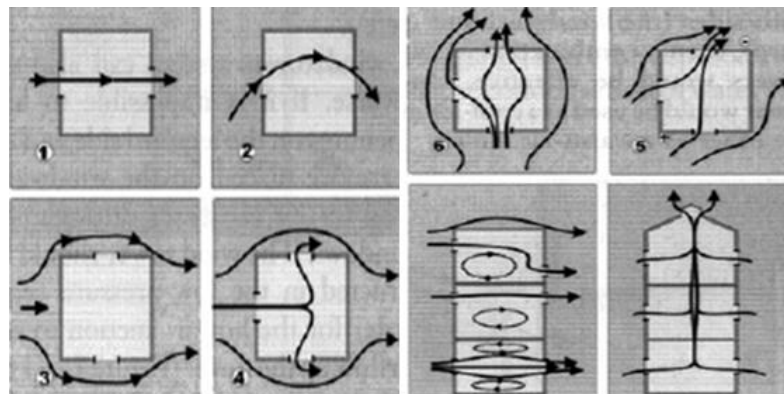


Figure 2- 13 Ventilation strategies by the arrangement of openings (Givoni, 1976).

CFD recently become immensely popular in assessing and presenting the building airflow, wind conditions and indoor environment. The contemporary CFD study of characteristics of natural ventilation of the wing wall carried out by



Mak et al. (2007). Large window openings may provide superior natural ventilation. “The best performance of the wing wall is at the wind angle of around 45 °. The study also shows that 3D CFD simulation produces a similar trend to the experimental results although there are some minor disagreements” (Mak & Niu, 2005; Mak, 2007).

## **2.7 APPLICATIONS OF NATURAL VENTILATION AND WING WALL DESIGN**

### **2.7.1 UMNO Tower**

“Wind wing wall” is a short barrier placed perpendicular to an opening in a building used to collect or charge the prevailing winds into the indoor building. Menara UMNO Tower in Penang (Figure 2-14), Malaysia was the first high-rise office building to employ a wind wing wall system. The architect of this building Ken Yeang, firstly introduced and developed to maximize the value of the prevailing winds by capturing a wider range of wind directions and increasing the indoor airflow for the purpose of natural ventilation. The vertical wing wall runs up the full height of the building and to develop wind from south, southwest

and northeast (Figure 2- 15) directions as marked in green color in Figure 2- 16 and Figure 2-17.



Figure 2- 14 UMNO Tower by Ken Yeang 1 (Tye, 2006).



Figure 2- 15 Wing walls on the southeast of UMNO Tower.

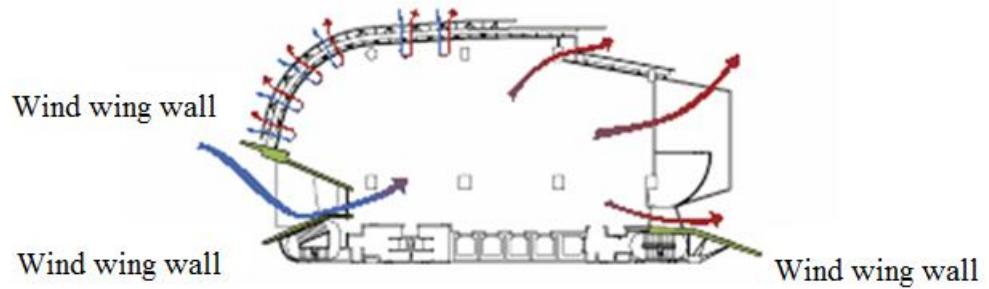


Figure 2- 16 Office floor plans (top).

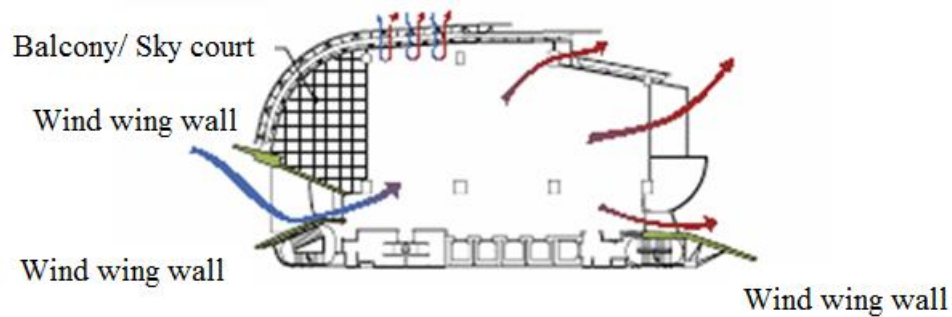


Figure 2- 17 Office floor plans (bottom).

CFD simulation had implemented at the design stage of the UMNO Tower building. It confirmed the pressure difference had increased by the wind wing wall as showed in Figure 2-18. The effectiveness of natural ventilation driven by wind wing wall had proven in the study; wing wall can direct a greater range of prevailing winds into the building. The use of the wing wall also minimized the risk of natural ventilation because of the dynamic changes in wind directions (Wood & Salib, 2012).

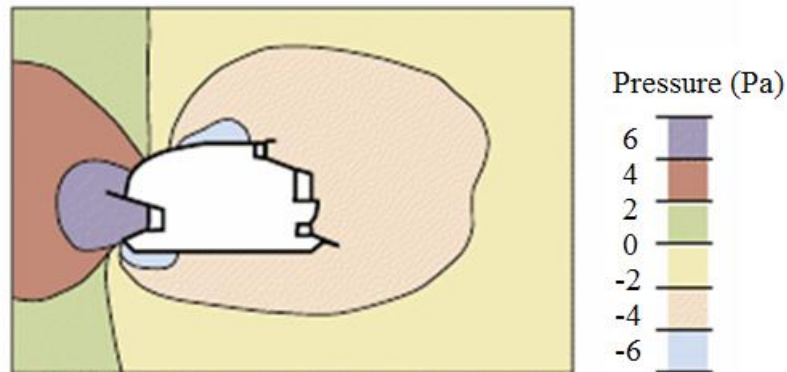


Figure 2- 18 CFD simulation of air pressure contours around the building (plan view) (Wood & Salib, 2012).

### 2.7.2 Post Tower

Post Tower in Bonn, Germany (Figure 2-19 and Figure 2-20) also used its extension of DSFs at the east end of the north façade and the west end of the south façade as wing walls to improve the performance of natural ventilation.

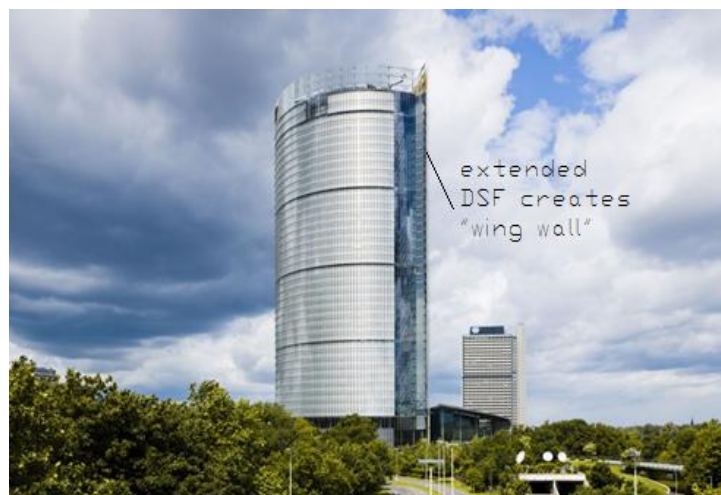


Figure 2- 19 Extended DSF creates “wing wall effect” in Post Tower (King, 2012).



Figure 2- 20 Post Tower, Germany (King, 2012).

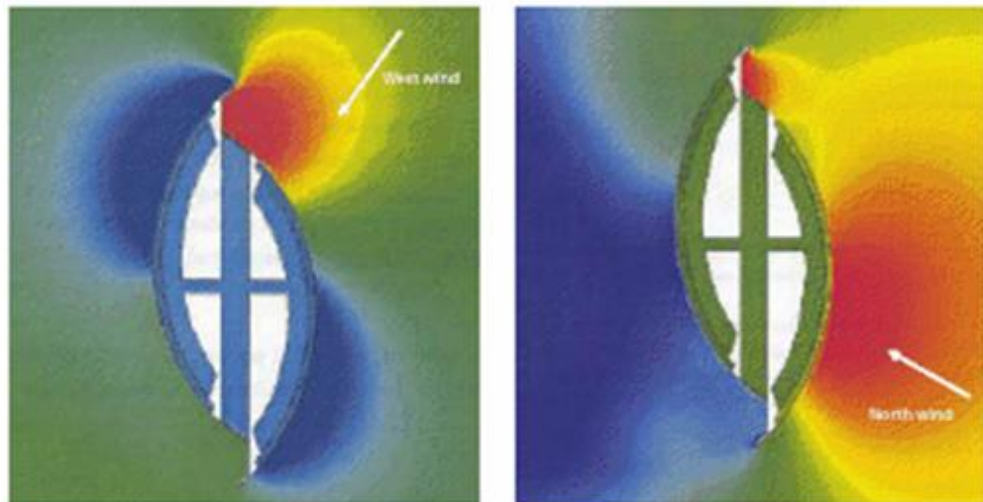


Figure 2- 21 CFD studies of the pressure difference for the wing wall in Post Tower, Germany (Wood & Salib, 2012).

CFD studies in Figure 2-21 had shown that the wing walls help create pressure differences to enhance the performance of natural ventilation. However,

traditional wing wall normally uses in a single function, either natural ventilation or noise screening. Therefore, the new design will incorporate both of the functions and try to maximize to establish architectural features of the restored building.

# **CHAPTER 3**

## **RESEARCH METHODOLOGY**

### **3.1 INTRODUCTION**

This research determines the effectiveness of the control of airflow and acoustic energy for ventilation system in sustainable building design. Steps have carried out different designs of wing wall and ventilated window with wing wall, and their performances have tested in each stage. The following objectives will carry out:

1. To determine systematic relationship between openings and airflow;
2. To investigate and assess the impact of noise attenuation of multiple quarter-wave resonators system;
3. To investigate and assess the development of ventilated window design from using straight duct to rounded-inlet duct;
4. To evaluate the effectiveness of ventilated window in acoustic energy and ventilation energy.

With the purpose of carrying out experimentally, lab-based small-scale experimental and full-scale experimental measurements, computational simulations, and flow visualization test need to be conducted.

### **3.2 RESEARCH GAPS**

The performance of wing wall in some measure has proven having an effective function in enhancing the effectiveness of natural ventilation, especially at particular opening conditions (Buratti, 2006; Hosaam et al., 2005; Naish et al., 2013; Tang, 2005) . However, the external wind speed in Hong Kong is inconsistent distributed all year round especially in summer time when sometimes there is no breath at all, whereas sometimes typhoons arrive with extreme high wind velocity.

The air quality yet did not as expected in most of the time although wing wall widely used in public housing in Hong Kong for decades. Nevertheless, based on the recent studies, wing wall is still a single functional design as it can only induce fresh air; wing wall itself is not enough for noise screening.



From the acoustic aspects, wing wall installed with sound absorption materials sometimes uses most of the time using foams to attenuate the noise pollution. However, foams also cause some negative impacts primarily to human health; as it is one of the sources of dust and require replacement and maintenance of ordinary. Quarter-wave resonators could be an option to replace traditional sound absorption materials as it requires less maintenance, allow air goes smoothing without harming human health but also with adequate noise screening effects.

Most of the studies in recent years pay attention to its role in industry (i.e. mufflers in engines); despite the fact that few studies concern its importance in the building environment. No panels with transparent materials have been studies since so far.

A combination of ventilated window with wing wall is the new concept contrasting with traditional open windows or wing wall. The goal of this design would be to make a balance between the positive relationship between acoustic energy and ventilation energy.

### 3.3 OVERVIEW OF THE APPROACH

According to the previous objectives described and literature reviews, this chapter will outline the methodologies in this research. Table 3-1 summarizes the proposed methods with the corresponding research objectives.

<b>Research objectives</b>	<b>Research methodology</b>
To determine systematic relationship between openings and airflow.	Small-scale experimental measurements, Ventilation measurements. CFD simulation. Flow visualization techniques.
To investigate and assess the impact of noise attenuation of multiple quarter-wave resonators system.	Acoustics measurements experiments.
To investigate and assess the development of ventilated window design from using straight duct to rounded-inlet duct.	Ventilation and acoustics measurements. CFD simulations Flow visualization techniques.
To evaluate the effectiveness of ventilated window in acoustic energy and ventilation energy.	Comparison made between CFD simulations and testing. Flow visualization techniques.

Table 3- 1 Research objectives vs. Research methodology

A combination of ventilated window with wing wall is a new concept contrasting with traditional open windows or wing wall. Study of ventilated window with MQWRs system combine with a wing wall system will carry out in both of acoustics and ventilation.

### **3.3.1 Small-scale experimental and Full-scale direct techniques for predicting ventilation**

The small-scale experiments use measuring techniques to predict ventilation performance with a reduced scale of regular residence space. Experiments and scale model tests covering to assess the effectiveness of natural ventilation of wing wall in the laboratory. A small-scale model (20% of original size) of wing wall will set up to take the first set of ventilation experiment.

Besides the measurements of different forms of wing wall design, the airflows measure in the room by using the anemometer to observe the effect of straight-inlet rectangular duct and rounded-inlet cylindrical duct; air flow velocities at different angles (0 °, 30 °, 45 °, 60 °, and 90 °) measure.

The ventilation performance of ventilated window with MQWR design has measured in the full-scale model experiments. In both small-scale experimental and full-scale experimental measurements, a Testo hot-wire anemometer shown uses in measuring the airflow velocity in the ventilation experiments, which include two main parts: a display shows the wind speed and a sensing probe. This type of anemometer can detect low speed air compared to other types of anemometer. The anemometer is easy and convenient to use. A handheld anemometer is typically extremely compact and extremely useful for gathering wind data (McWilliams, 2002). It gives a direct reading of velocity in meters per second (m/s).

Direct measurements by hot-wire anemometer have used for decades. Modera et al. (1995) found this type of anemometer can provide a valid means to achieve the desired airflow rate to calculate whole building ventilation rate. Paepe et al. (2009) also conducted ventilation measurements by hot-wire anemometers, which placed in the scale model. The results illustrated that the direct measurements by hot-wire anemometer had excellent agreement with the CFD results. The output of anemometer measurements is usually an analogue signal

that can be used for monitoring and control if the reasonable numbers of measurement points carefully design and choose (ibid, 2009).

Experiments by Chen use anemometers to measure velocities. He concluded the measurement is not particularly accurate when the wind speed is less than 0.1m/s (Chen et al., 2003). Small-scale ventilation experiments show similar functions in predicting ventilation performance with full-scale experimental models. It is cost-effective, less time-consuming and could be used to compare with and evaluate the information obtained from CFD simulation results (Lee et al., 2007)

### **3.3.2 Sound transmission loss Measurement**

The sound transmission loss of the wing wall, MQWRs and straight and rounded-inlet cylindrical ducts will carry out in this research. For the acoustic experiments, certain equipment such as loudspeakers and microphones will carefully select and apply in the experiment, sound source and receiving source will also be carefully design in order to get the most optimized testing results. On-site measurements then will conduct, and the data would be collected for further research and analysis.

Five sets of the trial had accomplished to examine the noise reduction of different combinations and absorption materials in the MQWRs, these include: 1) Quarter-wave resonator with membrane absorbers; 2) Membrane absorbers; 3) Polyester; 4) Quarter-wave resonator and 5) Control test with no absorbers in the duct.

A tube closes at one side and opened at the other create a quarter-wave resonator. Field and Fricke confirmed “the rigid end of the tube confines the resonator cavity” (Field & Fricke, 1998). Under certain conditions, this body of air can be brought to a state of resonant. The fundamental resonant can be formed is a quarter wave in a cavity. The displacement,  $d = (2n-1)\lambda/4$ , where  $n=0, 1, 2, 3, \dots$ ,  $d$  is the cavity depth.

### **3.3.3 CFD simulation**

Recent reviews have shown that the modern trend in using CFD for indoor environment where specific analyses of ventilation performance were crucial. However, in this research, the applications of CFD models only apply to examine and evaluate the movement patterns and ventilation effectiveness. In this

research, a variety of design options would be implemented at the beginning stage based on different concepts and strategy in response to the CFD predictions. Selection of the final design will base on the ventilation performance. Figure 3-1 shows the use of CFD for natural ventilation performance at the initial design stage.

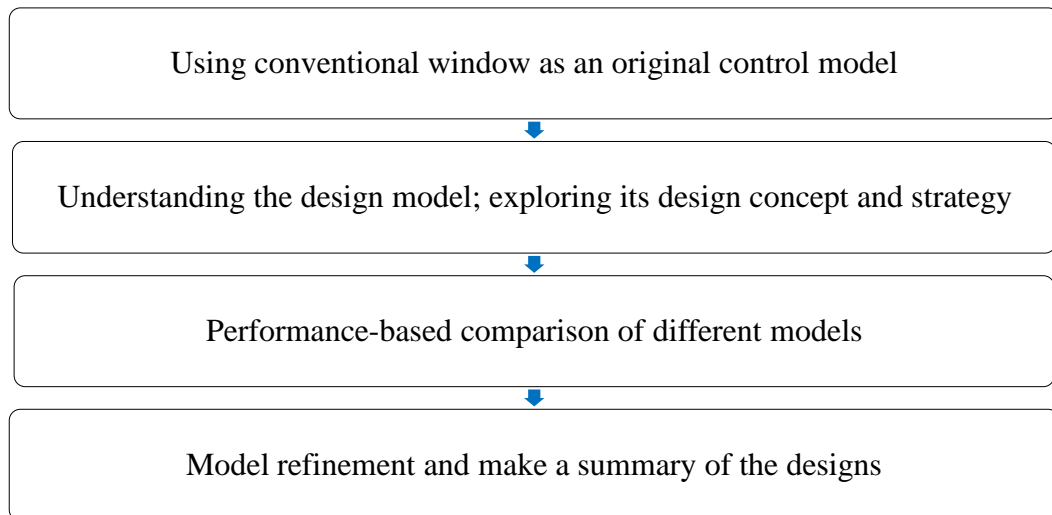


Figure 3- 1 The use of CFD for natural ventilation performance at the initial design stage.

Tsou (2001) used CFD to examine the effect of building ventilation performance and the development of designs on the concept of technologies. Chen et al. (2010) also suggested using a CFD model to replace traditional empirical models, which developed with a database. CFD selected in his research for predicting ventilation performance. However, when the CFD uses in this way, experimental

measurements or other techniques have to be carried out at the same time to verify the results. In this research, both experimental measurements and flow visualization techniques will accomplish. Comparisons among those models will perform.

### **3.3.4 Flow visualization techniques**

Flow visualization techniques involved in this research except the models discussed above. The analysis of various airflow simulations will perform with different physical scale models, using tracing method with a technique of direct injection of ink in the water, with a water table apparatus. It uses low speed of less than 2m/s, which are sufficient for incompressible outflows. It allows for an immediate and dynamic visualization of the airflow outside and inside the model, as well as a direct definition of the inlet and outlet openings. The photographic record of the experiments made with a Nikon digital camera, makes the airflow analyses a highly intuitive, effective and amusing task. Dark ink used as the indicator for the visualization of extended lines.



“Flow visualization is an essential tool to understand the nature of the flow field. The proper utilization may require appropriate information that will help in influencing the flow characteristics and superior design modification of ventilation systems. It is difficult to evaluate the values of flow visualization” (Mahmood, 2011). The test method of movement visualization bases on observations with eyes. Therefore, the precision and prejudice may occur during the observation process. Normally using a digital camera nowadays to record the results or record a video during the flow methodology for records for further investigations.

The reviews have proven the effectiveness of flow visualization in predicting the natural ventilation performance. Komatsu and his colleagues (2008) used both direct experimental measurements and flow visualization techniques to study the airflow at different wind directions. Pereira and Toledo (2004) also affirmed the feasibility of flow visualization comparing to the use of CFD predictions mostly due to its low cost. Nitatwichit (2008) in a case study approved the numerical results readily agreed with the experimental results.

### 3.4 SUMMARY

This chapter reported the assessments in this research have four types of models for predicting the performance of acoustics and ventilation performance in residential buildings. The model types were small-scale experiment, full-scale experiment, CFD and flow visualization. The advantages of methodology are shown in Table 3-2.

---

<b>Small-scale</b>	Inexpensive Direct view of airflow Good for selections at initial design Short time
<b>Full-scale</b>	Relatively expensive anechoic room with actual room size Actual room size, more reliable
<b>CFD</b>	Colorful and clear presentations of streamlines for simple model
<b>Flow visualization</b>	Direct view of the nature of movements Relatively easy to manage

---

Table 3- 2 Advantages of different models.

The small-scale experimental measurements can offer immediate and detailed information about the performance of acoustics and ventilation systems. Reliable

experimental results can be obtained with the basis of economy and less time-consuming. The full-scale experimental measurements are the actual room size; and our specially designed anechoic room gives more reliable test environment.

CFD prediction can consider single internal flows and heat transfer problems. The presentation of results can be shown in different ways, and the colorful vector movement and streamlines are obviously for people to understand the inner flows, circulations, and turbulence of each model. However, CFD required the operators to have solid expertise in understanding the software, which is not easy at all. The input at the beginning stage of the CFD prediction is extremely complex; therefore misleading results are relatively high due to its difficulty. The cost to purchase the software is expensive, and the use of this computational simulation is time-consuming.

Flow visualization is inexpensive and less time-consuming comparing to the CFD simulations. It also gives people a complete view of the water flow patterns in order to understand the air ventilation flow path of the model. The operation is relatively easy unless the water flow rate has to be carefully controlled.

## **CHAPTER 4**

### **NOISE CONTROL AND AIR VENTILATION**

#### **PERFORMANCE OF CONVENTIONAL WING WALL**

##### **4.1 THE CONCEPT OF WING WALL**

Maximum potentials currently still focus on the evaluation and improvement of thermal comfort. Development and integration of environmental, energy and ecological issues into building design are becoming far imperative in Hong Kong. In order to improve the environmental performance and sustainability of buildings, the Buildings Department, the Lands Department and the Planning Department of the Hong Kong SAR Government issued the first of a series of joint practice notes to promote the establishment of green and innovative features in residential buildings.

The use of wing wall as showed in Figure 4-1, one of the green features, is an alternative to creating effective natural ventilation. It shows the typical wing wall in Hong Kong. Natural ventilation considers being a successful passive cooling strategy in building design.



Figure 4- 1 Typical use of wing walls in Hong Kong.

Wing wall had widely used in public housing, in Hong Kong. It has two main functions in residence building design: 1) For ventilation purpose; it promotes the natural ventilation of a building, and 2) For noise screening, always used in forms of vertical fins.

Natural ventilation can be “an energy conserving design strategy reducing building cooling loads, and improving indoor thermal comfort in various hot climate areas” (Kindangen et al., 1997). According to the preceding literature review, the performance of the wing has proven having an effective function of enhancing the effectiveness of natural ventilation. However, based on the recent

studies, wing wall is still a single functional design as it can only produce fresh air and has particularly limited studies concerning its function in sound isolation and reduction performances.

## **4.2 MODEL EXPERIMENTS IN LABORATORY**

### **4.2.1 Acoustic experiments**

Transmission loss tests carried out in the laboratory on a ventilation opening (730mm x 100mm) at the middle center of the wall. A wood board (150mm extended from the opening; 50mm x 100mm on each side) served as a wing wall to create a dual-flow ventilated environment (Figure 4-2). Wedges placed around the microphone at the source side with the desire to reduce the sound reflection from the surroundings. Tests with or without membrane absorbers were both carried out. Layout of configuration of the experiment shows in Figure 4-3. An acoustic driver radiating white noise over the frequency range 20 Hz to 20 kHz used as the source of noise constantly in this mockup experiment. Six measurement points (indicated as M1, M2, M3, M4, M5, and M6) chosen and evenly distributed to measure the noise level in the receiving room (2900mm x

1800mm x 2500mm). Two microphones Type B&K#4189 and Type B&K#4189A21 use to determine the noise level, one mounts at the front of the ventilation opening at the same height, the source room and the other one located in the receiving room, respectively.



Figure 4- 2 Wood board wing wall models.

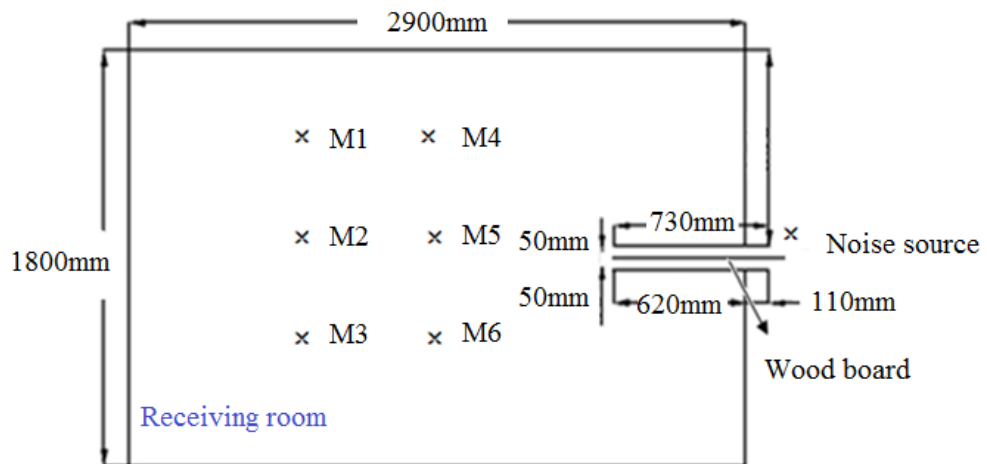


Figure 4- 3 Physical configurations and plan of the experimental set-up of the experiment.

Noise reduction between the control mode and the membrane absorber (Figure 4-4) in the source room and the receiving room shows in Figure 4-5.

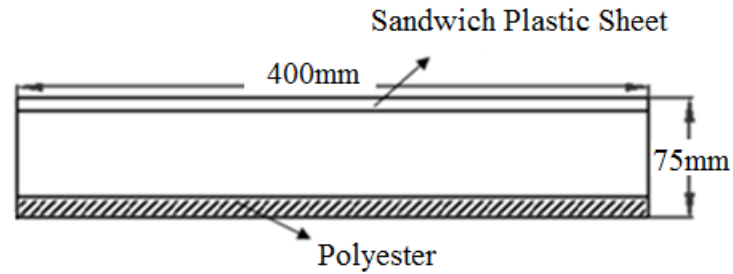


Figure 4- 4 Membrane absorber.

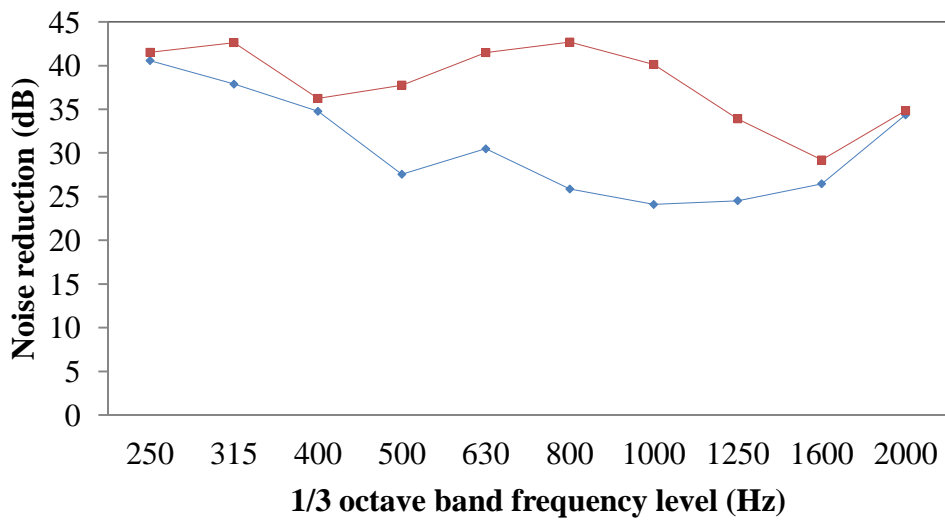


Figure 4- 5 Noise reduction between membrane absorber and control in source and receiving room. —◆— Control tests in two rooms; —■— tests with membrane absorbers in two rooms.

The performance becomes significant at frequency range from 400 Hz to 1.6 kHz.

The highest noise reduction achieves approximate 17 dB at frequency level of



800 Hz. However, noise reduction at a lower frequency level especially at 250 Hz to 400 Hz is irrelevant and also at 2 kHz, the sound attenuation is minimal. Best performance, therefore, occurs at frequency level range between 500 Hz to 1.25 kHz, the average noise reduction reaches 10 dB across the entire frequency range.

#### **4.2.2 Small-scale ventilation experiments**

In this experiment, airflow has tested with an electric blower with three grading. Grade 1 and Grade 3 of the electric fan uses. Grade 1 is of stronger wind, and Grade 3 is of weaker wind. As showed in Figure 4-6 and Figure 4-7, the blower locates 2m from the model.

Airflows measure in the room by using the Testo anemometer by placing the probe in the upper, middle and the bottom part of the duct with and without the wing wall of the mockup. To observe the effect of wing wall, airflow velocities at different angles ( $\theta = 0^\circ, 30^\circ, 45^\circ, 60^\circ, 90^\circ$ ) test for each mockup. It found that indoor ventilation can be achieved by adopting wing wall design.



Figure 4- 6 Experimental setups for airflow measurements.

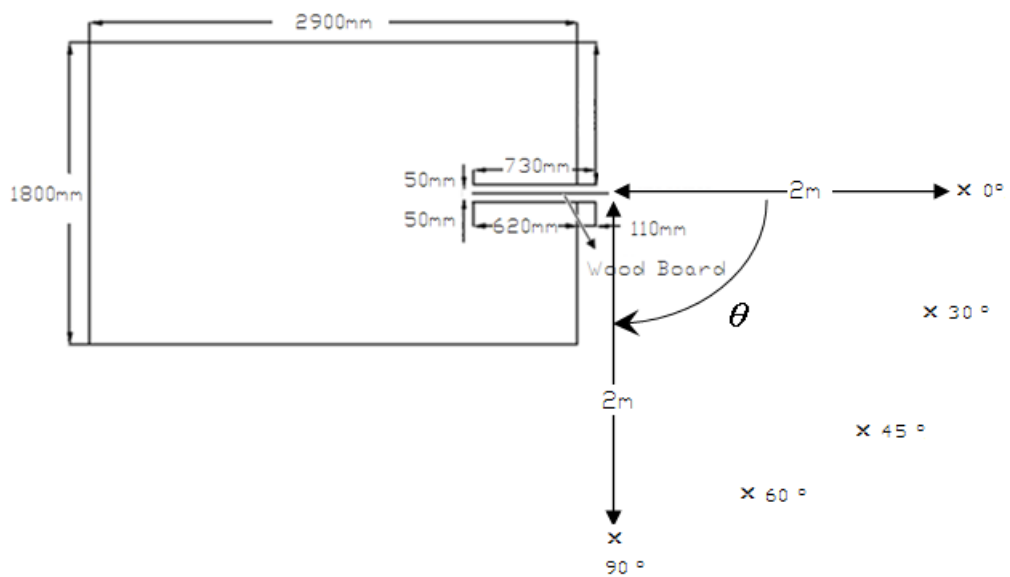


Figure 4- 7 Floor plans and layout configurations of the airflow measurements.

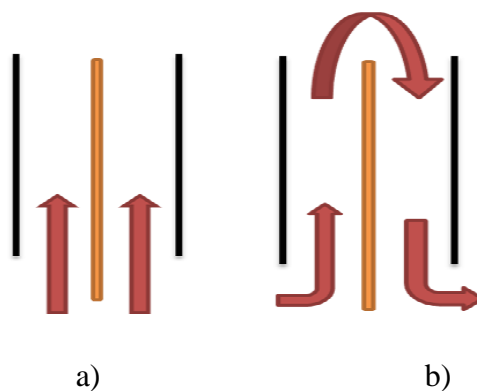


Figure 4- 8 a) Air flow directions in wood board wing wall mockup, at  $0^\circ$ ; b) Air flow direction in wood board wing wall mockup, at  $30^\circ$ ,  $45^\circ$ ,  $60^\circ$  and  $90^\circ$ .

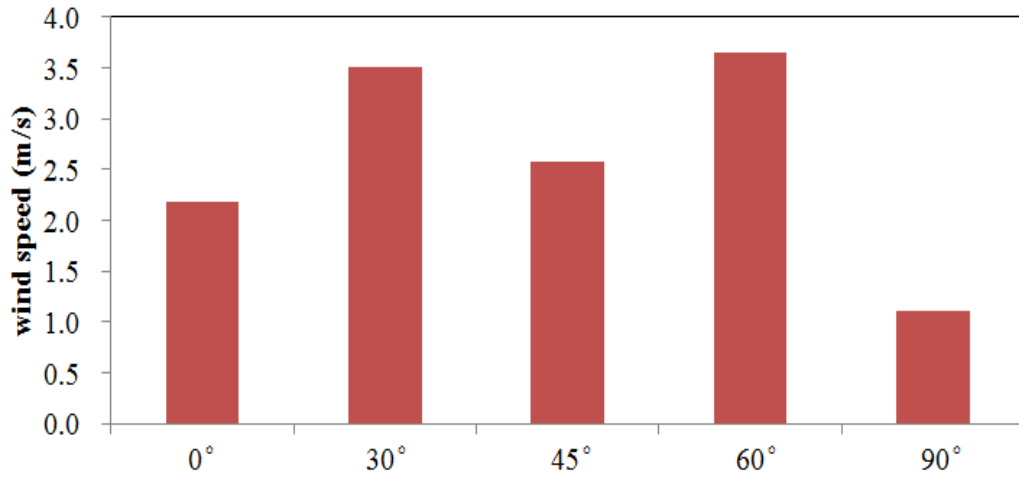


Figure 4- 9 Grade 1 wind at the duct with wing wall of designs.

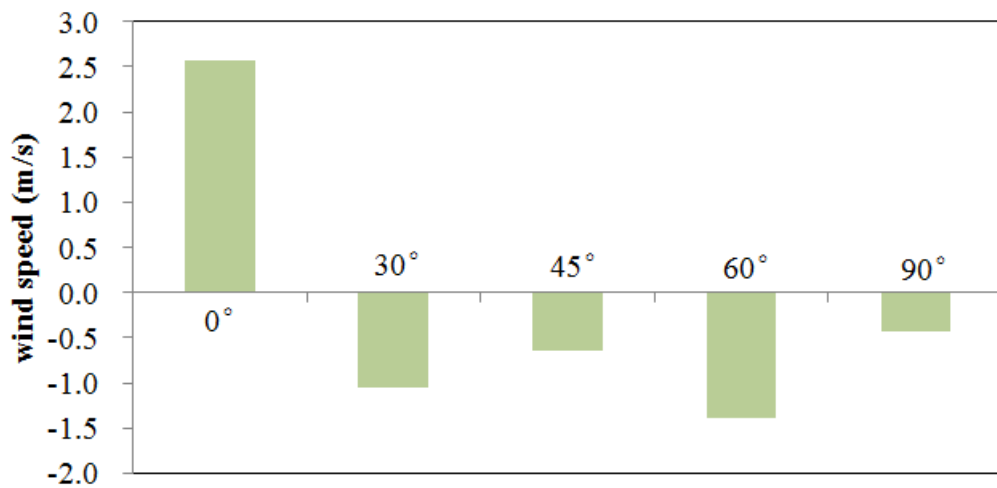


Figure 4- 10 Grade 1 wind at the duct without wing wall of designs.

Figure 4-9 summarized the wind speed, which went into the room when the electric fan was at Grade 1, which simulated strong wind condition. As showed in Figure 4-10, positive wind speed measured at electric fan located at 0° while

negative wind speed measured at 30 °, 45 °, 60 ° and 90 °. Destructive wind speed indicated that the wind was flowing out of the room via the duct.

When Grade 3 of the electric fan adopted the wind speed obtained was lower than that obtained at Grade 1 condition. The wind speeds at the duct with wing wall were averagely about 1.5m/s while the wind speeds were greater than 2m/s for Grade 1 condition.

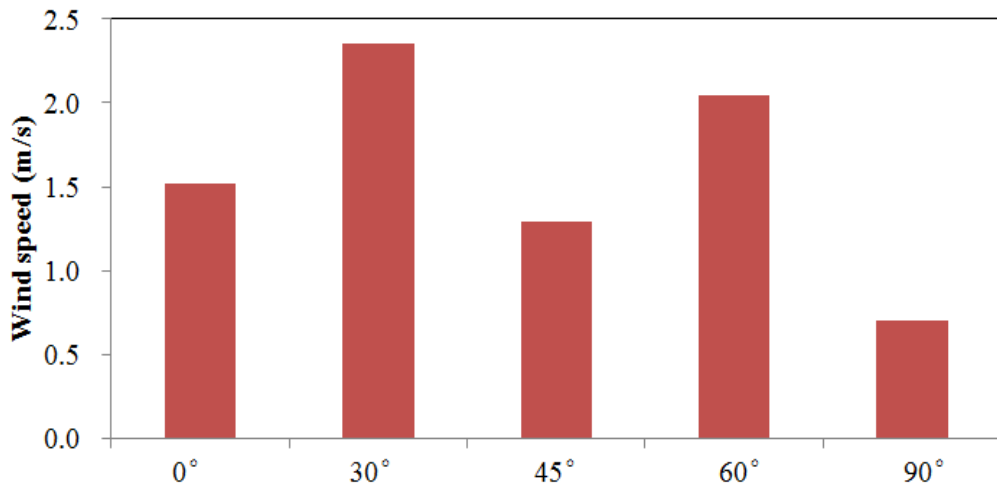


Figure 4- 11 Grade 3 wind at the duct with wing wall of designs.

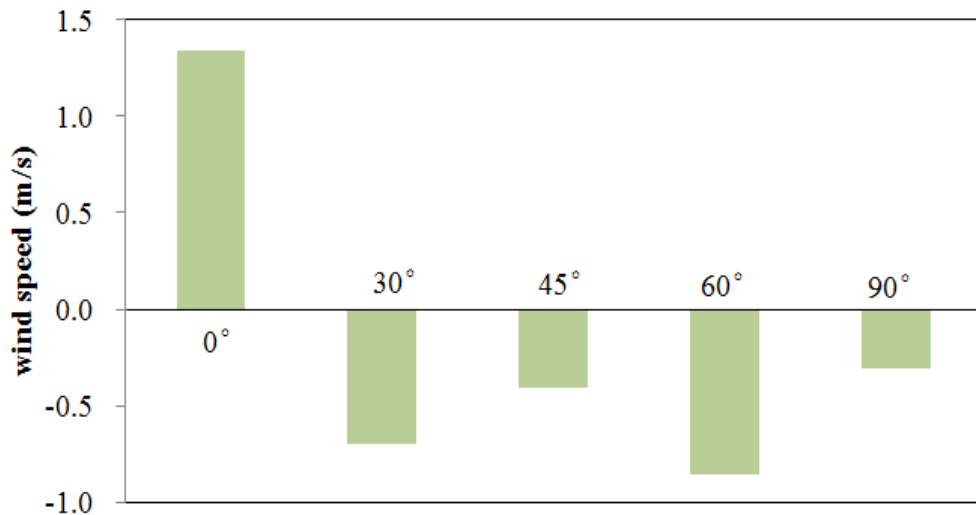


Figure 4- 12 Grade 3 wind at the duct without wing wall of designs.

By comparing 4-10 and Figure 4-12, it shows that the wind speeds measured at the duct without wing wall at Grade 3 conditions were slightly less than wind speeds at Grade 1 condition. This revealed that the incoming air affects the outflow of the air. Figure 4-9 and Figure 4-10 presented the data of freezing wind condition, which simulated autumn environment while Figure 4-11 and Figure 4-12 presented the data of poor wind condition, which simulated summer condition.

From the experiment, the observation showed that the gaseous exchange between the indoor and outdoor environment enhanced when the wind did not directly flow into the room. However, wind speed only measured in front of the duct.

Wing wall is an easily adopted feature that can be installed in the model room without massive amendment of the original design.

#### **4.2.3 Ventilation test for different types of dual-flow ventilated windows**

The experiments of ventilation have carried out through a 1: 10 scaled room with or without wing wall in the same layout configuration as showed in Figure 4-7 in different setups. Single side ventilation relates to the areas where there is the prevailing wind. In these regions, the air enters from its only entrance and passes through the building and at last leaves window, door or other exhausted segments. In aeronautical studies, the Reynolds number for the mockup and for the full-scale figure it represents should be the same. To satisfy this rule, a 1:10 mockup should be tested at wind velocities about 10 times greater than that of the prevailing winds, something not possible to accomplish. This scaled mockup simply uses a 15cm extended wood board from the opening to serve as a wing wall. Note that the area of the ventilated window was smaller in the actual area of a real open window, and the dimension and position of this ventilated window fixed during all experimental process.

Top view of each experiment set up and measurements clearly explain respectively in the present research. The wind direction along with the geometry of the wing wall performed for approaching air angles of  $45^\circ$ . The direction of dual-flow wing wall influenced the wind pressure distribution. Air flow rate on a given single ventilated room performed for different angles, which consisting of four cases (Figure 4-13): a) with a parallel wing wall; b) with a  $90^\circ$  wing wall (left side); c) without wing wall; and d) with a  $45^\circ$  wing wall (right-side).

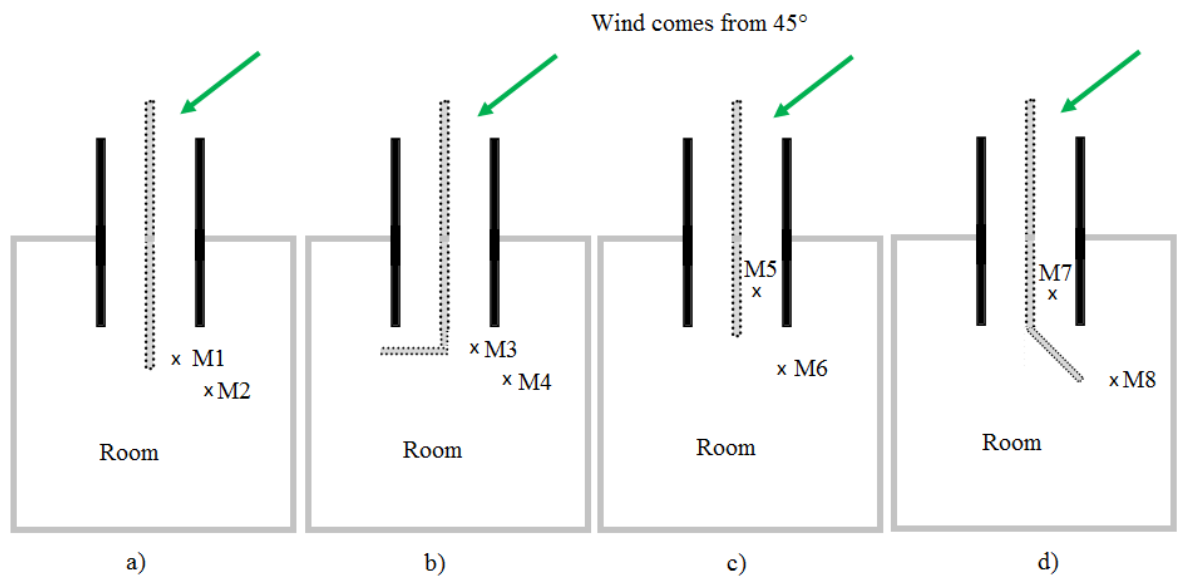


Figure 4- 13 Four different types of dual-flow ventilated windows. a) with a parallel wing wall; b) with a  $90^\circ$  wing wall (left side); c) without wing wall; and d) with a  $45^\circ$  wing wall (right-side).

All experimental tests carried out on a constant wind speed corresponding to 30 m/s and keeping energy conservation and acceptable indoor air quality in mind. The airflow rates for different angles present in Figure 4-14. Best performance in the duct happened at M7 at 2.1 m/s, which represent the airflow in the case (d) with a 45 ° wing wall (right-side). In case (b) with a 90 ° wing wall (left side) and (c) without wing wall, the wind velocity is relatively small comparing to the other two cases. It presented the wind velocity in the duct would not be increased without wing wall. Nevertheless, the air flow rate of all the four measurement points inside the duct is quite impressive comparing the measurement results of the four points in the room away from the duct in a short distance; hence the air flow velocity in any cases is negligible. The small-scale experimental mockup has used in this analysis using measuring techniques to estimate or predict ventilation performance with a scale of 1:10 of the room. The ventilated window in this test constructed in the laboratory attached to a scaled mockup of an actual room. There was no remedy made in the pressure measurements obtained with the configuration.



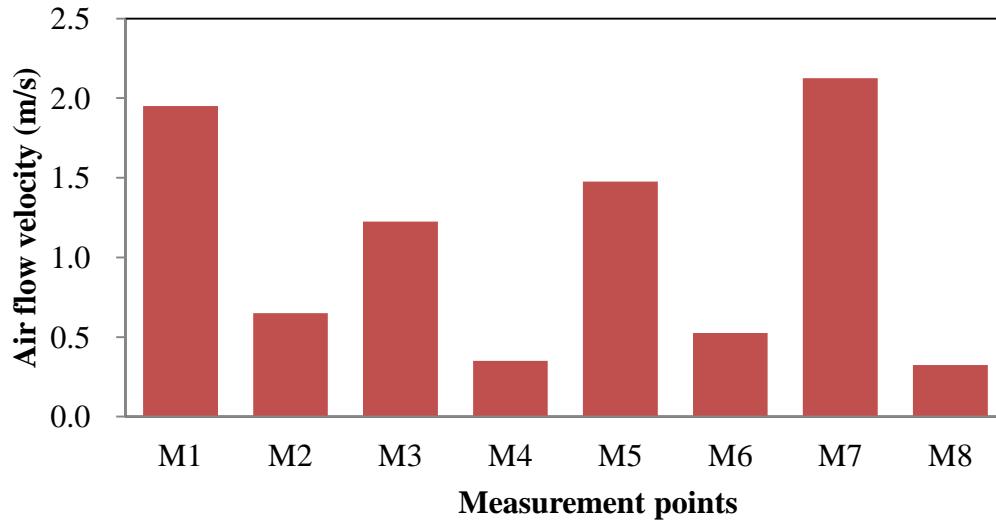


Figure 4- 14 Airflow speed for different angles in the four cases.

A blower used in the ventilation experiments making a mock wind-driven natural ventilation conditions. It may only show wind comes from certain directions. Prevailing wind direction often changes with the seasons and may change throughout the day. Wind speed usually varies daily and seasonally and typically dim at night in the absence of solar heating of the ground. However, this demonstration test could declare in some measure similarly to the real situation as many residential buildings in Hong Kong are siting closely to external obstructions to wind flow, the wind-driven natural ventilation may not as easily go through as it expects to be. Proper placement of wing wall can create positive and negative pressure zone thus allowing ventilation in rooms would be more weight. Conventional wing wall cannot improve ventilation in rooms with

openings on the leeward side only but can increase ventilation in rooms with openings only at the windward side.

#### **4.2.4 Single ventilation and cross ventilation performance in a wing wall design**

In the last experiment, there is a slight difference between the airflow rates of the dual-flow wing wall design with or without opening in the room; the effect of airflow velocity in single ventilation and cross ventilation environment is therefore additionally explored in the research. The ventilation test has divided into two cases: with and without panel absorber in the duct opening on each side of the wood board wing wall. The result in Figure 4-15 indicated the wind velocity with and without panel absorbers in a single-ventilated or a cross-ventilated room. However, the difference between the velocities is insignificant.

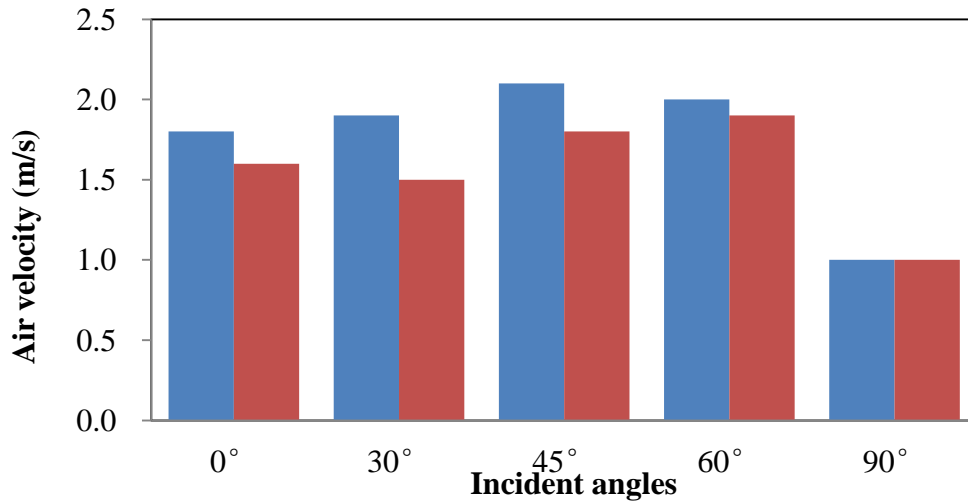


Figure 4- 15 Air velocities in a single-ventilated/ cross-ventilated room; ■ Air velocity in the single-ventilated room; ■ Air velocity in the cross-ventilated room.

The dual-airflow window could be used to conserve energy and improve indoor air quality in buildings because it works like a heat exchanger and can introduce outside air into buildings; supplying fresh outdoor air to the indoors and can conserve energy by recovering energy from the exhaust flow to the supply airflow. When the panel absorbers inserted in the ventilated duct, the duct area would diminish to half of the original size; thus there is no comparison should be made between the wind velocity merge with or without panel absorbers.

### 4.3 SUMMARY

For the acoustics aspect, conventional wing wall without any absorbers can achieve the maximum noise reduction at 17 dB at frequency level of 800 Hz. The transmission loss is significant between 400 Hz to 1.6 kHz across the entire band. However, the transmission loss is not perfect at a lower frequency level.

For the ventilation aspect, the ventilation rate has improved at the outlet compared with the inlet. Wind-driven natural ventilation is an effective way to preserve the luxurious and healthy indoor environment. The conventional wing wall design can achieve remarkably well in single-sided ventilation for this room configuration in the mockup experiments.

Single-sided ventilation incorporated with wing walls could significantly improve the interior air circulation compared with that without wing walls. Indoor ventilation can be achieved at each different angle (at 0°, 30°, 45°, 60°, 90°) measured in the test when the wood board serves as a wing wall.

Conventional windows need to be fully closed when the noise level is elevated outdoor; no natural wind can enter the indoor. The performance of dual flow is better than the existing conventional single-ventilated window thus has a

significant potential for conserving energy and improving air quality. Therefore, especially during summer time, the performance of natural ventilation to control indoor air quality and temperature to cold buildings by increasing indoor air movements can be further enhanced.

The limitation of the ventilation examination may be due to the simulated wind ventilation condition. To some degree, the experiment's setup provides ideal winds directions and wind speeds only. Future experiments need to be considered carefully. We will also examine how wing walls could help improve cross ventilation at each different prevailing wind direction to the windows. The effectiveness of the wing wall and the movement patterns of air movements will be examined in this research.

Wind-driven ventilation is a process that air movement through spaces due to the pressure difference flowing from high pressure to low pressure. The purpose for buildings to have proper ventilation is to provide clear and fresh air for occupants. Ventilation can help to maintain thermal comfort in the mockup room. In this test, wing wall uses to achieve natural ventilation. Natural ventilation achieves owing

to the pressure difference on either side of the wings, which improve air flowing into the model room and flowing out the other side of the wing.

Further studies should be focused on the indoor airflow. However, it does not specify in this research. The investigation of indoor airflow can help to analyze how effective the wing wall design facilities of the gaseous exchange between indoor and outdoor environment.

# **CHAPTER 5**

## **NOISE CONTROL OF MULTIPLE QUARTER-WAVE RESONATORS**

### **5.1 INTRODUCTION**

In designing a natural ventilation system, there is always a conflict between ventilation and acoustic requirements. Larger openings always expect in enhancing the effectiveness of natural ventilation; however, at the same time large openings may also produce higher noise levels.

It has known that low frequencies enter buildings can affect human comfort by openings such as windows. Using of absorbing materials is always a hot topic in building design. Gao and Lee (2011) found that admirable natural ventilation performance has to be controlled strictly by opening positions. Yin et al. (2010) considered the counteraction between wind and heat is one of the important reasons for affecting natural ventilation, but they did not consider pollution factor like noise in the study.

Field et al. (1996) had firstly investigated the use of MQWR system in noise attenuation. The result indicated the effectiveness of the noise attenuation of the multiple resonator system is feasible once the resonator system in normal position. Lower costs compared to sound insulation and minimal maintenance requirements. However, the efficiency of an in-duct active noise control system employed to resist an external sound source is unknown.

## **5.2 MODIFIED DESIGN OF VENTILATED WINDOW**

The MQWR system made of plexi-glass plastic sheet which replaces the traditional fibrous acoustic materials. The advantages of using plastic materials include: 1) it can replace traditional absorptive materials so it can improve the durability; 2) it can avoid small particle emissions, and 3) it can avoid poisonous gas due to fire. It requires little maintenance and allows air to pass straightly without harming human health but also with particularly significant noise screening effects. A combination of ventilated window with wing wall is a new concept contrasting with traditional open windows or wing wall.



Therefore, the modified ventilated window has consisted of two parts: 1) MQWR systems (showed in Figure 5-1); and 2) wing wall connected with ventilated window. The system provides the sound barrier screening effects and improves the quality and quantity of fresh air flows through the system.

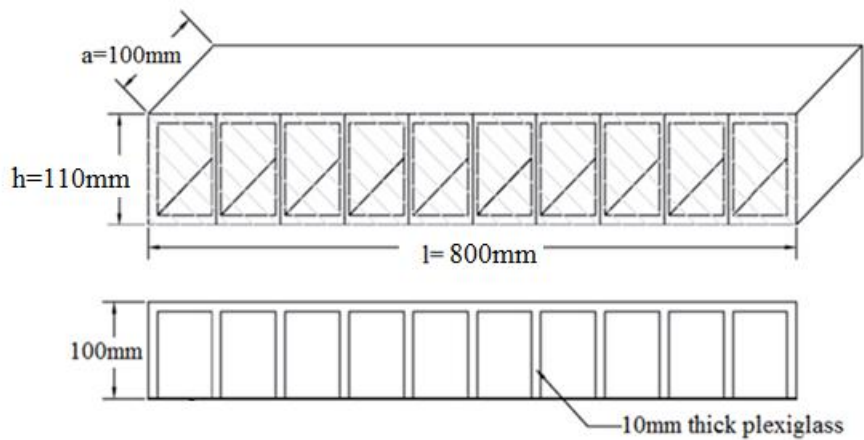


Figure 5- 1 3D-view and top-view of the multiple quarter-wave resonators.

Many studies have shown the effectiveness of noise control in enclosed rooms and other environments for cancelling engine noise and low frequency noise in general. However, there is no research on how both acoustic comfort and ventilation can be achieved. This study also asks whether there is any connection between transmission loss and ventilation; to study whether it is possible to make a balance between acoustic energy and ventilation.

### 5.3 THE TRANSMISSION LOSS OF QUARTER-WAVE RESONATORS

The resonant frequencies ( $f_n$ ) of quarter wave absorber can be clearly predicted from:

$$f_n = c(2n-1)/4d, \text{ where } n=0,1,2,3\dots \dots\dots\dots\dots\dots(5-1)$$

The resonance frequency increases with smaller depth of cavity  $d$ . The transmission loss corresponds to the effect of the quarter-wave resonator can be defined as the following equation:

$$TL = 10 \log \left( 1 + \frac{S_{sb}^2}{4S^2} \left( \frac{1}{r^2 + \cot^2 kd} \right) \right) \quad (5-2)$$

The transmission loss increases with larger length area ratio of  $\frac{S_{sb}}{S}$ , absorption  $\alpha$  and smaller thickness of the tube  $h$  (Figure 5-1). Sound attenuation of the new ventilated window design improved significantly by combining flexible absorber with or without quarter-wave resonators. Four types of combinations also used for the experimental measurements. Figure 5-2 to Figure 5-4 present different types of silencers used in this study.

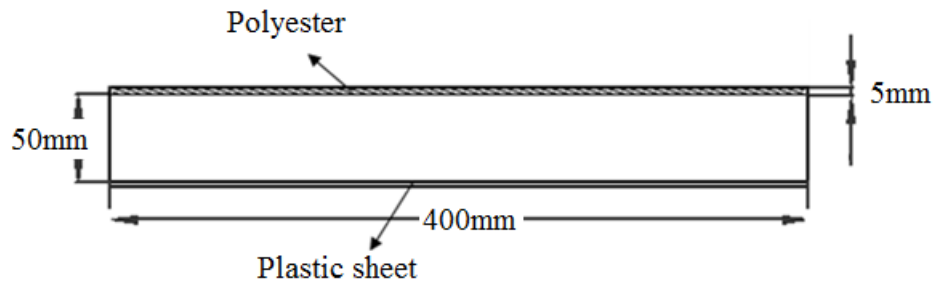


Figure 5- 2 Polyester panel absorber.

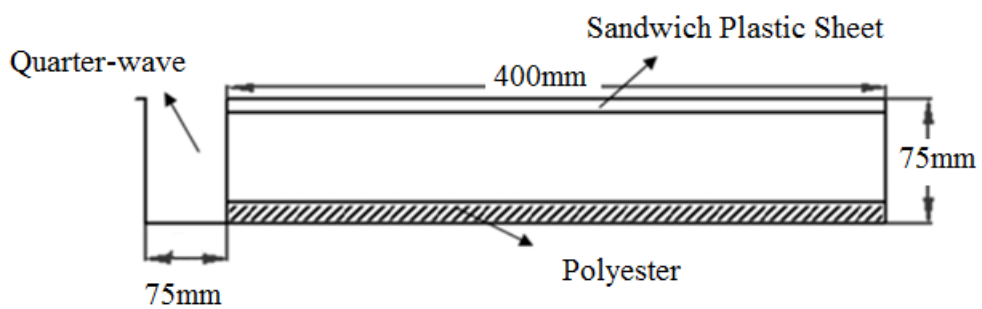


Figure 5- 3 Membrane absorber with quarter-wave resonators.

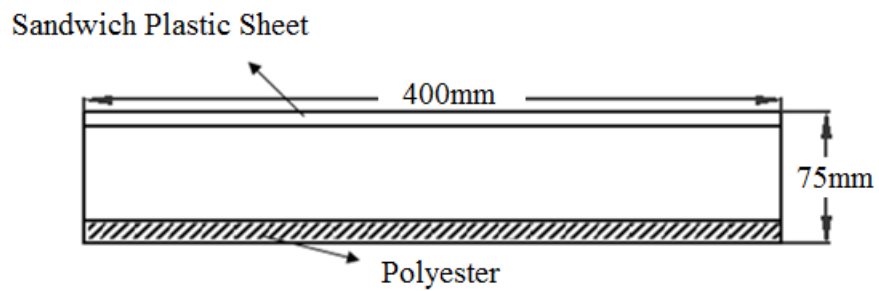


Figure 5- 4 Membrane absorber.

Transmission loss measured to examine and evaluate the transmission loss of MQWRs with or without the duct in the lab. A transparent duct with an opening area of 4mm x 10mm connected with the opening in the wall; a loudspeaker put

in front of the opening at the source room and used as a noise produced in this model test. One microphone (B&K4189) positioned at the source room, and the other one (B&K4189A21) placed at either in the duct or the receiving room. Figure 5-5 illustrated the configurations of acoustic measurements. a) Back side of the duct; b) front view of the transparent duct; c) duct combined with MQWRs.



a)

b)



c)

Figure 5- 5 a) Back side of the duct; b) front view of the transparent duct; c) duct with MQWRs.

Figure 5-6 pointed up the positions of the microphone at the receivers' room; a) showed the microphone put in the duct, and b) showed the microphone put in the room.



Figure 5- 6 Noise measurements a) in the duct and; b) noise measurement in the room.

Figure 5-7 shows the comparative results of tests carried in two rooms; duct only and duct with quarter-wave resonators. Muffler effect is visible between the coupled rooms for the cases. Duct with quarter-wave resonators performs better sound attenuation comparing with duct only test in two rooms; especially at a higher frequency level higher than approximately at the frequency level of 600 Hz.

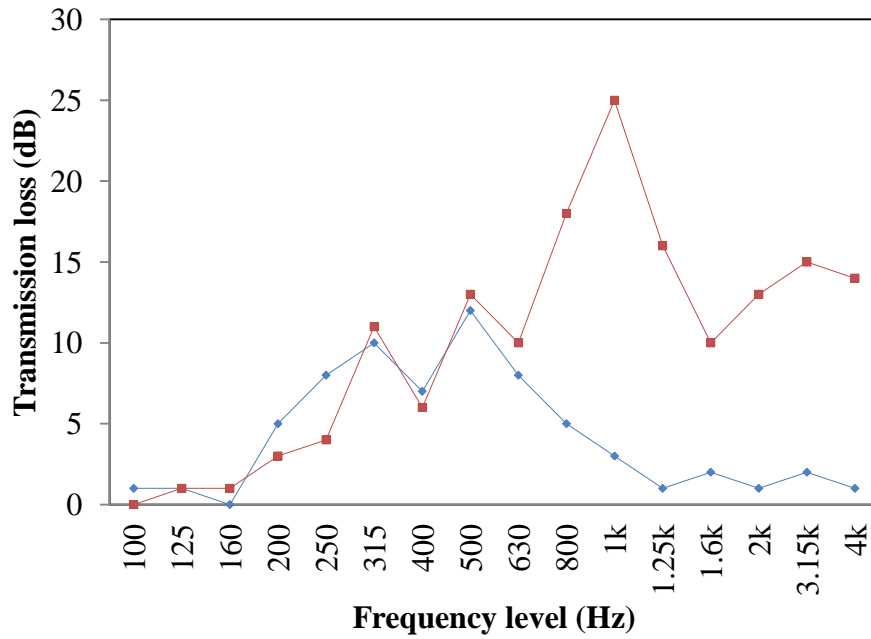


Figure 5- 7 Tests carried in two rooms: duct only and duct with quarter-wave resonators; —●— duct only- test in two rooms; —■— duct & quarter- test in two rooms.

From the experimental result, we obtained the highest transmission loss of 25 dB at frequency level of 1 kHz. In theory, the transmission loss duct with quarter-wave resonators test can be calculated from the equation of

$$TL = NR - 10 \log \frac{A}{S} \tag{5-3}$$

Where,

$A$  represents the area of the room

$S$  represents the area of the duct

The test result met the entire agreement with theory.

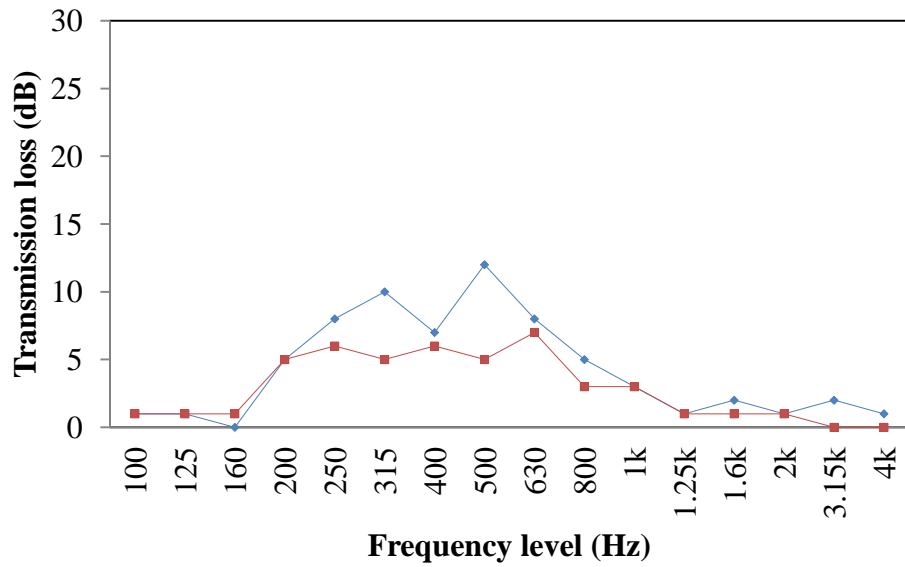


Figure 5- 8 Experimental results of duct only test in rooms and duct only test in the tube; —●— duct only- test in two rooms; —■— duct only- test in tube.

Figure 5-8 showed duct only test in two rooms and duct only test in the tube. Muffler effect is noticeable in the duct only test in two rooms between the frequency levels at around 200 to 800 Hz. However, duct only does not produce high satisfaction in the experiment. Highest transmission loss has detected at 12 dB at frequency level of 500 Hz in the duct only test in two rooms. Besides, from the calculation, the absorption coefficient  $\alpha$  is 0.2, therefore, the maximum transmission loss of duct only test in the tube, transmission loss is 7 dB.

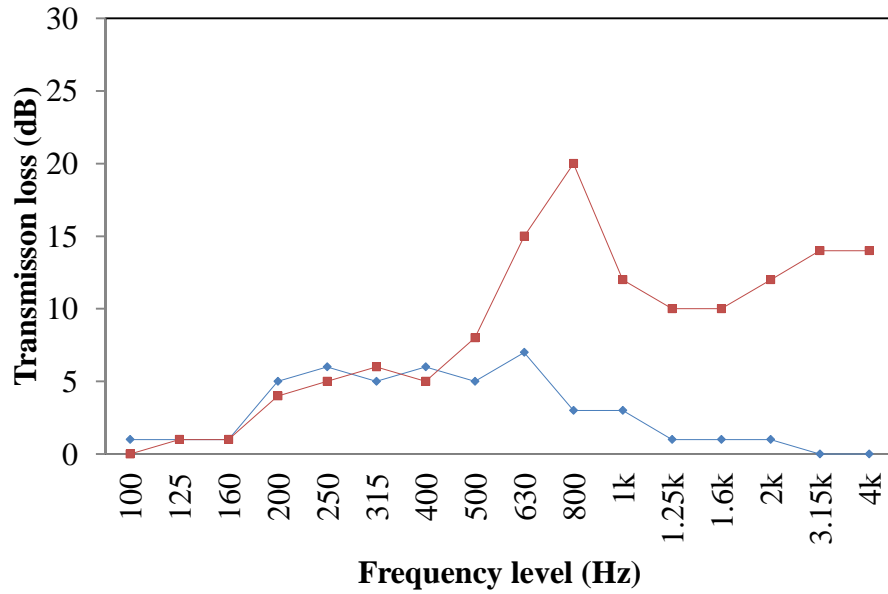


Figure 5- 9 Experimental comparisons between duct only test and duct with quarter-wave resonators in the tube; —♦— duct only- test in tube; —■— duct & quarter- test in the tube.

Figure 5-9 showed duct only test and duct with quarter-wave resonators in the tube. There is no muffler effect presenting in the duct only test in the tube. Therefore, duct in the test tube can also be calculated. From calculation, we obtain the absorption coefficient  $\alpha=0.2$ . Therefore, the transmission loss in duct only in the tube testing can be calculated in the equation of transmission loss is 7 dB.



Nevertheless, muffler effect can be examined by the test of the duct with quarter-wave resonators. Figure 5-10 presents the experimental comparisons between duct only test and duct with quarter-wave resonators in the tube.

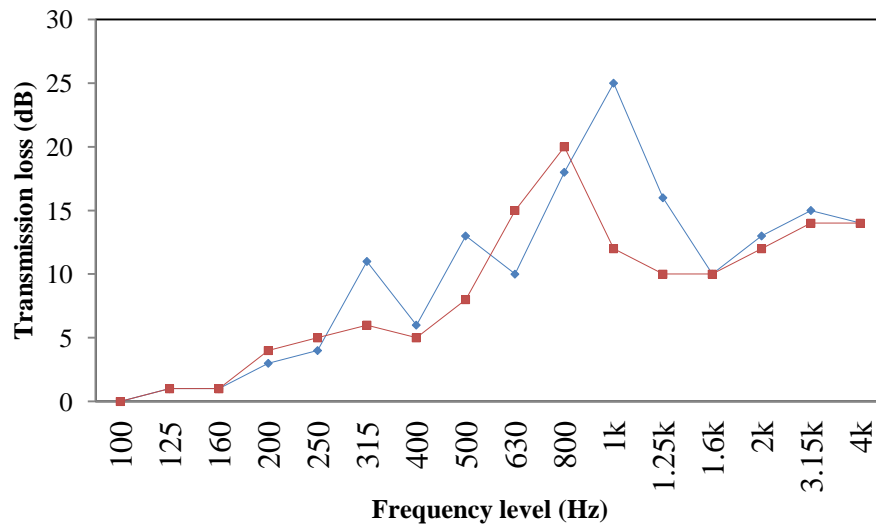


Figure 5- 10 Experimental comparisons between duct only test and duct with quarter-wave resonators in the tube; —◆— duct & quarter- test in two rooms; —■— duct & quarter- test in tube.

The frequency level can be calculated from:

$$C = \lambda f, \tag{5-4}$$

Where,

$C$  represents the velocity

$\lambda$  represents the wavelength

$f$  represents the frequency level

If the duct installed with quarter-wave resonators, the wavelength is 0.09m.

Therefore, the frequency,  $f = \frac{340}{0.09 \times 4} = 944\text{Hz}$ . The highest transmission loss can be found at frequency level of 944Hz.

The muffler effect is more significant in the test in two rooms rather than in the tube from shown in this figure.

$$C = \lambda f, \text{ therefore the frequency, } f = \frac{340}{0.8 \times 2} = 212.5 \text{ kHz.}$$

Thus transmission losses are high at frequency level of around 320Hz, 450Hz, and 900 Hz in theory. Further, the Transmission loss of duct with quarter-wave resonators test can be calculated from the equation of:

$$\text{Noise Reduction (NR)} = TL + 10 \log \frac{A}{S} \quad (5-5)$$

Where,

A represents the area of the room,  $A = 2 \times 2 \times 3 = 12\text{m}^2$ ;

S represents the area of the duct,  $S = 0.04 \times 0.1 = 0.004\text{m}^2$ ;

Therefore,  $TL = 58 \text{ dB (experimental measurement)} - 10 \log \frac{12}{0.004} = 58\text{dB} - 35\text{dB} = 23\text{dB}$

Figure 5-11 showed combined ducts with quarter-wave resonators test in tube both in the experiment and in theory. The experimental result shows that the

maximum acoustic reduction can reach 20 dB and the average transmission loss can be above 10 dB at frequency level between 630 Hz to 4 kHz. The performance of duct with quarter-wave resonator in the tube test is satisfactory. From imperative tube measurement, we obtain the absorption coefficient  $\alpha=0.3$ . Therefore in theory, the TL= 12 dB in the duct and quarter-wave resonators in the tube experiment can be calculated.

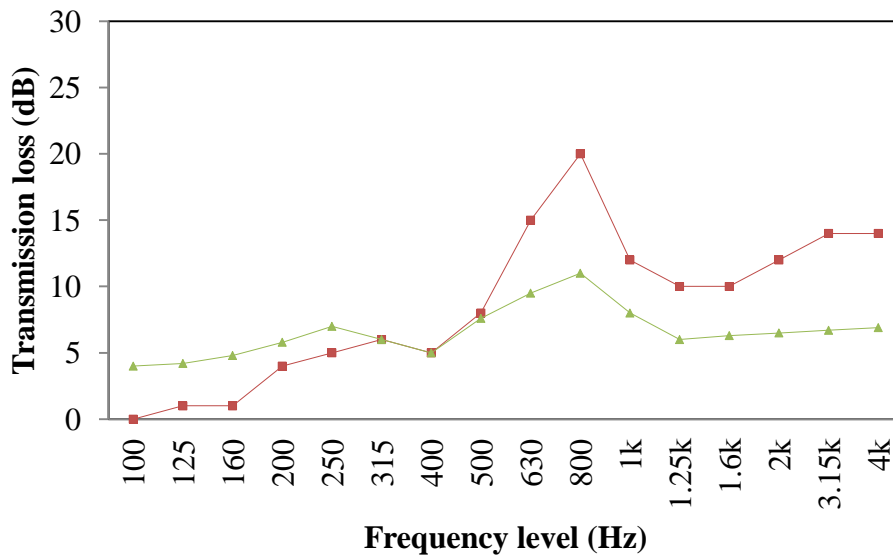


Figure 5- 11 Experimental comparisons between duct with quarter-wave resonators test in tube both in the experiment and in theory; —■— duct & quarter-test in tube experiment; —▲— duct & quarter- test in tube theory.

Figure 5-12 showed duct only test in both of the experiment and theory. However, the experiment result did not show a similar transmission loss performance comparing it is in theory. In theory, the transmission loss is 7 dB in the duct test

in the tube can get from calculations. The dips in the transmission loss near 315 Hz, 500 Hz and 800 Hz are due to the formation of standing wave along the length of the testing tube.

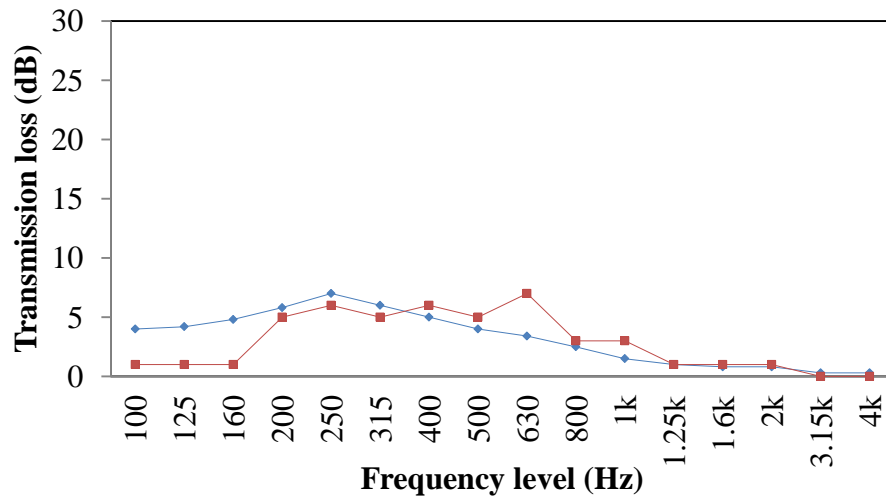


Figure 5- 12 Experimental comparisons between duct only test in both of the experiment and theory; —♦— duct only- test in tube experiment; —■— duct only- test in tube theory.

## 5.4 ACOUSTIC PERFORMANCE OF SILENCER FOR VENTILATED

### WINDOW MEASURED IN DUCT

#### 5.4.1 Formula of flexible absorber

The surfaces of the tube excite to be vibrated at resonances frequencies to dissipate energy when sound energy transmits in the tube of silencer. This terms as a flexible absorber. The transmission loss corresponds to flexible absorber effect can be predicted by

$$TL=10\log\left(\frac{2\alpha l}{h}\right)(dB) \quad (5-4)$$

The transmission loss increases with a large length of tube  $l$ , absorption coefficient  $\alpha$  and smaller thickness of the tube  $h$  (Figure 5-1); details list in Appendix II (Huang, 1999; Frommhold et al., 1994; Wang et al., 2006).

When sound energy comes across MQWRs, sound energy can be absorbed from reflection due to the impedance change at the outlet of each quarter resonator in resonant frequencies.

#### **5.4.2 Specimen and measurement setup**

Three types of full-scale silencer models for ventilated window construct to investigate their sound transmission loss in the duct. The cross-sectional views of

silencers presented in Figure 5-13. They made of plexi-glass plastic sheet with a thickness of 5mm. The first one is a conventional silencer with polyester in cavities. The second one is a designed silencer with multiple quarter-wave resonators in cavities. The third one is a tube with cavities closed with transparent plastic membrane.

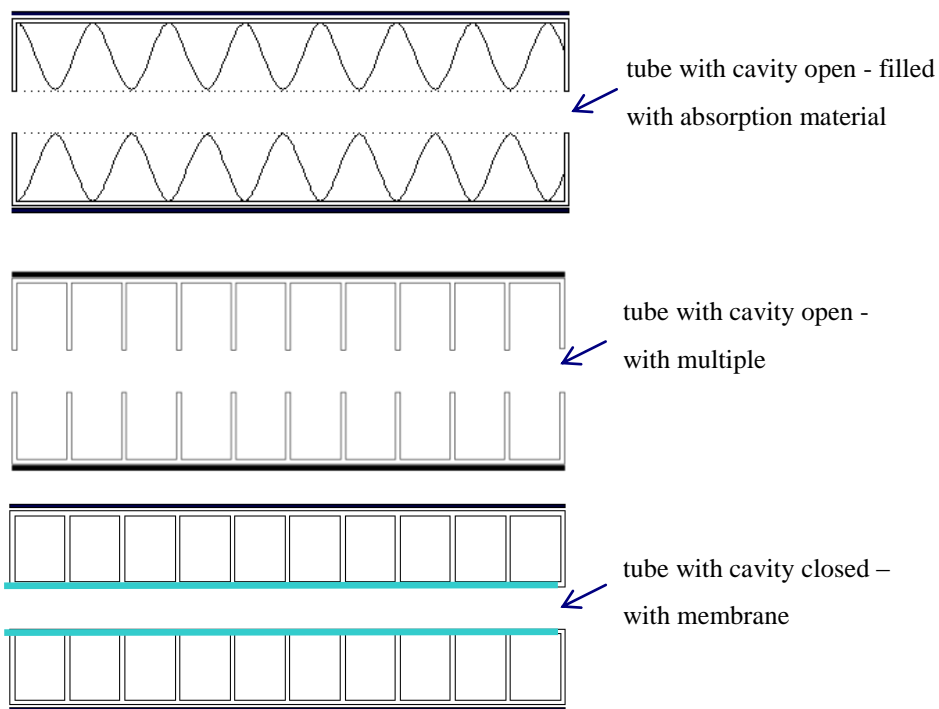


Figure 5-13 Multiple quarter-wave resonators installed inside the duct (Wang et al, 2014).

Figure 5-14 illustrates the noise reduction measurement set-up of the silencer in duct. The test methods in acoustics are in accordance with British Standard (ISO 7235: 2003). A loudspeaker placed on one side and fed with white noise in 1/3

octave bands. One microphone sets at the source side (B&K 4189), and the other microphone at the receiving side (B&K 4189), measures the noise levels in both sides at four positions halfway between the duct and wall and centerline.

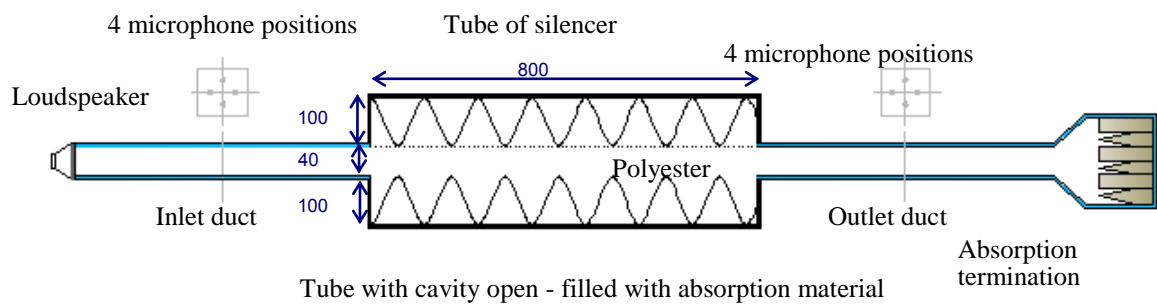


Figure 5- 14 Transmission loss measurement setup on silencer (for ventilated window) in tube (all dimensions in mm) (Wang et al, 2014).

The sound pressure levels measured in 1/3 octave band frequencies from 100 Hz to 4 kHz. The transmission loss in the duct can be determined by noise reduction.

$NR = L_1 - L_2$ .  $L_1$  and  $L_2$  are the average sound pressure levels in the source side and receiving side, respectively. The noise reduction is equals to transmission loss in this case because of the absorption termination (Wang et al, 2014).

### 5.4.3 Transmission loss results measured in duct

The results of transmission loss for the three types of ventilated silencers present in Figure 5-15. The vibration of the plate surface in the silencer can dissipate some of energy at resonant frequencies; this terms as flexible absorber. The dominate energy dissipation for the silencer with cavity closed with membrane should be due to the effect of flexible absorber of the tube. Silencer with cavity closed with membrane possesses the transmission loss of 3 dB to 7 dB in the frequency range of 100 Hz to 630 Hz bands. (Figure 5-15). Prediction of transmission loss agrees well with experimental results (Figure 5-16).

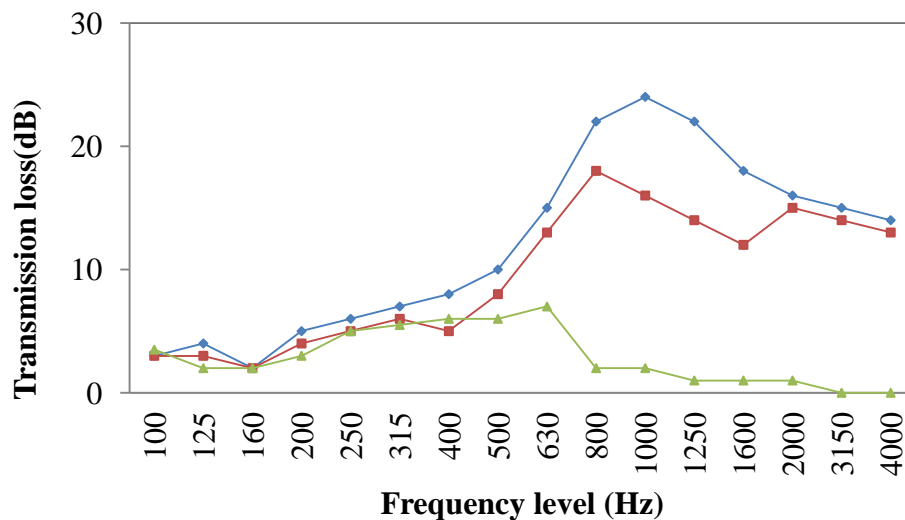




Figure 5-15 Transmission loss measurement results measured in duct for three types of silencer (for ventilated window); — tube with cavity open - filled



with absorption material;  tube with cavity open - with multiple quarter-wave resonators;  tube with cavity closed with membrane.

The energy dissipation for silencer with multiple quarter-wave resonators corresponds to both flexible absorber and quarter-wave absorber effect. The transmission loss below 800 Hz bands is similar to the silencer with membrane; since both of them have the same effect of flexible absorber. The higher transmission loss at the frequency above 630 Hz band corresponds to muffler effect, especially at 800 Hz and 2 kHz bands (Figure 5-15). This agrees with the first two quarter-wave resonant frequencies are 850 Hz, 2550 Hz, where the cavity depth is 0.1m. The additional transmission loss at 1 kHz may be due to the standing wave effect in the tube.

The energy dissipation for silencer with polyester corresponds to both flexible absorber and porous absorption effect. Again, the transmission loss in the low frequency region below 800 Hz bands is similar to the other two silencers owing to the same effect of flexible absorber (Figure 5-15). The higher transmission loss at the frequency above 400 Hz bands corresponds to porous absorption effect since polyester is usually effective in the higher frequency range. Parallel

performance of noise reduction can be achieved by silencer with quarter-wave resonators and silencer with porous material. Therefore, quarter-wave resonators can be an option to replace absorption material as it requires little maintenance, avoids the small particle emission and even toxic gas in the fire (Wang et al, 2014).

#### **5.4.4 Acoustic performance of ventilated silencer in a room**

A practical application of ventilated silencer installs on building ventilation openings to allow the natural ventilation and reduce the noise radiation from outside. Three types of silencers installed into building openings to analyze their practical application for noise reduction.

Figure 5-16 illustrates the transmission loss measurement set-up of silencers in building opening. A loudspeaker placed on the source side and fed with white noise in 1/3 octave bands. One microphone (M1) set at the source side (B&K 4189), and the other one (M2) at the receiving side (B&K 4189), measuring the noise levels in both sides at six positions. The sound pressure levels measured in 1/3 octave band frequencies from 100 Hz to 4 kHz.

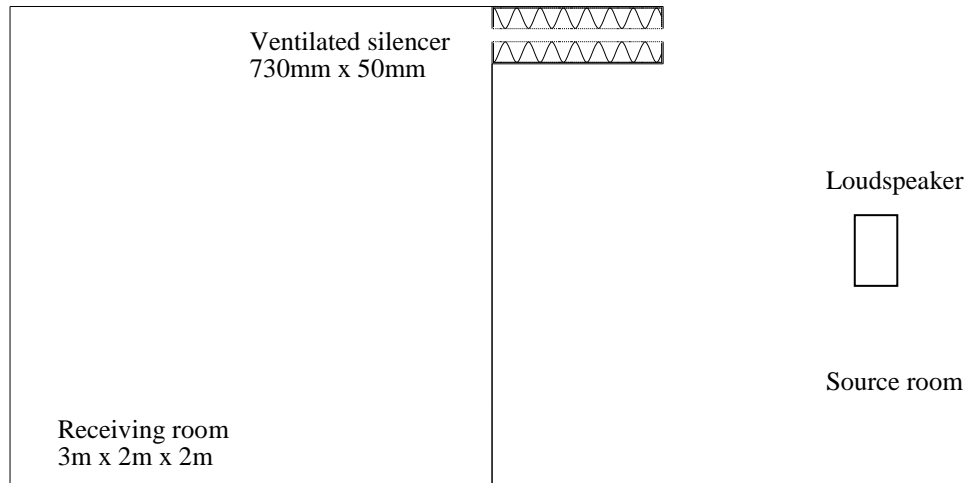


Figure 5-16 Noise measurement setup on ventilated silencer in room.

The  $NR = L_1 - L_2$ .  $L_1$  and  $L_2$  are the average sound pressure levels in the source side and receiving side, respectively. The room with the dimensions of 2m (L) X 3m (W) X 2m (H) covered with absorption material with known absorption coefficient as showed in Table 2. Thus, the transmission loss of the ventilated silencer can be calculated from the equation of

$$NR = TL + 10 \log \frac{A}{S} \quad (5-5)$$

The results of transmission loss in room calculated from the experimental noise reduction results presented in Figure 5-17. Therefore, quarter-wave resonators can be an option to reduce the noise in residential building environment. This can avoid the particle emission and toxic gas in the fire of porous material.

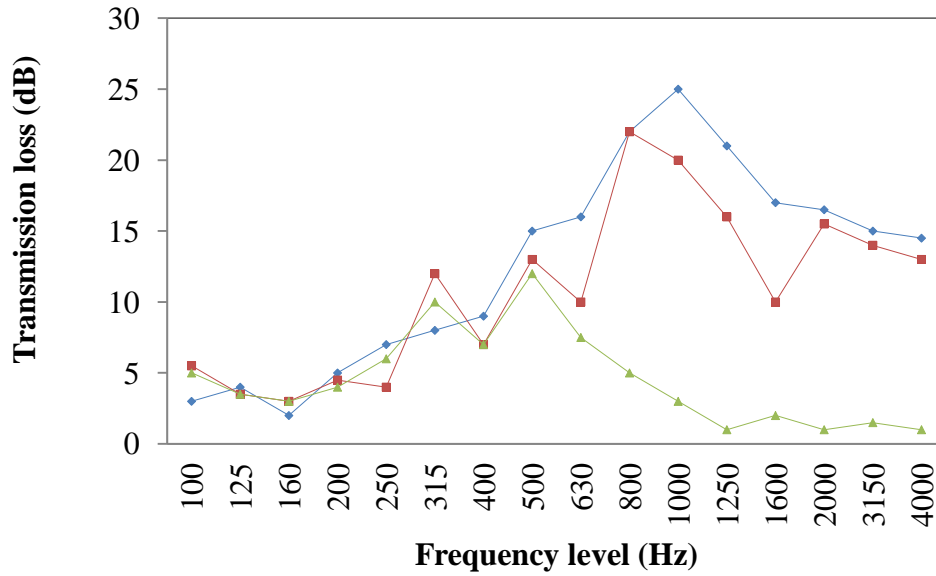


Figure 5-17 Transmission loss measurement results measured in two rooms for three types of silencer (for ventilated window); — tube with cavity open - filled with absorption material; — tube with cavity open - with multiple quarter-wave resonators; — tube with cavity closed with membrane.

## 5.5 FULL-SCALE MOCKUP EXPERIMENTS IN FO TAN

Mockup experiments were also conducted in this research. Layout of configuration of the experiment is presented in Figure 5-18. Microphone Type B&K#4189 and Type B&K #4189A21 have been used in the source room and receiving room respectively. The configuration of ventilated window is shown in Figure 5-19. One set of ventilated duct is at each side of the window glass. It

consists of sixteen small ventilated duct as shown in the graph. The dimension of each small ventilated duct is 150mm x 150mm x 400mm.

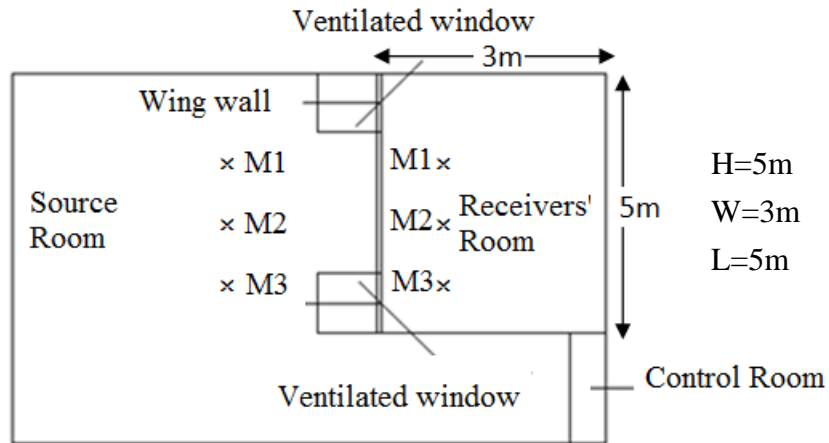


Figure 5- 18 Physical configurations of the acoustic test; Receiving room: 3m (W) x 5m (L) x 5m (H).

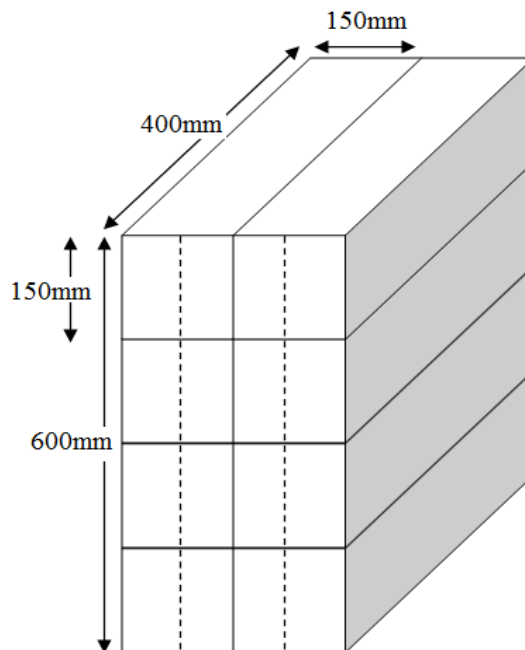


Figure 5- 19 Configuration of ventilated window.

An acoustic driver radiating white noise over the frequency range 20 Hz to 20 kHz was used as the source of noise constantly in this scaled mockup experiment. Six different points have been measured at the receiving room in each case. Three measurement points (M1, M2 and M3; each repeat twice at different heights) have been chosen at each side in the source room and the receiving room. Ventilated windows are distributed in the two sides on both of the left and right side of the lighting glass window (non-openable). Membrane absorbers are put into both sides of the ventilated windows.

Figure 5-20 shows the full-scale mockup of the experimental design; a) Back side view of the design; b) Front side view of the design; c) Ventilated duct of the wing wall design and the membrane absorbers in the ventilated duct. A large amount of absorptive wedges are placed in the receiving room, which can create more reliable outdoor testing environment regarding to simulate the testing of traffic noise.



a)



b)



c)

Figure 5- 20 a) Back side view of the design; b) Front side view of the design; c)  
Ventilated duct of the wing wall design and the membrane absorbers in the

ventilated duct.

Five sets of experiment had been accomplished to examine the transmission loss of different combinations and absorption materials, these include: 1) Quarter-wave resonator with membrane absorbers; 2) Membrane absorbers; 3) Polyester; 4) Quarter-wave resonator and 5) Control test with no absorbers in the duct.

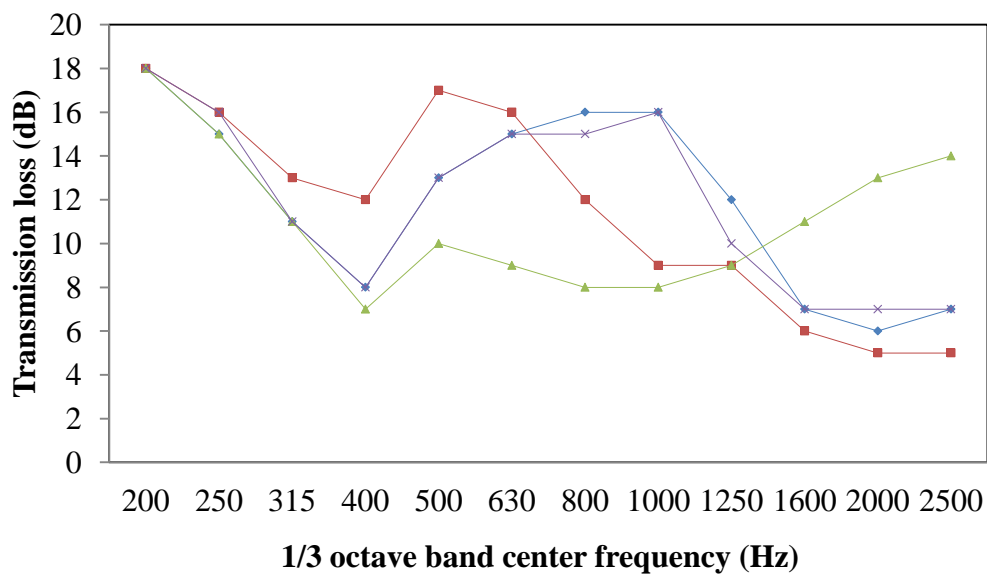


Figure 5- 21 Transmission loss in the full-scale mockup experiment; —◆— quarter and membrane; —■— membrane; —▲— polyester; —×— quarter-wave.

The results of this full-scale mockup experiment are presented in Figure 5-21. Quarter-wave resonators with membrane absorber and quarter-wave absorber



have similar noise attenuation across the entire 1/3 octave band. Their transmission loss meets the same high level with polyester at a frequency range from 200 Hz to around 315 Hz but relatively low noise attenuation after 1.6 kHz. Polyester does not perform well at lower frequency level, but it becomes much better than the other three types at higher frequency level above 1.6 kHz. Membrane absorber has the greatest performance of transmission loss at low frequency level below 630 Hz but fallen considerably afterwards. Polyester has the best performance at a higher frequency level but at low frequency level, its transmission loss performance is the worst comparing with the other three presentations. For lower frequency level from 200 Hz to 630 Hz, no doubt, membrane absorbers have the most significant transmission loss.

Clearly, measurements obtained from a full-scale mockup experiment are the most realistic and the data obtained is more reliable. Such detailed flow information cannot be able to be obtained with analytical and empirical models. However, the full-scale mockup experiment would be much more expensive and took longer time to complete.

According to the previous literature review, the performance of the wing wall in some measure has been proven having an efficient function in enhancing the

effectiveness of natural ventilation, especially at specific opening conditions. However, external wind speed in Hong Kong is unevenly distributed all year around especially in summer time when sometimes there is no wind at all whereas sometimes typhoons appear with extreme high wind velocity. Nevertheless, based on the recent studies, wing wall is still a single functional design, as it can only induce fresh air but has very limited studies concerning its function in noise insulation and reduction.

From the acoustic aspects, wing wall installed with noise absorption materials sometimes is used, most of the time using foams to attenuate the noise pollution. However, foams also bring some negative impacts especially to human health; as it is one of the sources of dust and requires replacement and maintenance of ordinary. Quarter-wave resonators could be an option to replace this kind of sound absorption material, as it requires little maintenance, allow air goes smoothing without harming human health but also with very good noise screening effects. Most of the studies in recent years put attention in its function in industry (i.e. mufflers in engines); despite the fact that very few studies concern its application in building environment. A combination of ventilated window with wing wall is the new concept contrasting with traditional open

windows or wing wall. At the same time, MQWRs system will be installed in the wing wall system to study its performance in both of acoustics and ventilation.

In this study, the noise attenuation is designed to be in the dominant frequency range of traffic noise i.e. 250-2000 Hz.

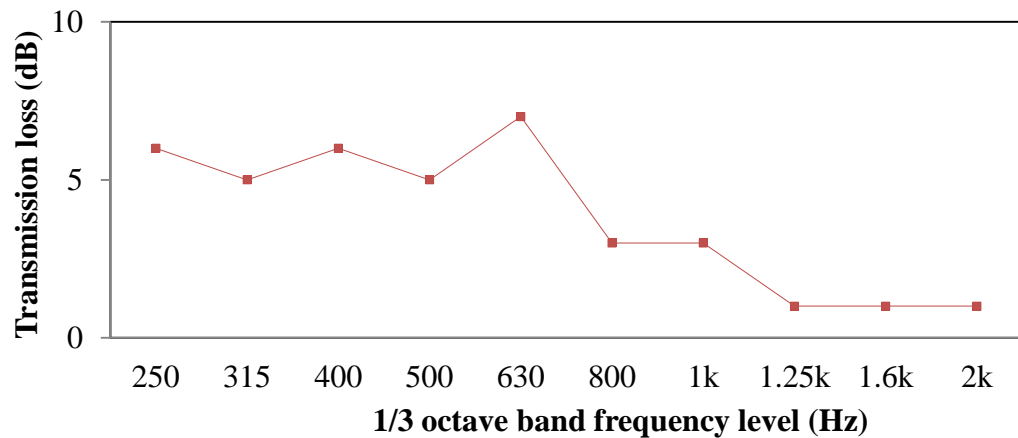


Figure 5- 22 Transmission loss of the panel absorber; —■— duct only- test in tube.

Target to reduce traffic noise by 10 dB  $\pm$  1 dB from 200 Hz to 1 kHz; and reduce traffic noise by 5 dB  $\pm$  1 dB between 1 kHz and 2 kHz. The duct is simply to be fabricated and the durability is much higher than that of the conventional fibrous acoustic material. Experiments have been carried out; and the measured values of the attenuation are found to be in good agreement with the theory. The test of transmission loss of the panel absorber is carried out in the testing duct in the

laboratory as showed in Figure 5-22. The result shows the peak transmission loss is at 7 dB at frequency level of 630 Hz.

## **5.6 TESTING IN AN ANECHOIC SOURCE ROOM**

In an acoustic testing room, the walls, ceiling and floors are lined with 700mm deep wedges of acoustic foam. The aim of this construction is to provide an acoustic test environment in which the noise emissions even of relatively quiet equipment can be investigated.

The test methods in acoustics are in accordance with relevant ISO140 procedures in an anechoic source room, which is a space designed to acoustically control which without affecting acoustic performance but can totally absorb reflections of sound within the environment. Transmission loss of 10 dB to 22 dB can be achieved in our experiments. Figure 5-23 explains the difference between a mockup traditional room conditions and a revised anechoic experiment room environment. The two rooms are absolutely isolated. The source room and receivers' room are in the same condition in Figure 5-23a, both of them present the indoor environment, but it has reflections. However, as shown in Figure

5-23b, one room represents indoor condition; absorptive wedges are placed in the other room to create environmental reliability (traffic noise outdoor) ((Kang, J. & Brocklesby, M.W. 2005; Kang, J. & Li, Z. 2007; Wong et al., 2012). Source room is semi-anechoic when the receiver's room is reverberated.

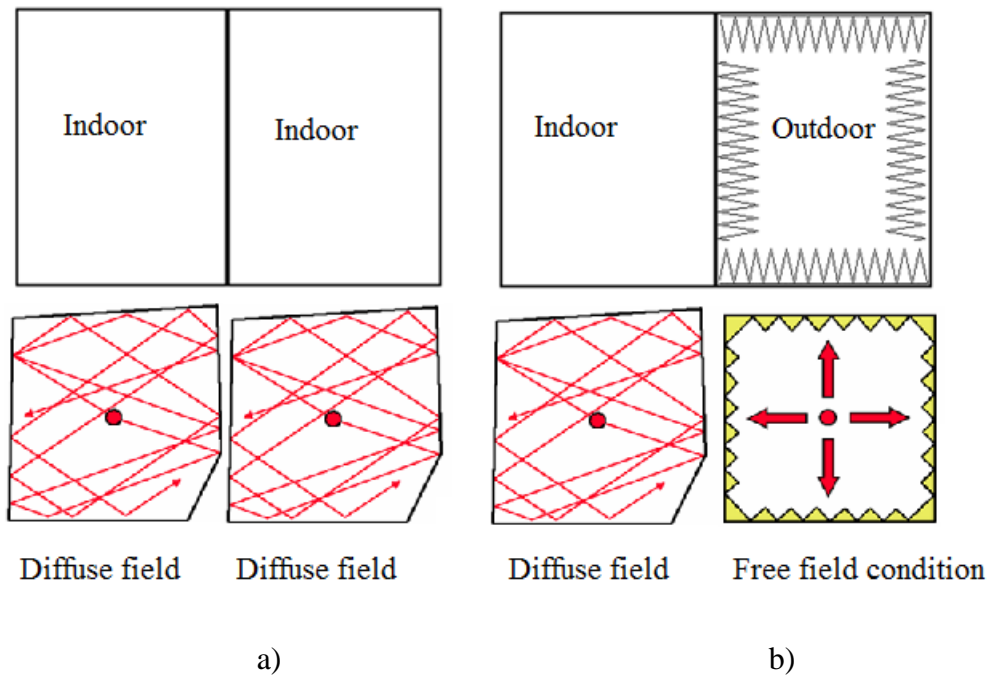


Figure 5- 23 a) Traditional experimental mockup room; b) Revised anechoic experiment mockup room.

## 5.7 SUMMARY

The significant transmission loss has been observed between the control test and using membrane absorbers; especially at the frequency level between 400 Hz to

1.6 kHz across the entire 1/3 octave band of the acoustics experiment of the scaled mockup laboratory experiment results.

The mock-up acoustics experiments have been carried out in Fo Tan in an anechoic source room. Membrane absorbers have the most significant transmission loss at lower frequency level. The duct is simply to be fabricated and the durability is much higher than that of the conventional fibrous acoustic material. Experiments have been carried out; and the measured values of the attenuation are found to be in good agreement with the theory.

It is obvious that the acoustic performance of ventilated window is considerable, but the silencer alone does not carry out considerably in noise attenuation. However, both of ventilated window and silencer would not block any wind coming through the opening in our experiments. After considering the acoustic and ventilation performances of ventilated window and silencer, we carried out a new design of wing wall which combines ventilated window and silencer altogether to evaluate and try to improve the acoustic and ventilation performance at the same time. Inlet has been built larger than the outlet after considering the maximum ventilation cooling is estimated. Considering the

experimental results, easily to find out the noise attenuation performance of the wing wall is significant, noise level tested in the receiving room is much lower than that in the source room, hence both the length of the silencer and the resonators inside to some extent help in minimizing the transmission of noise.

Of the acoustics aspect, mockup experiments examined the noise attenuation performance of different types of silencers. From the previous results, it is obvious that the acoustic performance of ventilated window is considerably using membrane absorber and quarter-wave resonators. At the same time, both of ventilated window and silencer would not block any wind coming through the opening in our experiments. The noise attenuation performance of the wing wall is significant, noise level tested in the receiving room is much lower than that in the source room in both scaled and full-scale experiment, and hence both the length of the silencer and the resonators inside to some extent help in minimizing the transmission of noise. Multiple quarter-wave absorber and multiple resonators with membrane absorber have significant noise attenuation at lower frequency levels. Quarter-wave resonators with membrane absorber and quarter-wave absorber have similar noise attenuation across the entire 1/3 octave band; their transmission loss meets the same high level with polyester at a

frequency range from 200 Hz to around 315 Hz but relatively low noise attenuation after 1.6 kHz. Membrane absorber has the greatest performance of transmission loss at low frequency level below 630 Hz but fallen considerably afterwards. For lower frequency level from 200 Hz to 630 Hz, no doubt, membrane absorbers have the most significant transmission loss. The noise attenuation mechanism for silencers includes the flexible vibration of the tube structure. Another noise attenuation mechanism for the MQWRs is the reflection due to the impedance change at the outlet of resonators.



# **CHAPTER 6**

## **VENTILATION AND ACOUSTICS PERFORMANCE**

### **OF NEW VENTILATED WINDOW DESIGN**

#### **6.1 INTRODUCTION**

The experimental results from acoustic and ventilation performance of multiple quarter wave resonators have good agreements with the theory. Beside the multiple quarter wave resonator plus wing wall design, we innovated boldly a design without using any absorbers but only by ventilated duct with extended inlet and outlet on each side. The cylindrical ventilated duct, which has a rounded-inlet at the front of the duct can prevent unexpected noise from the front directly and would not affect the airflow at the same time. Rounded-inlet duct installed between two rooms acts as “an expansion chamber with extended inlet and outlet” (Craggs, 1976; Lee & Kim, 2009). The simplest reactive muffler is believed to have sound attenuation due to muffler effect from room to room when there is a sudden expansion or contraction in the cross section of the sound flow path.

Figure 6-1 indicates the physical configuration of rectangular duct and cylindrical duct. There are three aims in this chapter: 1) to research and evaluate the experimental and theoretical sound screening of rounded-inlet cylindrical ventilated duct; and 2) to compare the ventilation performance between straight duct and rounded-inlet duct.

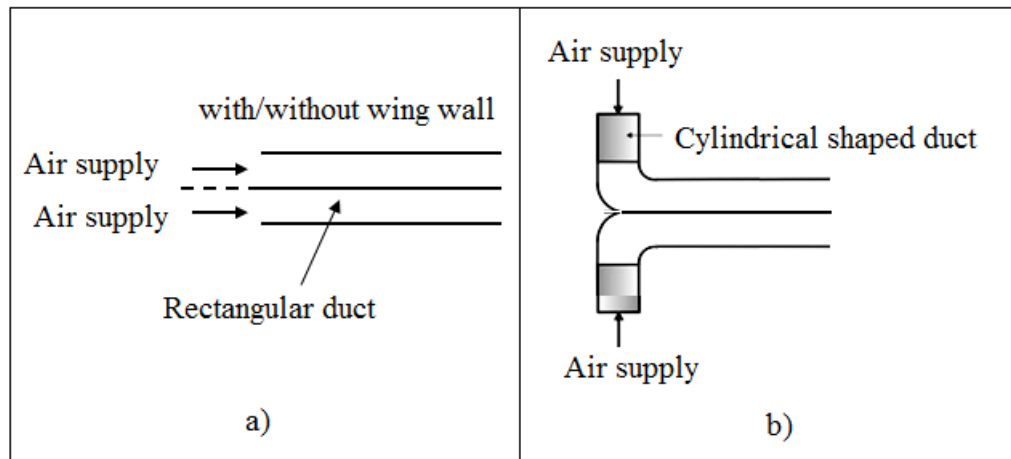


Figure 6-1 a) straight-inlet rectangular duct; b) rounded-inlet cylindrical duct.

Scale mockup measurements have been carried out in this research to examine the effectiveness of different design shapes (straight-inlet duct and rounded-inlet duct) of ventilated duct in attenuating sound transmission. Ventilation experimental measurements have also been carried out at different wind direction (i.e.  $0^\circ$ ,  $45^\circ$ ,  $60^\circ$  and  $90^\circ$ ) for dual-flow ventilated window and rounded-inlet cylindrical duct ventilated window. Both acoustics performance and ventilation performance have quantified.

## 6.2 ACOUSTICS PERFORMANCE OF THE NEW ROUNDED-INLET CYLINDRICAL VENTILATED DUCT DESIGN

### 6.2.1 Rounded-inlet cylindrical ventilated duct

A rounded-inlet cylindrical ventilated duct has inserted in the wall right between the source room and receiving room as showed in Figure 6-1 a) the front view at the source side and b) the back view in the receiving room.



a)

b)

Figure 6- 1 Rounded-inlet cylindrical ventilated duct; a) front view of the duct; and b) back view of the duct.

Loudspeaker has positioned at the same height at the microphone in the source side. Absorptive wedges surround it in order to minimize reflections.



a)

b)

Figure 6- 2 Photos of the experimental set-up; a) noise source; b) positions of the microphone at the source side.

The methodology of experiments has clarified as followed:

1. Noise source: Loudspeaker;

2. The speaker located about 2m away with incident angles at  $0^\circ$ ,  $30^\circ$ ,  $45^\circ$ ,  $60^\circ$  and  $90^\circ$  (Figure 6-3) on floor;
3. Microphones set at the source and recipient's room;
4. The measurement took for an interval of 20 seconds;
5. The data collected and analyzed by a computer program.

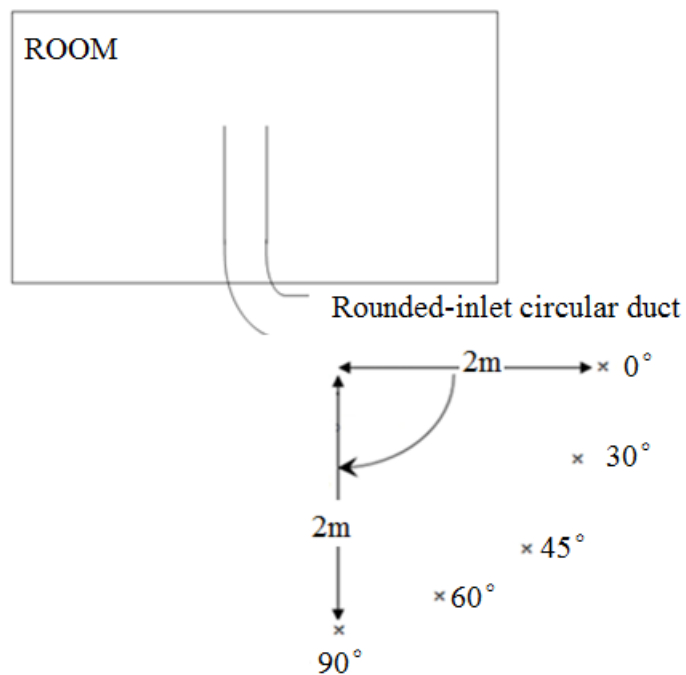


Figure 6- 3 Incident angles of measurements in the experiment.

The transmission loss test facility has a source room and a receiving room. An acoustic driver radiating white noise over the frequency range 200 Hz to 2 kHz used as the source of noise constantly in this mockup experiment. Two microphones B&K#4189 and B&K#4189A21 used to measure the noise level.

One mounted on the front of the ventilation opening at the same height in the source room and the other one located in the receiving room, respectively.

Layout of the experimental set up showed in Figure 6-4 when the microphone at the receiver's side placed in the room.

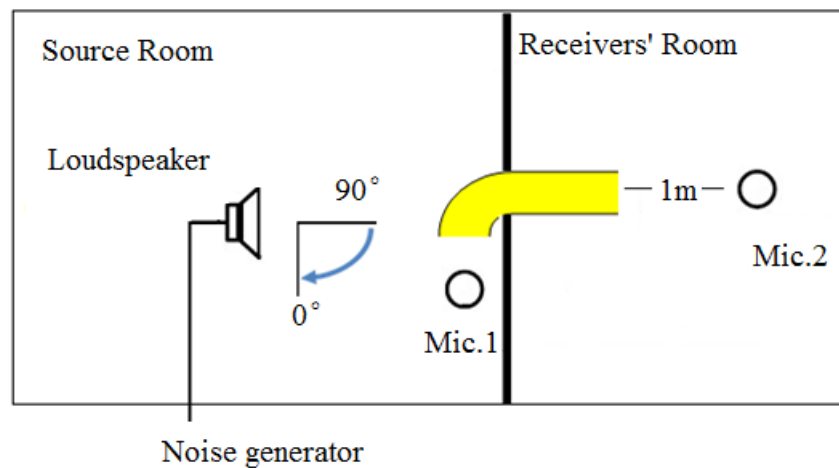


Figure 6- 4 Layout of scaled mock up measurements in the room.

The noise reduction results in the room at different incident angles showed in Figure 6-5. Best performance has found at 90° when the average reduction reaches 29 dB across the entire frequency band between 200 Hz and 2 kHz. At 30°, 45° and 60°, the noise reductions do not have large disparities. When the sound comes straightly to the opening from 0°, the noise reduction is much lower as indicated in the figure especially between 500 to 1.6 kHz. However, even at 0°

the noise reduction is still much better than the performance of conventional window, which only has an average reduction of around 7 dB.

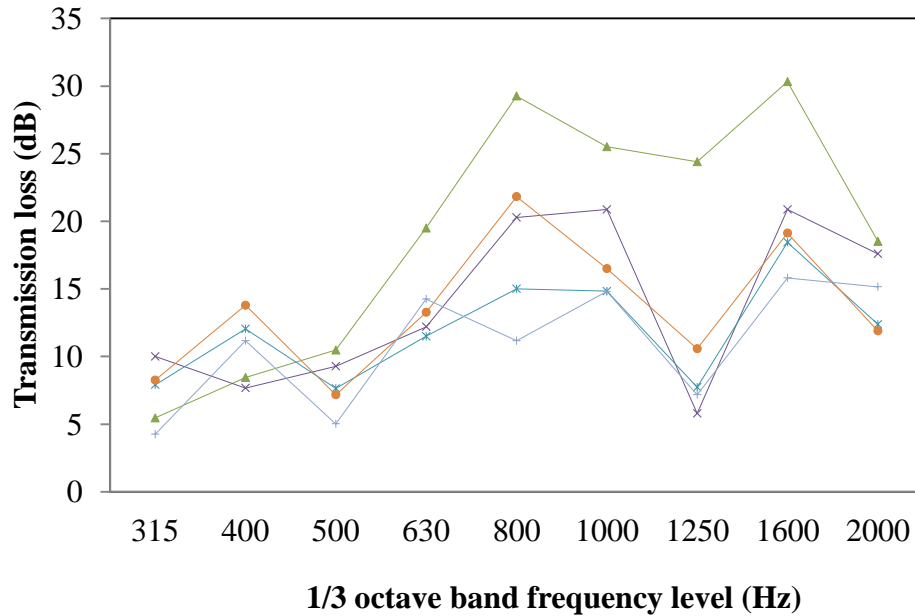


Figure 6- 5 Transmission loss of round inlet ventilated duct in the room; —▲— 90° in the room; —×— 60° in the room; —\*— 45° in the room; —●— 30° in the room; —+— 0° in the room.

### 6.2.2 Acoustics test with absorber in the rounded-inlet cylindrical ventilated duct

We also carried out noise measurement in the same experimental setups in combination of an absorber inside the ventilated duct. Measurements results obtained at both 0° and 90° with or without the absorber. Figure 6-6 showed the set up for the test.



Figure 6- 6 Acoustics tests (with absorber in the ventilated duct) when the microphone put in the room.

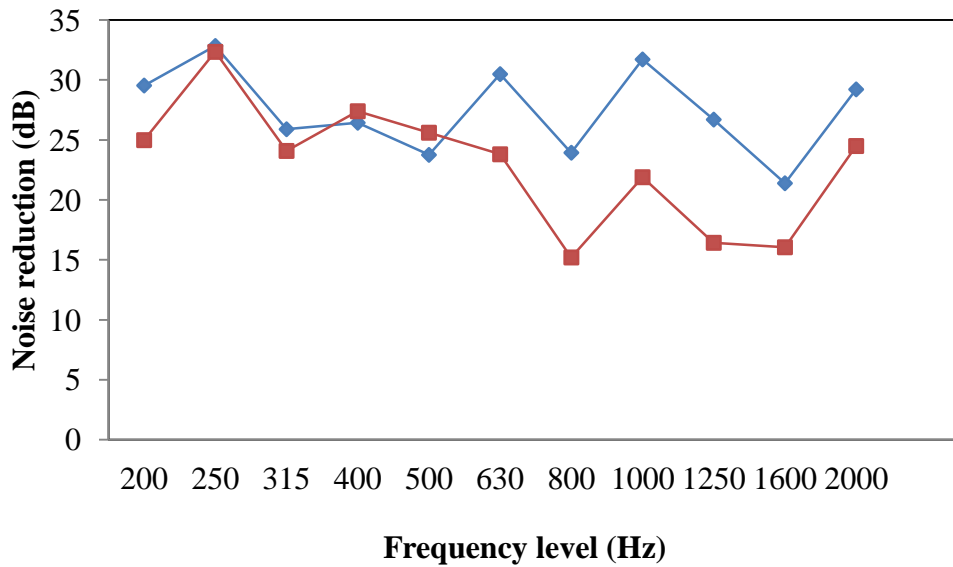


Figure 6- 7 Noise attenuation of absorber at 0° in the rounded-inlet ventilated duct; —◆— 0° with absorber in the room; —■— 0° in the room.

The average noise reduction with absorber in the duct at 0° is 26.5 dB while the noise reduction in the room without putting absorber in the duct is 22.9 dB. The performance is about 4 dB better than that without absorber. Figure 6-7 clearly

clarifies the difference of performance is negligible, which open appears at the frequency level between 630 Hz and 2 kHz.

At 90°, the average reduction across the entire frequency range is even lower.

The sound attenuation performance is also negligible as indicated in Figure 6-8.

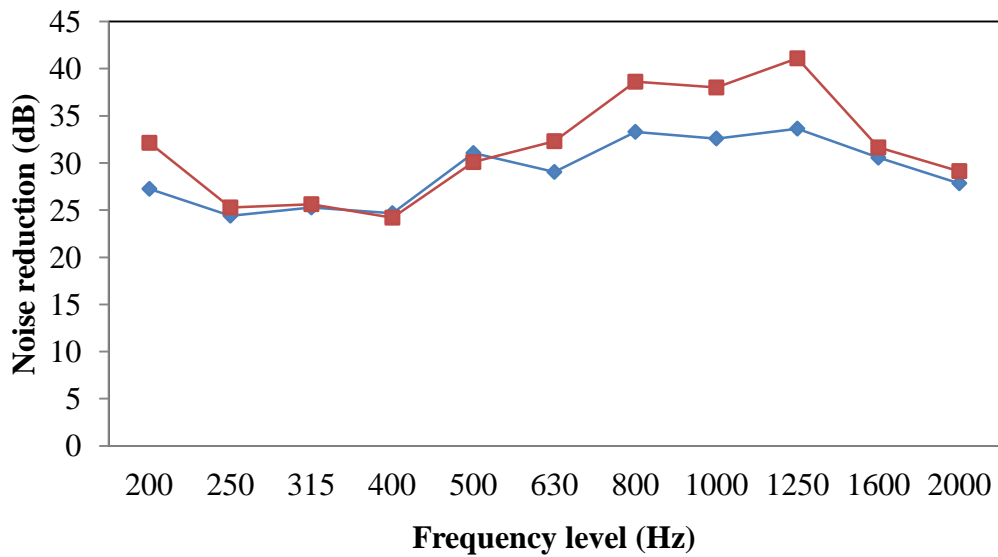


Figure 6- 8 Noise attenuation of absorber at 90° in the rounded-inlet ventilated

duct; —◆— 90° with absorber in the room; —■— 90° in the room.

### 6.2.3 Calculations of the Transmission loss of the round inlet duct

Sound attenuation owing to muffler effect happens when there is a rapid expansion or contraction of the cross section of the sound flow path. Sound wave



of certain wavelengths then reflected back towards the source; portions of the sound energy can be prevented from transmitting along the sound flow path. Sound wave passes through the inlet tube then experience a rapid expansion then contracts again when leaving through the outlet tube. The greater the ratio of expansion or contraction chamber to the inlet or outlet tube is the greater will be the sound reduction. The equation of transmission loss for expansion type muffler is as follows:

Where,

$l$  is the length of muffler, m

$S_1$  is the cross-sectional area of inlet chamber,  $m^2$

$S_2$  is the cross-sectional area of muffler,  $m^2$

Expansion chamber operates most efficiently in applications involving discrete frequencies rather than broad band noise (Kutz, 2005). “The transmission loss through an expansion chamber is defined as the difference in sound pressure level of the incident sound wave and the transmitted sound pressure level” (Byrne et al., 2006). In the case (Figure 6-9), when  $S = S_2/S_1$ ,  $k = 2k = 2\pi/\alpha$ , the transmission loss is calculated by:

$$TL1 = 10\log_{10}\left\{1 + \frac{1}{4}\left(s + \frac{1}{s}\right)^2 \sin^2 kl\right\} \quad (6-1)$$

Similar to a standard expansion chamber is the extended inlet and outlet expansion chamber, where the inlet and outlet tube are extended into the expansion chamber as shown in Figure 6-10 (Chaitanya & Munjal, 2011). The benefit of such a design is that part of the chamber between the extended pipe and the sidewall acts as “a side branch resonator therefore improving the transmission loss” (Craggs, 1976).

$$TL2 = 10\log_{10}\left\{1 + \left[\frac{s}{2s} \cot(kl)\right]^2\right\} \quad (6-2)$$

Therefore, the transmission loss in rounded-inlet ventilated duct will be:

$$TL = TL1 + TL2 \quad (6-3)$$

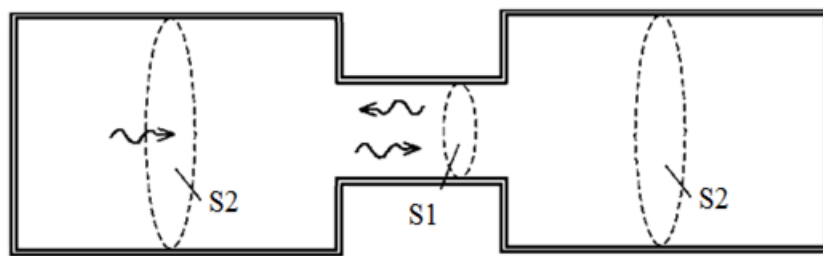


Figure 6- 9 Two rooms linked with a duct- muffler effect.

The ideal example of prediction of the expansion chamber with extended inlet and outlet is presented in Figure 6-10. It shows the predicted transmission loss of

a single-chamber silencer with  $L_1/L=0.5$  and  $L_2/L=0.25$  as well as its estimated performance variation with steady-flow changes. This design exhibits the best overall broadband performance features among all single-chamber silencers. This variation is also typical in application. Such variation coupled with modeling simulation and procedural simplification tends to diminish some of the forecast benefit. However, in this design, we only use the figures to describe the design formula, but not deeply exploring the modeling.

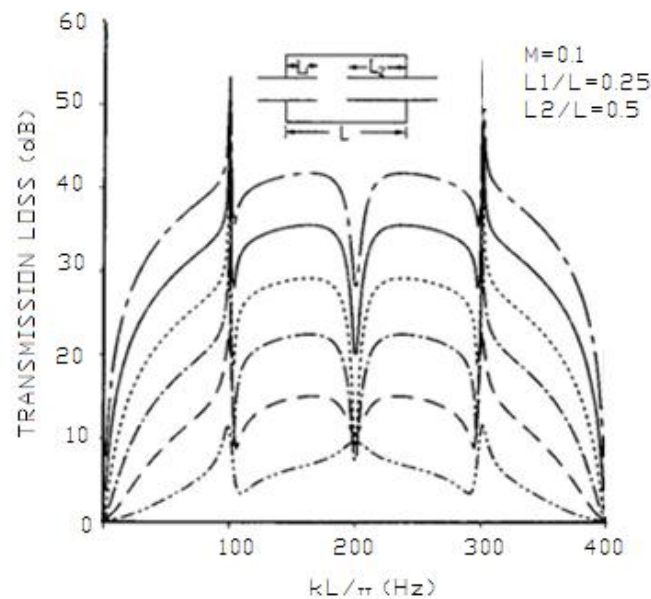


Figure 6- 10 Theoretical predictions of transmission loss of side branch resonator.

Figure 6-10 above may be used to determine the overall trend, but in practical applications, the tangible benefits must also be confirmed through direct

measurements (Munjal, 1987). Thus, we verify the calculations by carrying out experimental study. Figure 6-12 shows the transmission loss by using rounded-inlet ventilated duct in this test. Target of the design is to achieve at least 10 dB noise reduction comparing with using conventional window. The overall performance of this design is acceptable. The dip points in the graph are due to the formation of standing wave along the length of the duct.

Because of the study carried out in the laboratory and the source room is too large, the valid data only between about 200 Hz to 800 Hz chosen to perform in Figure 6-11 due to these limited conditions. Muffler effect in the design is only appropriate and helpful at a lower frequency level.

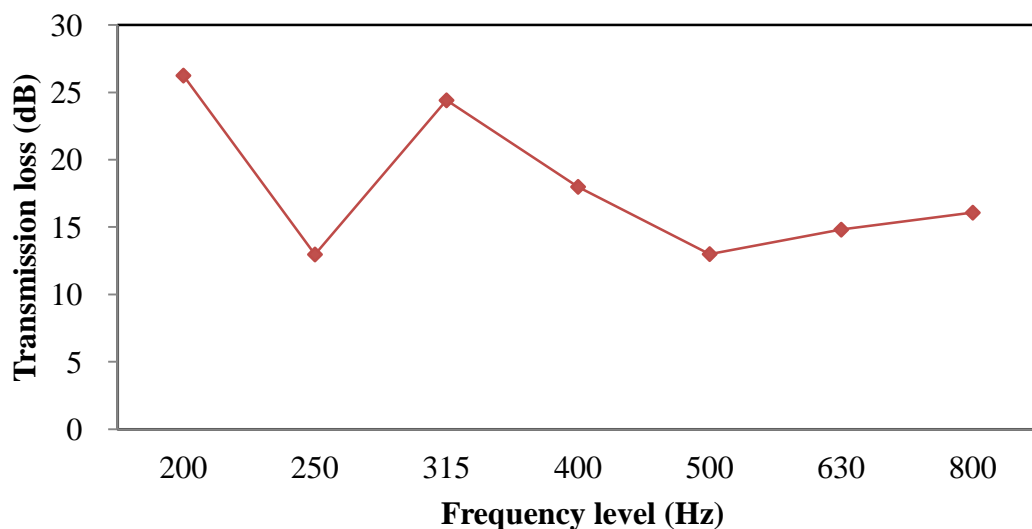


Figure 6-11 Transmission loss by using rounded-inlet ventilated duct-experimental; —◆— transmission loss.

Experimental and theoretical resonance peaks well matched to each other. A similar trend observed in the result although some of the theoretical resonance peak values are higher or smaller than the experimental values. A dip point observed at approximately 250 Hz and another one at 500 Hz. Two peaks found at around 200 Hz and 315 Hz.

#### **6.2.4 Comparing the noise reduction between straight-inlet rectangular duct and rounded-inlet cylindrical duct**

We also conducted the same test set up to determine the noise reduction of straight-inlet rectangular duct. The aim is to compare the noise reduction of straight ventilated duct and rounded-inlet ventilated duct. Based on the results, we would like to assess whether the sound attenuation performance would be affected by geometry. The experimental setup clarified in the following:

1. Noise source: Loudspeaker;
2. The speaker located about 2m away with incident angles at 0°, 30°, 45°, 60° and 90° (see Figure 6-12 and Figure 6-13) on floor;
3. Microphones set at the source and recipient's room;

4. The measurement took for an interval of 20 seconds;
5. The data collected and analyzed by a computer program.

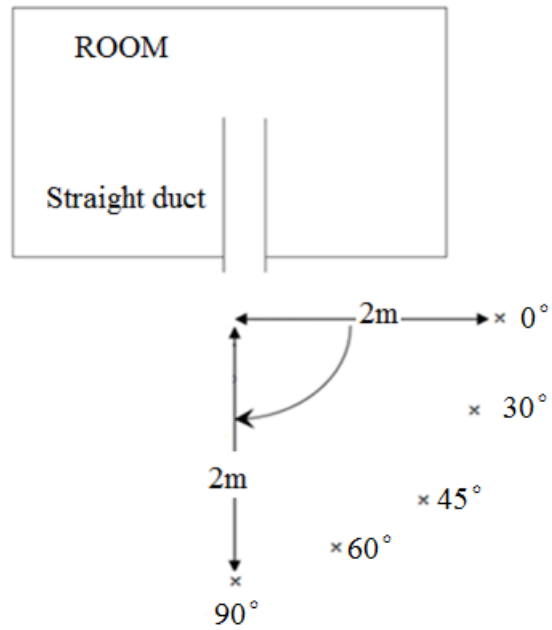


Figure 6- 12 Incident angles of measurements in the experiment.

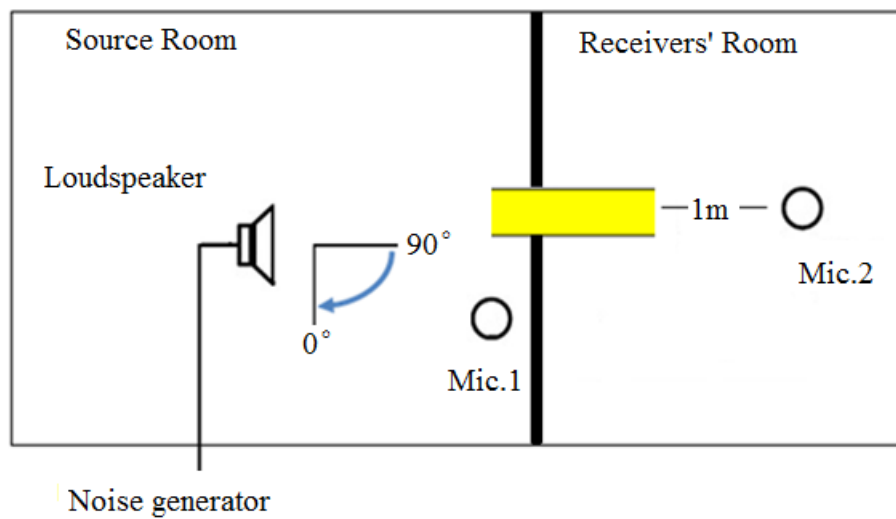


Figure 6- 13 Layout of scaled mock up measurements.

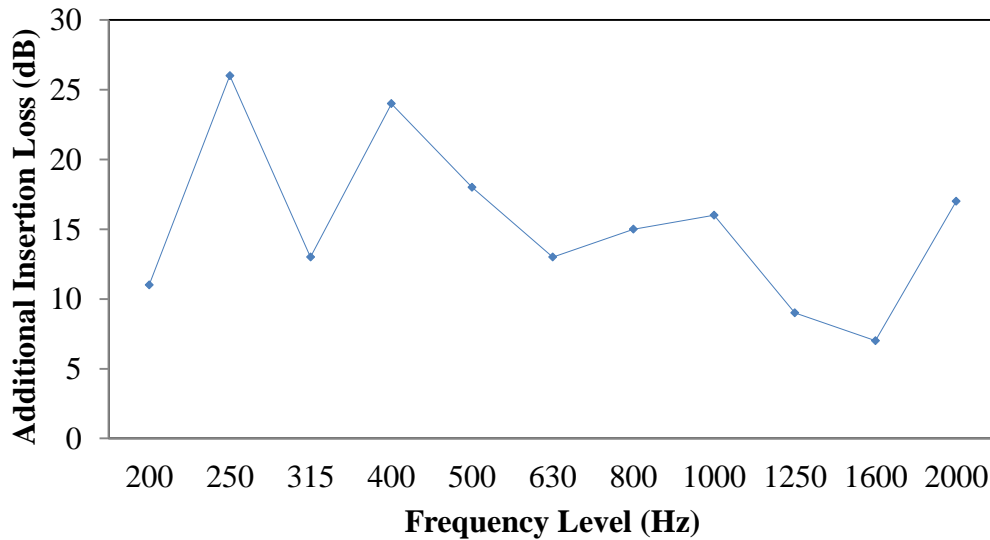


Figure 6- 14 Additional Insertion loss in the rounded-inlet cylindrical ventilated duct — 0°.

Regarding to Figure 6-14, the transmission loss of the rounded-inlet ventilated duct is high at frequency level between 200 Hz to 630 Hz. Two highest points observed at 250 Hz and 400 Hz. The average transmission loss at this frequency range reaches 10 dB.

Transmission loss of rounded-inlet ventilated duct is higher at a higher frequency level between 400 Hz to 2 kHz according to Figure 6-16. The average transmission loss at this frequency range reaches 10 dB. Test results show that the ventilated duct (with a rounded-inlet) performs better sound attenuation than

straight-inlet rectangular duct both at low frequency at 0° and high frequency at 90°.

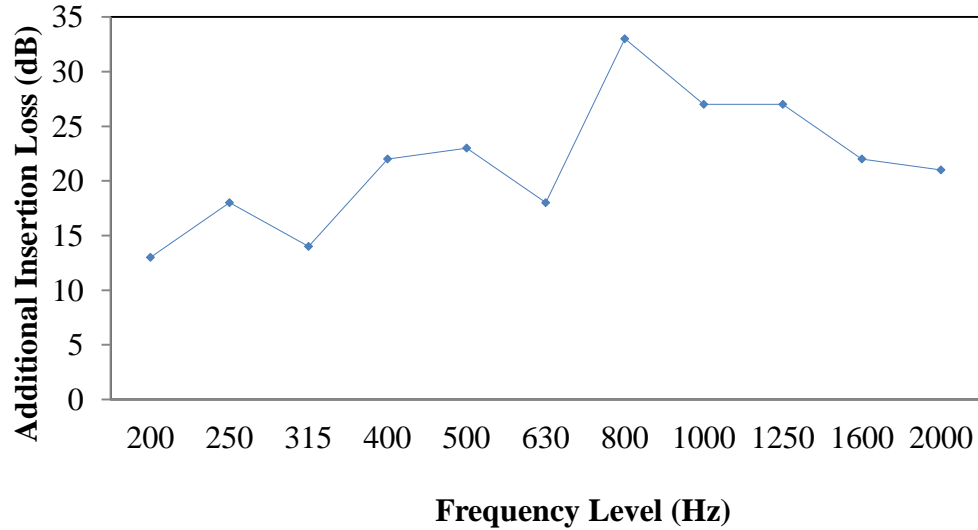


Figure 6- 15 Additional Insertion loss in the rounded-inlet cylindrical ventilated duct —◆— 90°

### 6.3 VENTILATION TEST FOR ROUNDED-INLET CYLINDRICAL VENTILATED DUCT

In the measurement, airflow has tested with an electric fan at free wind of 3.7m/s.

Airflows measured in the room by using the Testo anemometer by placing away from 1m from the ventilated duct. To observe the effect of straight-inlet rectangular duct and rounded-inlet cylindrical duct, airflow velocities at different



angles ( $0^\circ$ ,  $30^\circ$ ,  $45^\circ$ ,  $60^\circ$ ,  $90^\circ$ ) measured. Figure 6-17 and Figure 6-18 demonstrate the layout of each model, respectively.

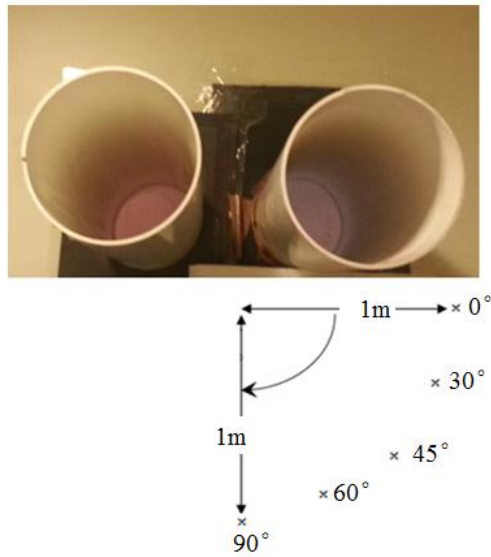


Figure 6- 16 Incident angles to the wall of ventilation measurements for straight-inlet rectangular duct.

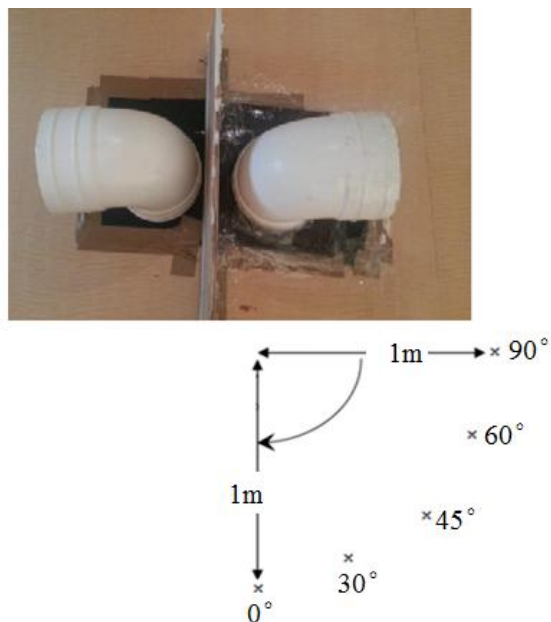


Figure 6- 17 Incident angles to the wall of ventilation measurements for rounded-inlet cylindrical duct.

Straight-inlet duct (m/s)		Rounded-inlet duct (m/s)	
Inlet	Outlet	Inlet	Outlet
90°	0.3	0.5	0.4
60°	1	1.1	1.1
45°	1.5	1.3	1.1
30°	1.2	1.5	1.3
0°	1.4	1.8	1.6

Table 6-1 Ventilation measurements for rounded inlet duct and straight-inlet rectangular duct.

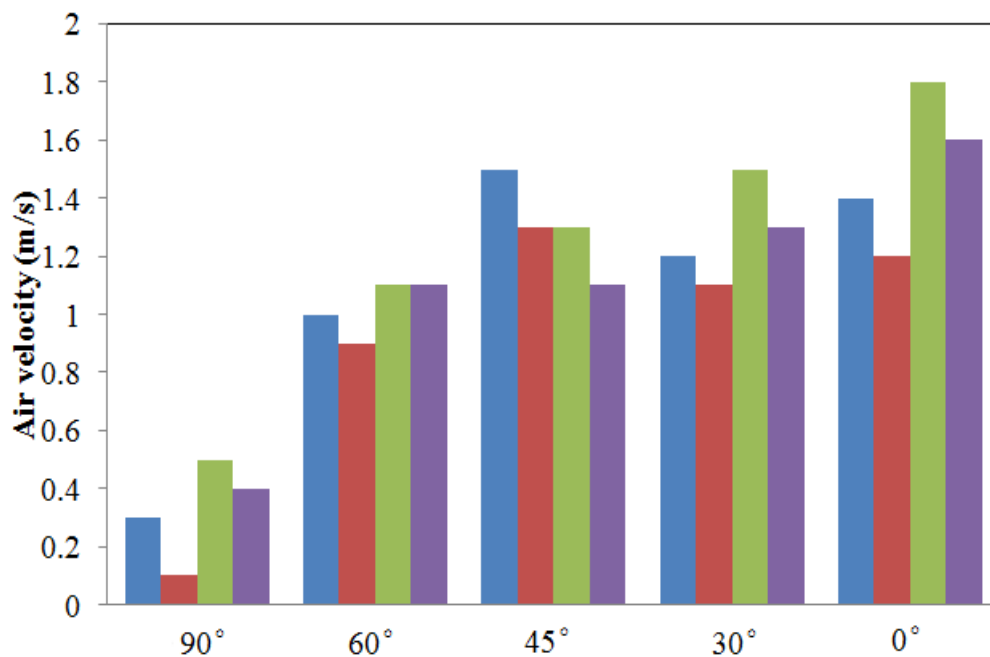


Figure 6-18 Ventilation measurements comparisons between straight-inlet rectangular duct and rounded-inlet cylindrical duct at incident angles to the opening; ■ Inlet (straight-inlet rectangular duct); ■ Inlet (rounded-inlet cylindrical duct); ■ Outlet (straight-inlet rectangular duct); ■ Outlet (rounded-inlet cylindrical duct).

Figure 6-19 indicates the ventilation measurements comparisons between straight-inlet rectangular duct and rounded-inlet cylindrical duct at incident angles to the opening. At incident angles at 0°, 30°, 60° and 90° to the opening of the duct, the rounded-inlet cylindrical duct shows better ventilation performance comparing with straight-inlet rectangular duct. Inlet and outlet flow are similar in both straight-inlet rectangular duct and rounded-inlet cylindrical duct.

#### **6.4 SUMMARY**

Scale mockup measurement carried out in this research to examine the effectiveness of different design shapes of ventilated duct in attenuating sound transmission from outdoor to indoor. Rounded-inlet cylindrical duct systems have many advantages compared with rectangular systems. Rounded-inlet cylindrical ventilated duct has quite satisfactory performance in noise attenuation at any incident angle of the noise source. Even without combining with any acoustic absorptive materials, the ventilated duct can still operate much better than the conventional window. The length and the open area of the duct are also prominent in acoustics performance fitting to measurements of the transmission loss inside the duct. Further ventilation measurements will carry out to assess the

performance. Comparisons between the ventilation performance of the rounded-inlet cylindrical ventilated duct and right rectangular type inlet ventilated duct will further evaluate.

Similar to a standard expansion chamber are the extended inlet and outlet expansion chamber. Rounded-inlet ventilated duct is where the inlet and outlet extending into the expansion chamber. The value of such a device is that part of the chamber between the extended pipe and the sidewall acts as a side branch resonator thus improving the transmission loss.

The wind speed in this study has tested only in front of the inlet and outlet opening but not in the room, and the test is not free of errors. The results can only give a comprehensive description of airflow movements' patterns but cannot be used as accurate information for calculations and measurements.

Additional studies of the routines of airflows of different designs of the ventilated windows will study in the next chapters. The investigation of indoor air flow can help analyze how effective design facilitates the air exchange and human thermal comfort between the indoor and outdoor environment.

# CHAPTER 7

## COMPUTATIONAL SIMULATION

### 7.1 INTRODUCTION

CFD widely used as a prediction tool in assessing indoor environment in certain conditions in specific basic building geometries and environments due to “the growing consciousness of the environmental performance of buildings in Hong Kong” (Mak et al., 2005), . This technique provides an alternative method other than wind tunnel test that is expensive and the weakness of resources in Hong Kong.

CFD is an effective way to visualize a current phenomenon of a single building geometry. In this research, we begin this technique in the early stage of planning and design phase in the natural ventilation performance. The movement patterns and turbulence episode will perform in this research by simplifying the simulation exercise based on a number of case studies.

The first experiment investigated the effectiveness of air flow by wing wall firstly carried out by Givoni in the 1960s (Givoni, 1976). His results show that single-sided room plus wing wall could significantly increase natural ventilation (Mak et al., 2007). CFD applied into two categories in the previous studies: 1) studied the effect of a factor on the fluid dynamic performance, and 2) examined the individual performance and found out any factors could affect it. Using the CFD techniques, we investigated the ventilated window with wing wall model to investigate the natural ventilation effectiveness numerically. Givoni (1976) and Prof. Mak et al (2007) have already proven the best performance of wing wall appears at wind direction at incident angle of  $45^\circ$ ; so wind direction at incident angle of  $45^\circ$  is acquiesced in the small scale CFD simulations. In this CFD simulation I follow Prof. Mak's (2007) procedures and workflows.

ANSYS ICEM CFD 11.0 software uses for this simulation. The CFD simulation sets up only to find the internal inlet air flow and outlet external airflow. Thermal calculations have been disabled. There is three essential parts in CFD, consisting of 1) CFX pre-processor; 2) solver and 3) CFX post-processor. Figure 5 presents a flowchart of the entire computational simulation work in this study.

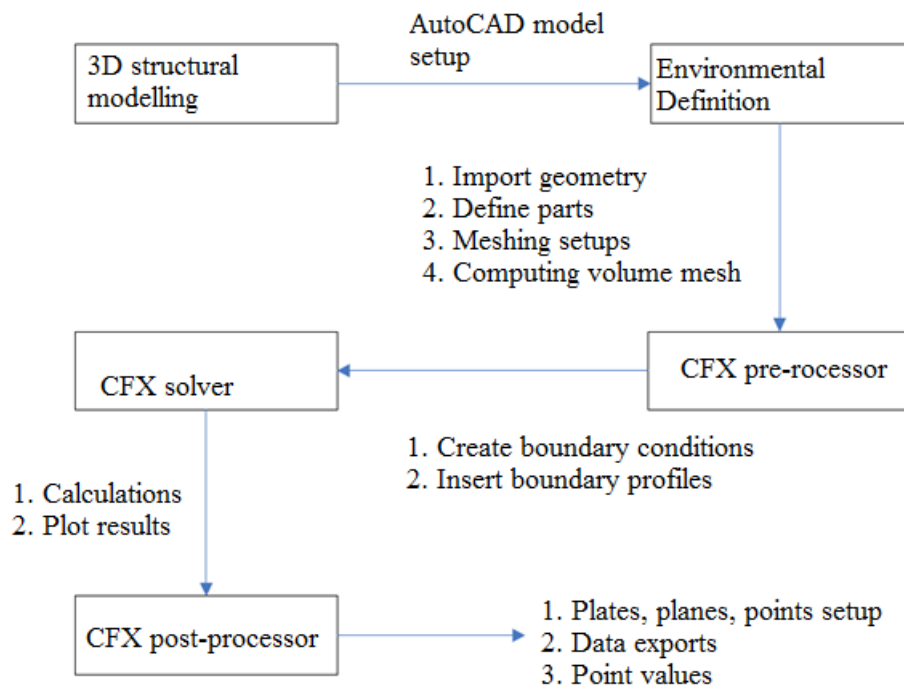


Figure 7- 1 Computational simulation work flowchart.

## 7.2 K-EPSILON (k-ε) TURBULENCE MODEL

K-epsilon (k-ε) turbulent model is chosen in the computational simulation in my study. “The baseline two transport-equation model solves for kinetic energy k and turbulent dissipation ε. Turbulent dissipation is the rate at which velocity fluctuations dissipate. This is the default k-ε model. Coefficients are empirically derived, valid for fully streamlines only. In the standard model, the eddy viscosity is determined from a single turbulence length scale, so the calculated turbulent diffusion is that which occurs only at the specified scale, whereas in

reality all scales of motion will contribute to the turbulent diffusion. This model uses the gradient diffusion hypothesis to relate the Reynolds stress to the mean velocity gradients and the turbulent viscosity” (Menter, 1994; Etheridge & Sandlberg, 1996; Awbi, 2003; Asfour & Gadi, 2008; E-epsilon model, 2014).

The advantages and limitations of k-ε turbulence model are listed in Table 7-1.

<b>Advantages of k-ε model</b>	<b>Disadvantages of k-ε model</b>
<ul style="list-style-type: none"> <li>➤ The most common model to simulate turbulence condition</li> <li>➤ Suitable for simple flows</li> <li>➤ Easy to implement</li> <li>➤ Relative cheap and lower computational time</li> <li>➤ Suitable for initial iterations and design;</li> <li>➤ Look on overall performance of the device and offer a stable solution</li> </ul>	<ul style="list-style-type: none"> <li>➤ Performs poorly for complex flows involving severe pressure gradients;</li> <li>➤ Separation and strong streamline curvature;</li> <li>➤ Lack of sensitivity to adverse pressure gradients;</li> <li>➤ Numerical stiffness when equations are integrated through the viscous sub-layer which is treated with damping functions that have stability issues.</li> </ul>

Table 7-1 Advantages and limitations of k-ε turbulence model.



### 7.3 COMPUTATIONAL SIMULATION OF CONVENTIONAL WINDOW

#### *Geometry*

Detailed geometry enters to create a representation model (Table 7.2). To set up this review, physical, thermal constants and boundary conditions define and proceed with proper calculations. AutoCAD software creates a 3D room design at the beginning of the simulation. Figure 7-2 showed the top view and front view (with dimensions), respectively. The model in this simulation is a 1:10 scaled model.

<b>Geometry</b>	<b>Values</b>
Wind speed	0.06m.s <sup>-1</sup>
Static pressure	0 Pa
Wind incident angle	0°

Table 7- 2 Geometry of conventional window in computational simulation.

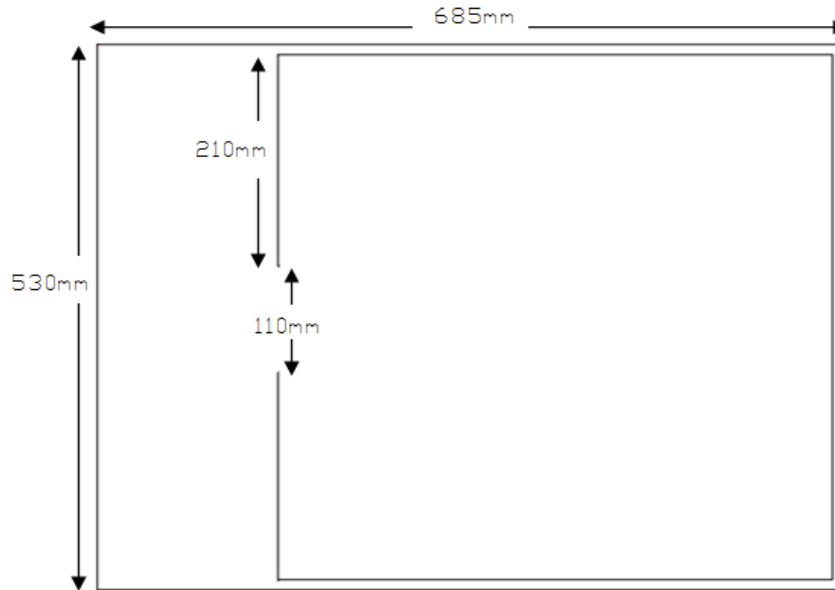


Figure 7-2 Physical configurations of conventional window.

### ***Boundary conditions***

The hypothetical model is placed in the environment. The “inlet” and “outlet” of the model room is defined as “opening”; whereas the wall faces the openings is defined as “inlet” and the wall behind the model is defined as “outlet” boundary condition in order to prevent fluid from flowing into the domain. The thickness of wall is ignored. The fluid name is defined as “air” at room temperature of 25 °C.

### ***Numerical grids***

This series of investigations carried out using computer simulation technique.

K-ε turbulence model is adopted. Figure 7-3 illustrated the meshing of grids of the control model. The number of grids is around 70,000 for this smaller scale simulation.

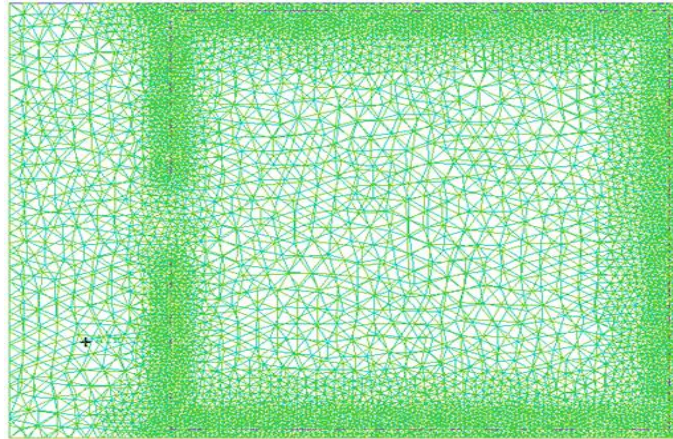


Figure 7- 3 Grids of the simulation model.

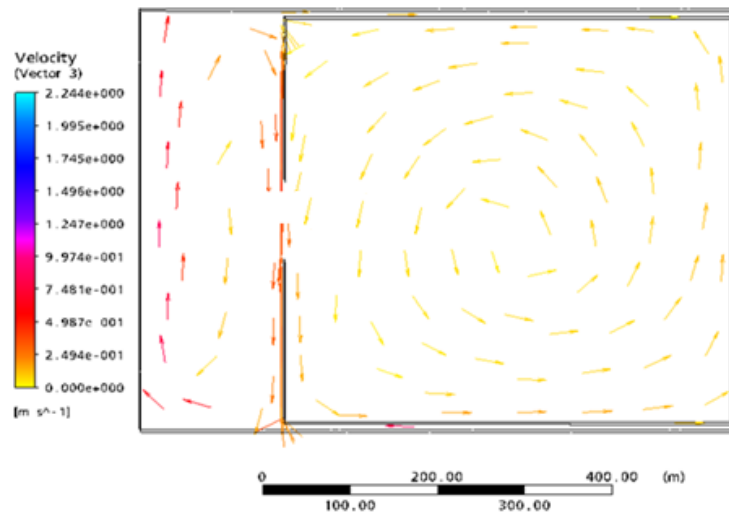


Figure 7- 4 Plan views of the vector diagram for a conventional window at the wind angle of  $45^\circ$  and wind speed of 0.06m/s.

Airflow concentrates at the opening of the room as showed in Figure 7-4 only

few can go into the room, but most of the flows circulate within the room so the ventilation inside the room is rather limited. This model presents the conventional window as a control model to examine the differences in the following tests.

## 7.4 COMPUTATIONAL SIMULATION OF WING WALL

### 7.4.1 Conventional wing wall

#### *Geometry*

Detailed geometry enters to create a representation model (Table 7.3). Physical constants, thermal constants and boundary conditions define and proceed with appropriate calculations in this study.

<i>Geometry</i>	<i>Values</i>
Wind speed	0.06m.s <sup>-1</sup>
Static pressure	0 Pa
Wind incident angle	0 °

Table 7- 3 Geometry of conventional wing wall in computational simulation.

Figure 7-5 explained the physical configuration of the conventional wing wall model in a room.

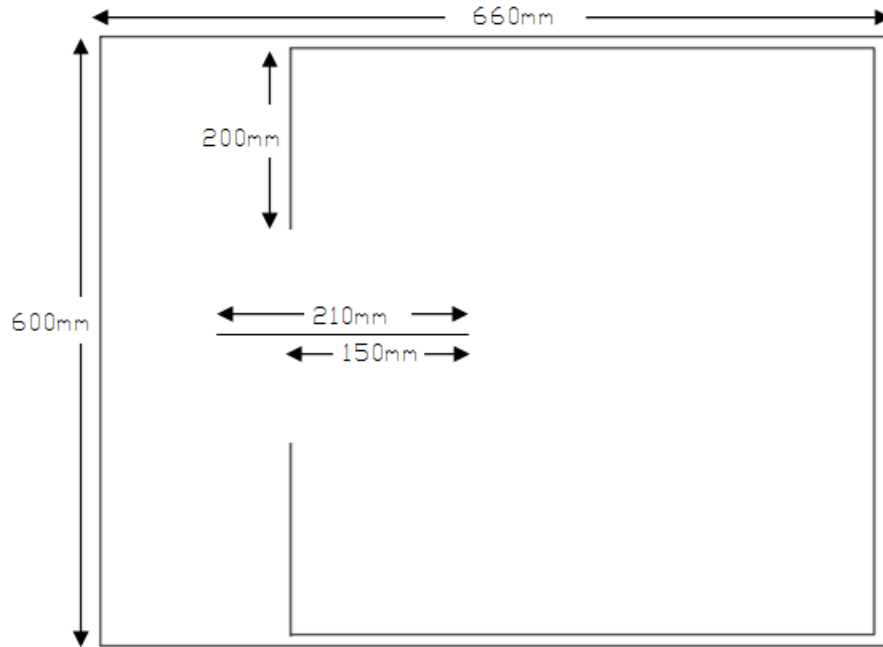


Figure 7- 5 Physical configurations of conventional wing wall.

### ***Boundary conditions***

The hypothetical model is placed in the environment. The “inlet” and “outlet” of the model room is defined as “opening”; whereas the wall faces the openings is defined as “inlet” and the wall behind the model is defined as “outlet” boundary condition in order to prevent fluid from flowing into the domain. The thickness of wall is ignored. The fluid name is defined as “air” at room temperature of 25 °C.

### ***Numerical grids***

This series of investigations carried out using computer simulation technique. A commercial CFD package FLUENT in this study to simulate the wind around the room and the airflow through the window openings and within the room. An absolute standard (two-equation)  $k-\epsilon$  turbulence model adopts through it inevitably introduces some errors. It has indicated by other investigators that the overall direction of airflow parameters such as pressure and air velocity can be reasonably predicted. Both structured and unstructured grid have used. Figure 7-6 illustrated after meshing of grids of the conventional wing wall simulation model. The number of grids is around 70,000 for this smaller scale simulation.

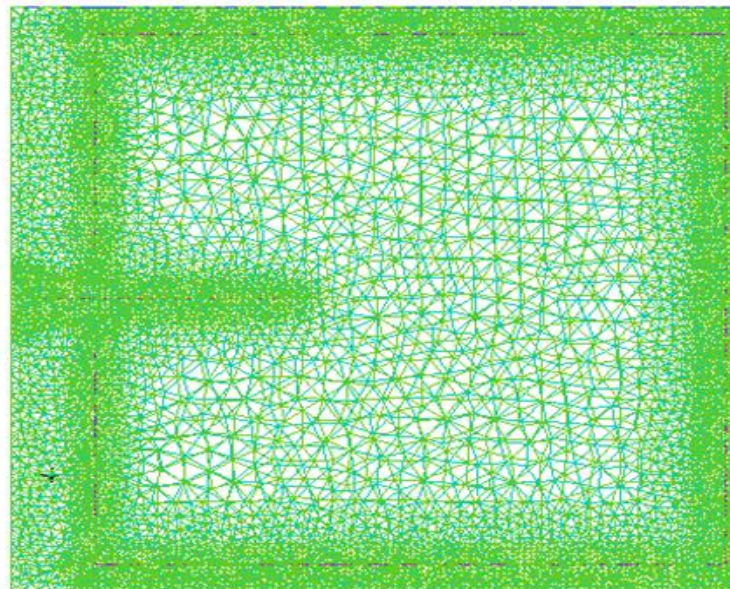


Figure 7- 6 Grids of the simulation model.

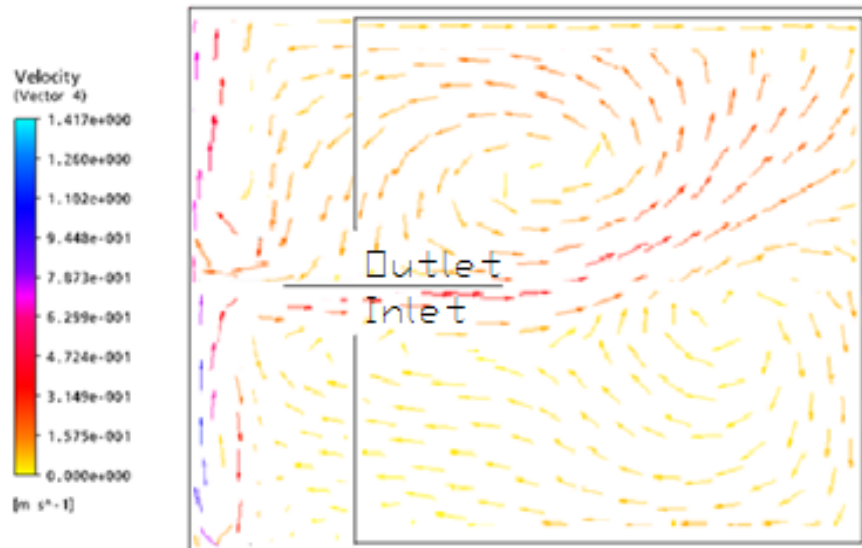


Figure 7- 7 Plan views of the vector diagram for a conventional wing wall at wind angle of  $45^\circ$  and wind speed of 0.06m/s.

The conventional wing wall in-between the opening has a role in accelerating the airflow rate as showed in Figure 7-7. In this case, the wing wall inserts in between the opening and the longer part places in the indoor space. There is a distinct flow in but the flow out is negligible. There are two separate circulations at each side of the wing wall in the indoor area. Comparing with the control model (conventional window), the wind speed has increased at the inlet, outlet and the opening.

## **7.5 COMPUTATIONAL OF WING WALL WITH BARRIERS ON EACH SIDE**

### 7.5.1 Conventional wing wall with two barriers

#### *Geometry*

Detailed geometry enters to create a representation model (Table 7-4). To set up this study, physical, thermal constants and boundary conditions define and follow with appropriate calculations.

<i>Geometry</i>	<i>Values</i>
Wind speed	0.06m.s <sup>-1</sup>
Static pressure	0 Pa
Wind incident angle	0 °

Table 7- 4 Geometry of conventional wing wall with two barriers in computational simulation.

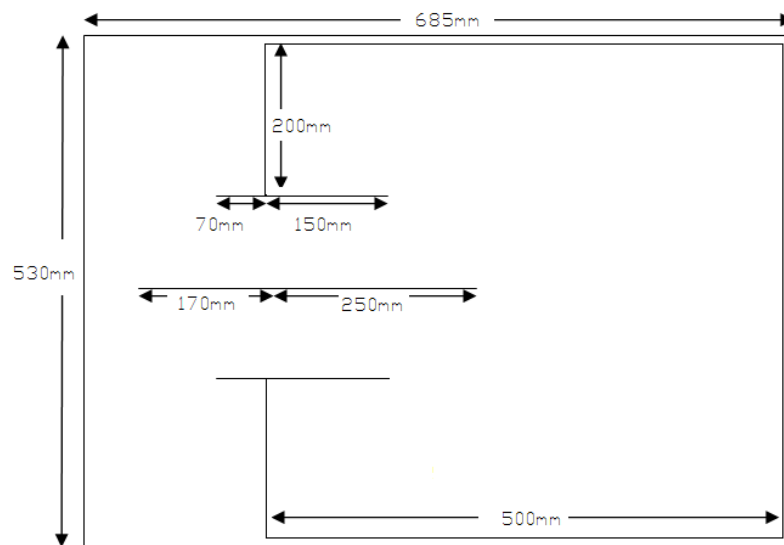


Figure 7- 8 Physical configurations of conventional wing wall with two barriers.



Figure 7-8 explained the physical configuration of the conventional wing wall model in a room.

### ***Boundary conditions***

The hypothetical model is placed in the environment. The “inlet” and “outlet” of the model room is defined as “opening”; whereas the wall faces the openings is defined as “inlet” and the wall behind the model is defined as “outlet” boundary condition in order to prevent fluid from flowing into the domain. The thickness of wall is ignored. The fluid name is defined as “air” at room temperature of 25 °C.

### ***Numerical grids***

This series of investigations carried out using computer simulation technique. K- $\epsilon$  turbulence model is adopted. Both structured and unstructured grid have used. Figure 7-9 illustrated after meshing of grids of the conventional wing wall simulation model. The number of grids is around 70,000 for this smaller scale simulation.

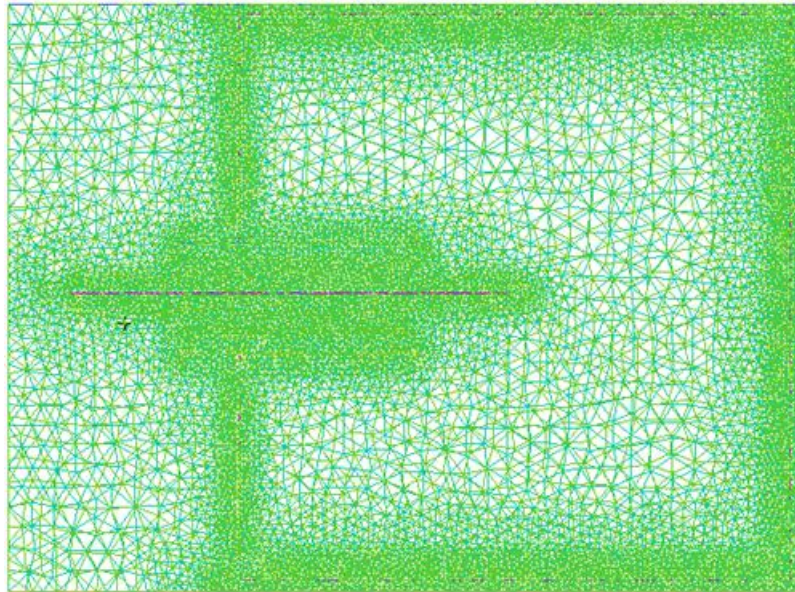


Figure 7- 9 Grids of the simulation model.

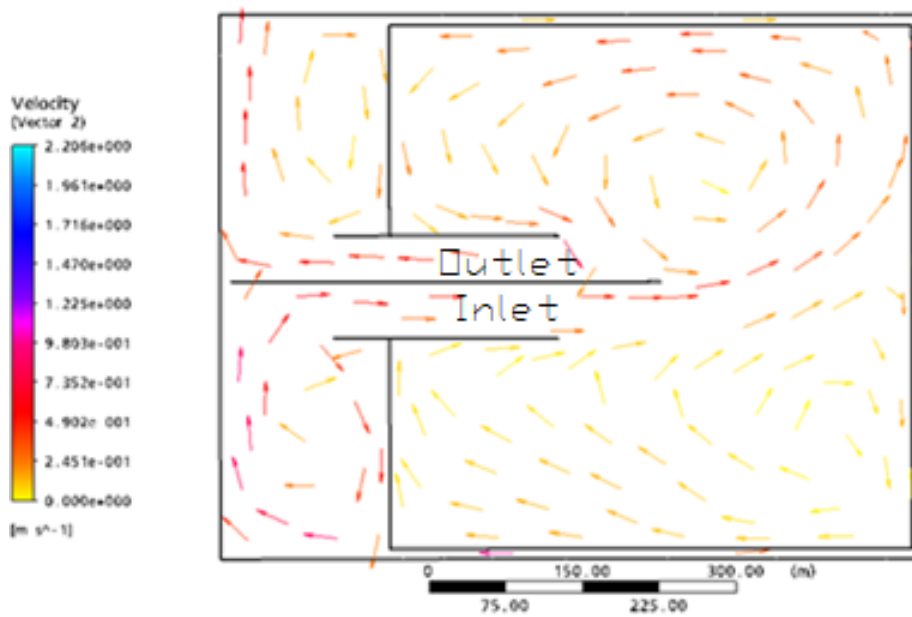


Figure 7- 10 Plan views of the vector diagram for a conventional wing wall with two barriers to wind angle of  $45^\circ$  and wind speed of 0.06m/s.

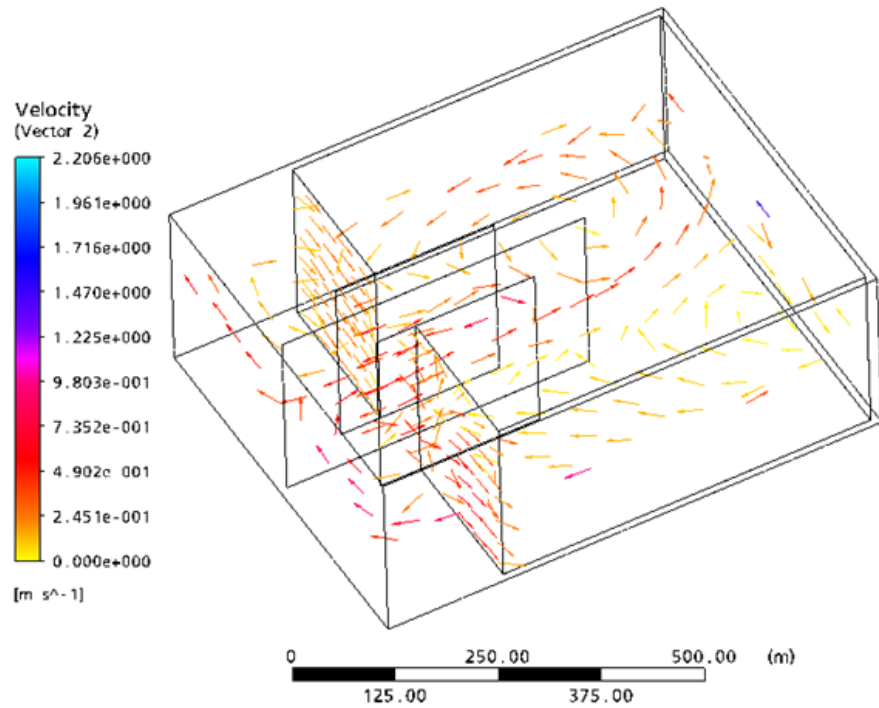


Figure 7- 11 3D views of the vector diagram for a conventional wing wall with two barriers to wind angle of 45 °and wind speed of 0.06m/s.

Figure 7-10 and Figure 7-11 showed the plan view and 3D view of the vector diagram for a conventional wing wall with two barriers at wind angle of 45 °and wind speed of 0.06m/s as calculated from the database obtained, respectively. Outlet velocity is greater than the inlet, which means the barrier in-between the opening has a purpose in accelerating the airflow velocity at the outlet. The airflow speed is much higher than the result of the control case.

## 7.5.2 Ventilated window with wing wall at 45 °

### *Geometry*

From the experiments above we found the best performance of airflow was to the wind direction of 45 °. The revised ventilated window design has also verified in the computational analysis. The configuration of the model has indicated in Figure 7-12. Two barriers change into shorter lengths, and a little triangular-shaped extension adds one side of the wing wall.

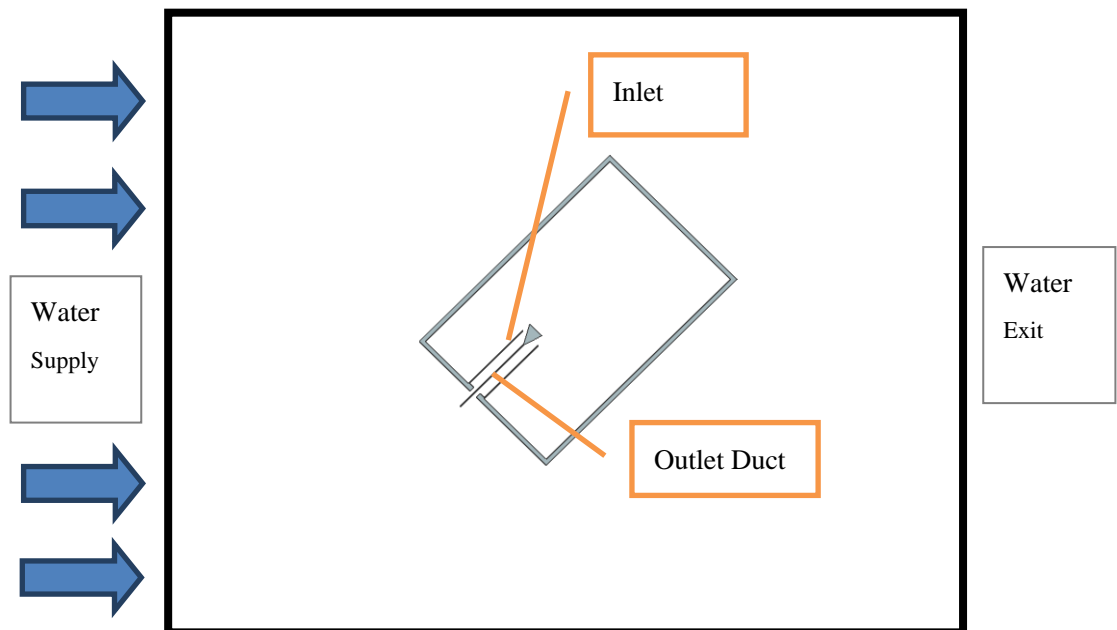


Figure 7- 12 Configuration of ventilated window with wing wall at 45 °.

### ***Boundary conditions***

The hypothetical model is placed at the center in the environment. Large boundary will not adversely affect the boundary conditions at the domain outflow (Figure 7-12). The “inlet” and “outlet” of the model room is defined as “opening”; whereas the wall faces the openings is defined as “inlet” and the wall behind the model is defined as “outlet” boundary condition in order to prevent fluid from flowing into the domain. The thickness of wall is ignored. The fluid name is defined as “air” at room temperature of 25 °C.

### ***Numerical grids***

This series of investigations carried out using computer simulation technique. K-ε turbulence model is adopted. Both structured and unstructured grid have used. The number of grids is around 1,000,000 for this large scale simulation.

---

<b>Water Supply Velocity</b>	<b>mm/s</b>	<b>1</b>	<b>5</b>	<b>10</b>	
<b>Inlet Duct</b>	<b>Velocity</b>	mm/s	0.0337	0.7903	1.4414
	<b>Pressure</b>	Pa	0.0053	0.0587	0.3094
<b>Outlet Duct</b>	<b>Velocity</b>	mm/s	0.0336	0.7882	1.4598
	<b>Pressure</b>	Pa	0.0046	0.0412	0.2398

---

<b>Room Average Velocity</b>	mm/s	0.0024	0.0723	0.1529
------------------------------	------	--------	--------	--------

Table 7- 5 Flow statistics of 2D ventilated window with wing wall at 45 ° at different water supply velocity.

Flow statistics of the wing wall at 45 ° present in Table 7-5. It noticeably shows at a higher water supply velocity. The inlet duct velocity and outlet duct velocity get higher. The highest inflow and outflow velocity obtain at water supply velocity of 10mm/s while the pressure at this speed is of the biggest. At all the three speeds of 1mm/s, 5mm/s and 10mm/s, the inflow velocity and outflow velocity are similar. The streamline and flow path of the wing wall at 45 ° at water supply velocity of 1mm/s present in Figure 7-13 and Figure 7-14. At low water supply velocity, there is no significant inflow and outflow in the image.

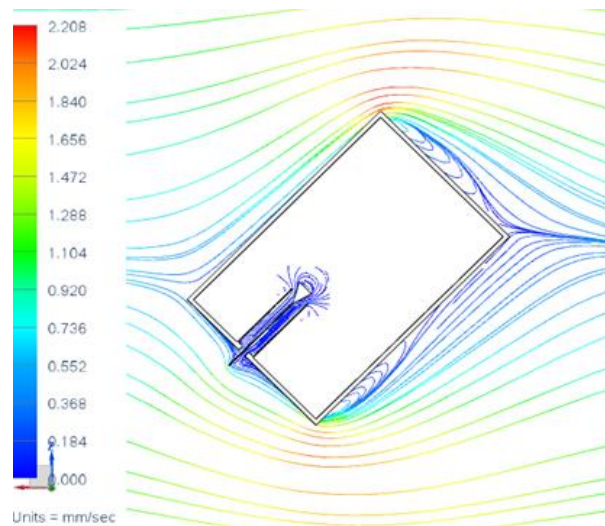


Figure 7- 13 Streamlines when the model places at 45 ° at water supply velocity of 1mm/s.

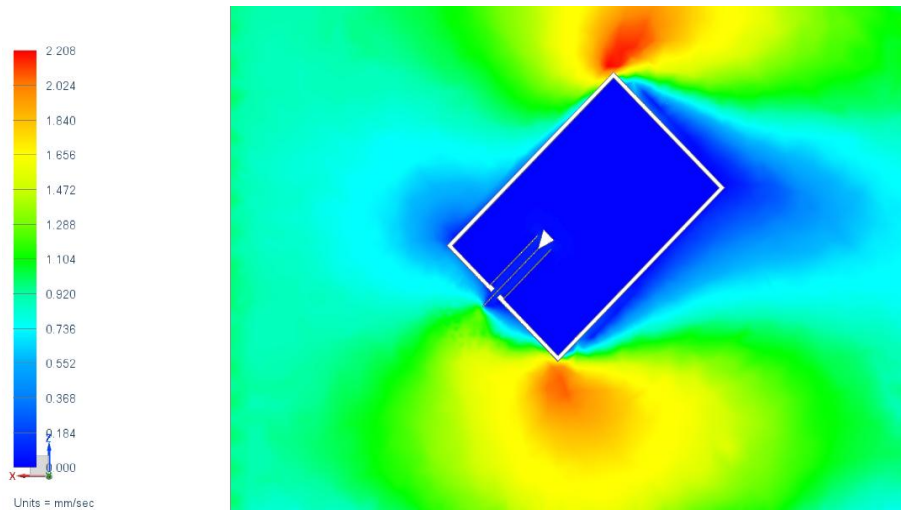


Figure 7- 14 Flow paths when the model places at 45 °at water supply velocity of 1mm/s.

Therefore, we have accelerated the speed up to 5mm/s. The streamlines and flow path shown in Figure 7-15 and Figure 7-16, correspondingly. There is a more visible inlet, and outlet flow comparing with the speed at 1mm/s, but the velocity is still low.

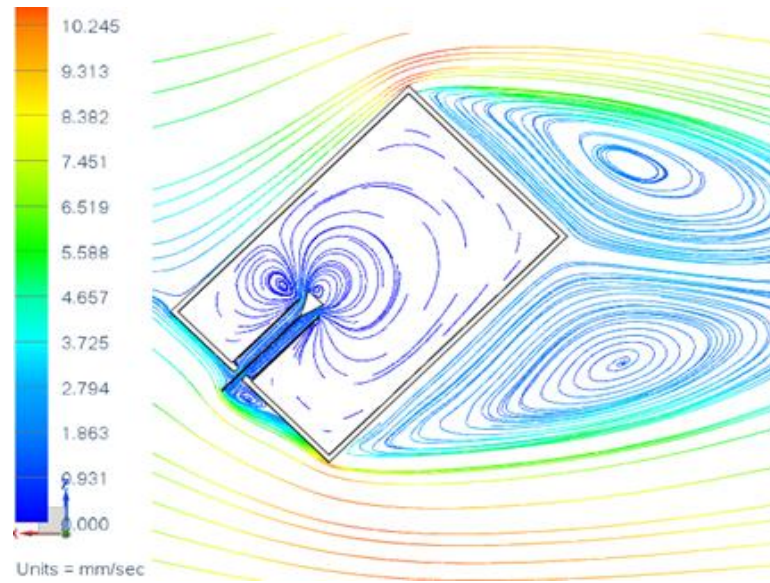


Figure 7- 15 Streamlines when the model places at 45 °at water supply velocity of 5mm/s.

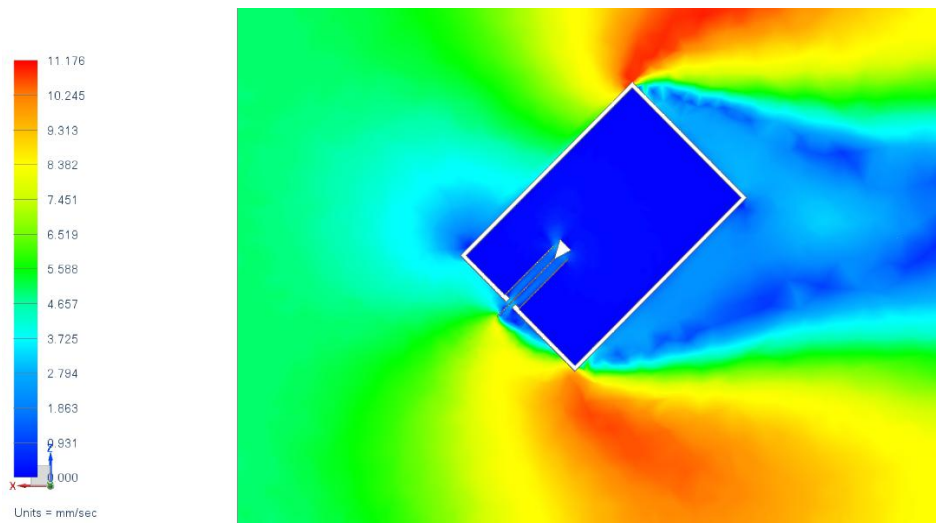


Figure 7- 16 Flow path when the model places at 45 °at water supply velocity of 5mm/s.

Again, we have to speed up the speed up to 10mm/s. The streamlines and flow path show in Figure 7-17 and Figure 7-18, correspondingly. There is a more



visible inlet and outlet flow comparing with the speed at 1mm/s and the speed at 5mm/s.

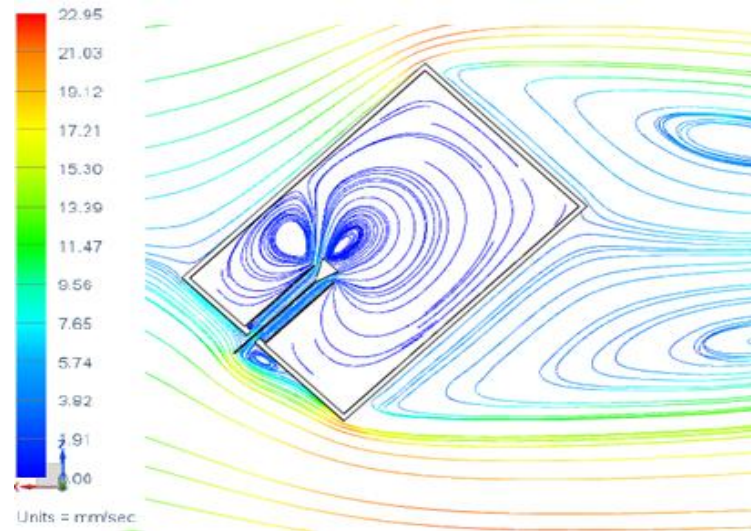


Figure 7- 17 Streamlines when the model places at 45 °at water supply velocity of 10mm/s.

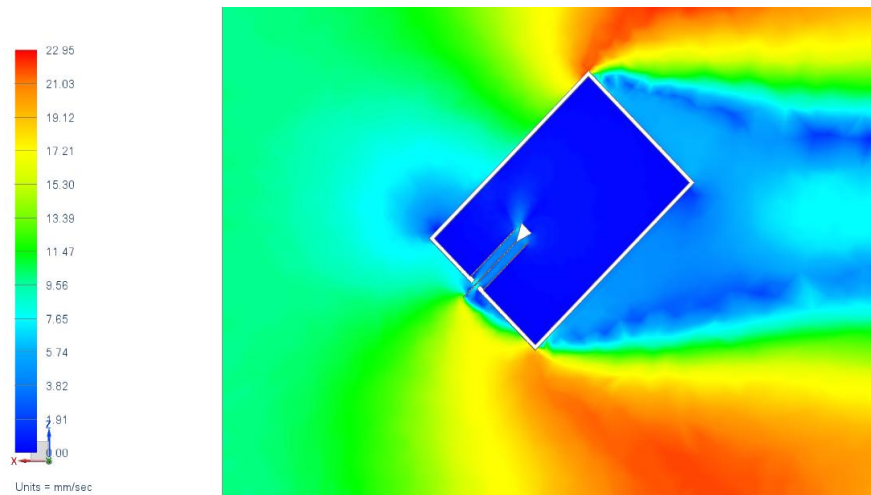


Figure 7- 18 Flow path when the model places at 45 °at water supply velocity of 10mm/s.

## 7.6 ROUNDED-INLET WING WALL AT 0 °, 45 ° AND 90 °

### *Geometry*

The improvement of airflow pattern has verified in this research. Modification of the design has carried out by: 1) adding two rounded-shaped triangular at each side of the wing wall and 2) making the two barriers at the two sides of the opening with a rounded-shape inlet. Figure 7-19 shows its configuration.

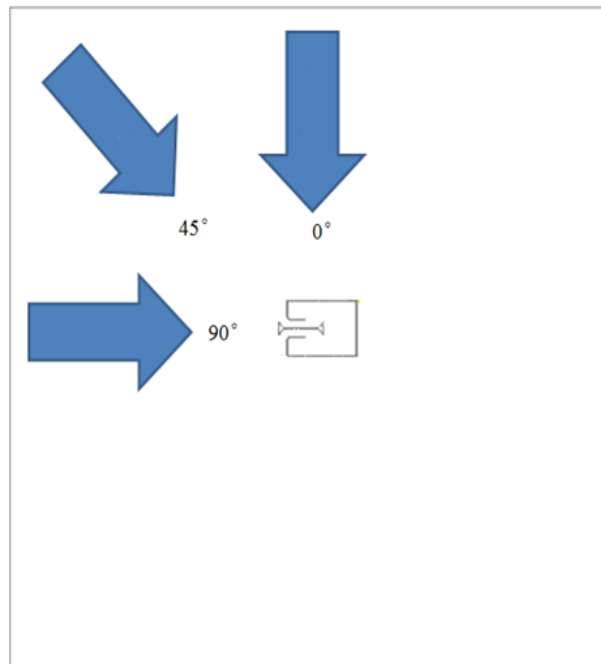


Figure 7- 19 Configuration of ventilated window with wing wall at 45 °.

### *Boundary conditions*

The hypothetical model is placed at the center in the environment. Large boundary will not adversely affect the boundary conditions at the domain

outflow (Figure 7-19). The “inlet” and “outlet” of the model room is defined as “opening”; whereas the wall faces the openings is defined as “inlet” and the wall behind the model is defined as “outlet” boundary condition in order to prevent fluid from flowing into the domain. The thickness of wall is ignored. The fluid name is defined as “air” at room temperature of 25 °C.

***Numerical grids***

This series of investigations carried out using computer simulation technique. K-ε turbulence model is adopted. Both structured and unstructured grid have used. The number of grids is around 1,000,000 for this large scale simulation.

The computational simulation of the revised design at 0 °, 45 ° and 90 ° in a water supply velocity of 5mm/s has carried out. The airflow statistics show in Table 7-6. At 0 ° to the prevailing wind, the inlet and outlet flow can achieve the greatest velocity.

<b>Flow Angle</b>	<b>Water Supply Velocity</b>		<b>5 mm/s</b>
<b>90 °</b>	Maximum Outlet Velocity	mm/s	0.0576
	Maximum Inlet Velocity	mm/s	0.0580

45 °	Maximum Outlet Velocity	mm/s	2.2284
	Maximum Inlet Velocity	mm/s	2.2738
0 °	Maximum Outlet Velocity	mm/s	2.8455
	Maximum Inlet Velocity	mm/s	2.9165

Table 7- 6 Airflow statistics at 0 °, 45 ° and 90 ° at a water supply velocity of 5mm/s.

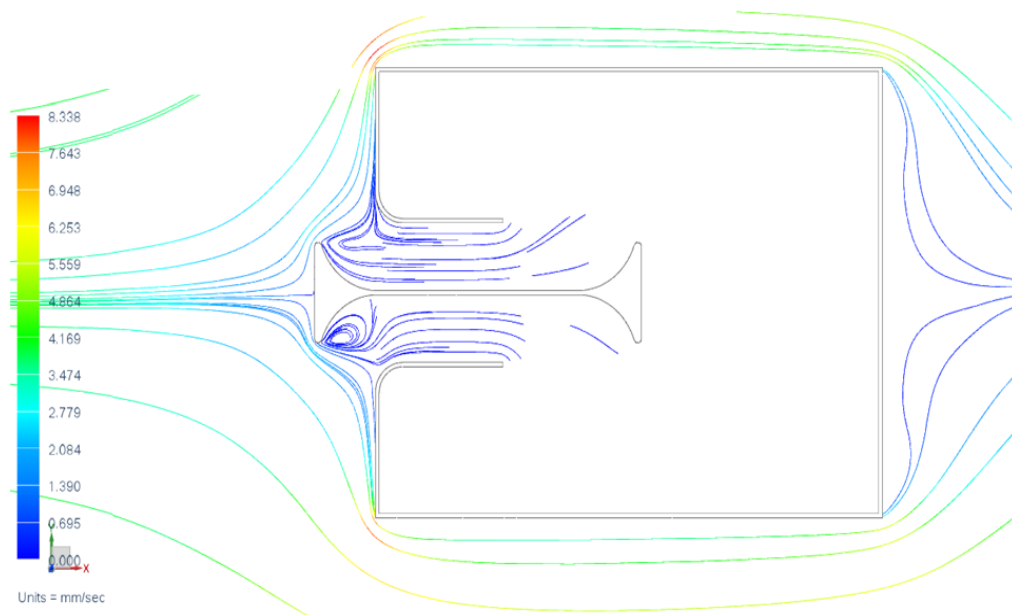


Figure 7- 20 Ventilated window with wing wall and rounded-inlet cylindrical ventilated duct in wind direction of 0 °.

Figure 7-20 shows the streamlines of rounded-inlet wing wall at wind direction of 0 °. The flow enters the room model through both the inlet and outlet duct at both sides of the wing wall. However, no airflow streamline can be observed

inside the room hence the ventilation is quite limited when the wind coming straightly. At 45° and 90°, visible inlet flow and outlet flow can be observed from the appearance of computational simulations from Figure 7-21 and Figure 7-22 respectively. The inflow and outflow velocity are higher at prevailing wind at 90° rather than at 45°. However, the turbulence at the top left corner of the image is bigger when the wind comes from a 90° than that comes from 45°.

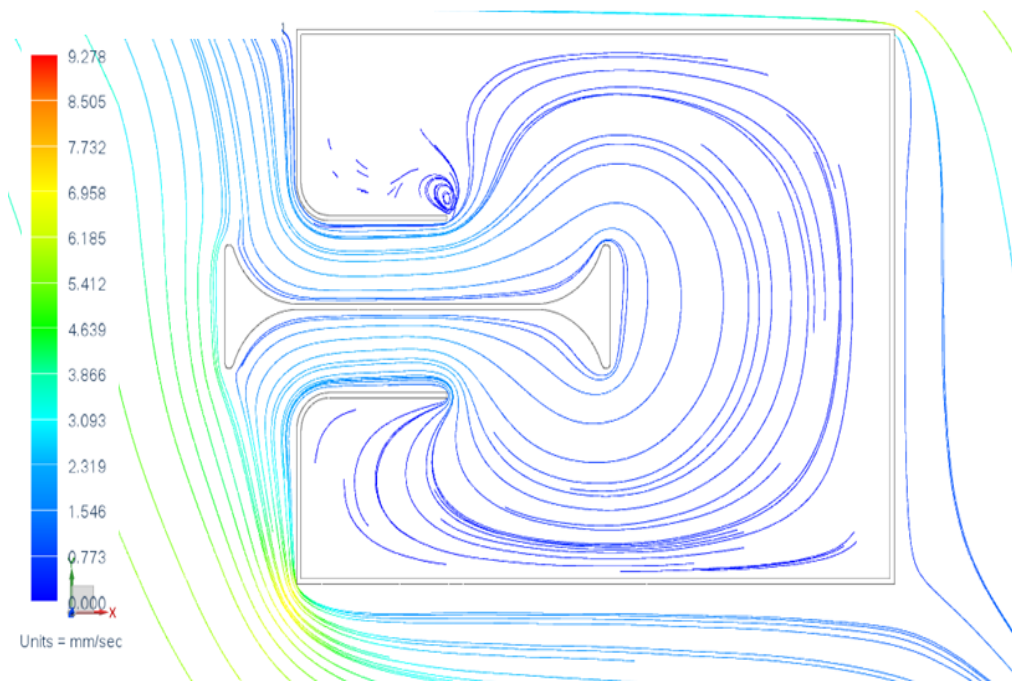


Figure 7- 21 Rounded-inlet wing wall at wind direction of 45°.

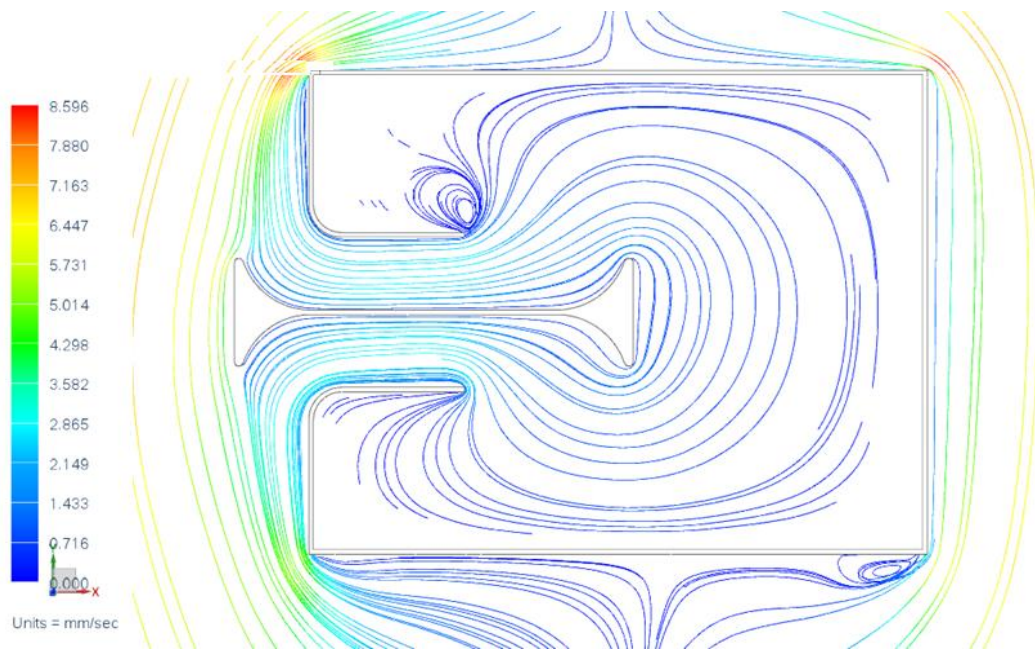


Figure 7- 22 Rounded-inlet wing wall in wind direction of 90 °.

## 7.7 DISCUSSION

With the application of CFD, the effects of wing wall and rounded inlet wing wall were studied. Figure 7-23 shows the percentage of air speed to wind speed by CFD at incident angle 45 ° for conventional window, conventional wing wall and with wing wall and barrier configuration. Inlet velocity and outlet velocity is low by using conventional window (no wing wall); and its performance is much better once installed with wing wall and barriers.

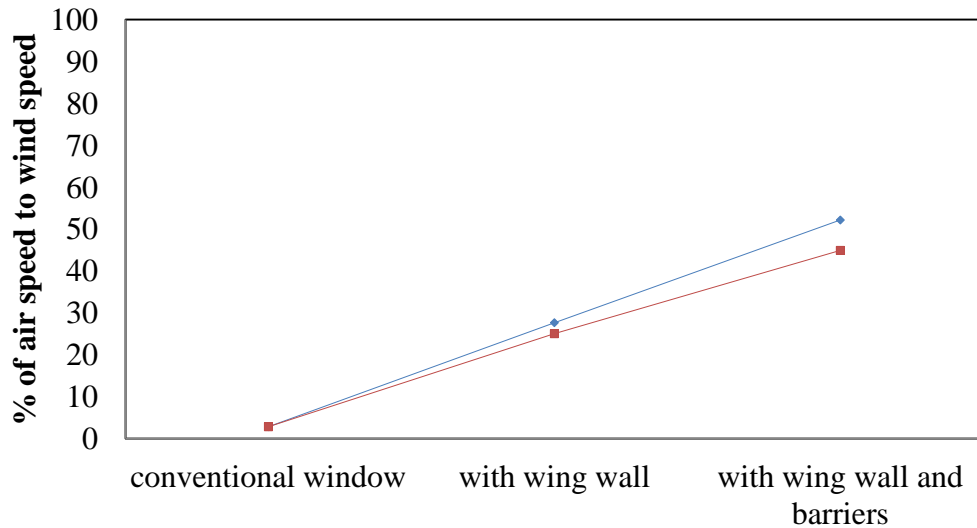


Figure 7- 23 Percentage of air speed to wind speed by CFD at incident angle of 45 ° for different configurations; —◆— inlet velocity; —■— outlet velocity.

Due to the good performance of ventilation of conventional window with wing wall and barrier design, the percentage of air speed to wind speed by CFD and by experimental at incident angle of 90 °, 45 ° and 0 ° for rounded-inlet wing wall is further carried out in Figure 7-24. At 90 °, the percentage of air speed to wind speed of inlet and outlet velocity is very low. Both CFD simulation and experimental measurement showed the best performance is at 0 °. There is positive correlation between CFD results and experimental results; hence there is a good agreement between the two methodologies.

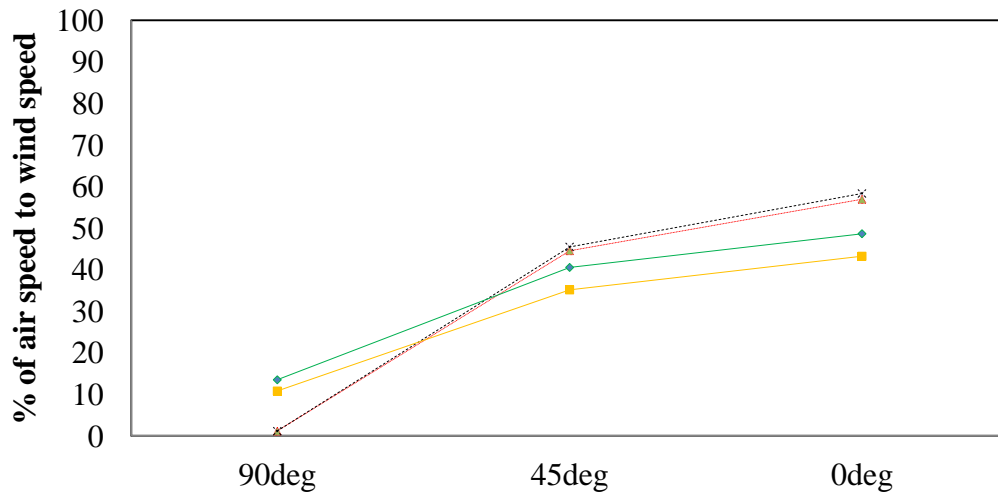


Figure 7- 24 Percentage of air speed to wind speed by CFD and by experimental at incident angle of 90 °, 45 ° and 0 ° for rounded-inlet wing wall; -x- outlet velocity-CFD; -x- inlet velocity-CFD; -■- outlet velocity- experimental; -◆- inlet velocity- experimental.

## 7.8 SUMMARY

The ventilation rate has improved in the receiving room comparing with that in the source room. Wind-driven natural ventilation is an effective way to preserve the luxurious and healthy indoor environment.

The application of CFD at the beginning of the model presents in this chapter. In a total of four groups of cases discuss in this chapter, which contain 1) conventional window; 2) conventional wing wall and the revised case; 3)



conventional wing wall with two barriers and the revised case; and 4) rounded-inlet wing wall. Among the case studies, rounded-inlet wing wall at prevailing wind at  $45^\circ$  has the best ventilation performance after considering all the factors, and this has a valid agreement with the Givoni's experimental results. The comparisons for effectiveness in natural ventilation illustrate in Table 7-6. The rounded-inlet wing wall can perform remarkably well for single ventilated room configurations in the model experiments. Wing wall with two barriers can also gain a greater ventilation performance, and it requires a higher prevailing wind than the revised rounded-inlet wing wall design.

Traditional windows need to be fully closed when the noise level is high outside; no natural wind can enter the indoor. Single-sided ventilation with wing wall can improve air circulation. The implementation of dual flow is better than the existing traditional single airflow window, which has a considerable potential for conserving energy and improving air quality. Therefore, especially during summer time, the performance of natural ventilation to control indoor level and temperature to cool buildings by increasing indoor air movements can be further enhanced.

# **CHAPTER 8**

## **FLOW VISUALIZATION**

### **8.1 INTRODUCTION**

Natural wind-driven ventilation due to the wind power is crucial to provide users thermal comfort in hot and humid weathers such as Hong Kong. Both CFD simulations and flow visualization analysis carry out in this research. The advantage of visualization technique of airflow is low cost compared with CFD simulation which takes much longer time and are still complex and cumbersome to be used by designers and architects because it needs higher initial cost and the necessity of in-depth knowledge on the computer and numerical modeling.

In this chapter, we describe the analysis of various airflow simulations performed with different physical scale models, using tracing method with a technique of direct injection of ink in the water, with a water table apparatus. It allows for an instantaneous and dynamic visualization of the airflow outside and inside the model, as well as a direct definition of the inlet and outlet penings. The photographic record of the experiments made with a Nikon digital camera, makes

the airflow analyses a highly intuitive, useful and amusing task. Dark ink used as the indicator for the visualization of extended lines. In this analogical experiment, we used tracing method and direct injection technique using continuous low speed.

### **8.1.1 Water Table Apparatus**

The main body of the experimental setup consisted of a) water inlet which controlled water flow; b) a removable color tray which supplied the injection directly into the clear water which is also easily removed and cleaned; c) a drainage pipe to collect the used water and make it easily to flow out. Physical configurations and dimensions showed in Figure 8-1. The water table consists of a horizontal glazing tray made of plastics over which the water flows in a certain direction. The transparency of the water tank design is simply for observers to determine the water flow.

The investigation conducts in a low-speed velocity of water at 0.57m/s corresponding to the flow Reynolds number of 4,680 (Wakeling & Ellington, 1997; Tavoularis, 2005); creating the field of the experiments and observations.

Water allows to flow evenly across the table on which about 1.5 to 2cm deep horizontal or vertical slice of a model placed. Water can flow through the opening of the different models. After a steady-state movement has achieved, dyed water pours into the color tray, to create parallel turbulent flow. As these dyed streams pass through the model, it is possible to determine where water is moving and where it is stagnant.

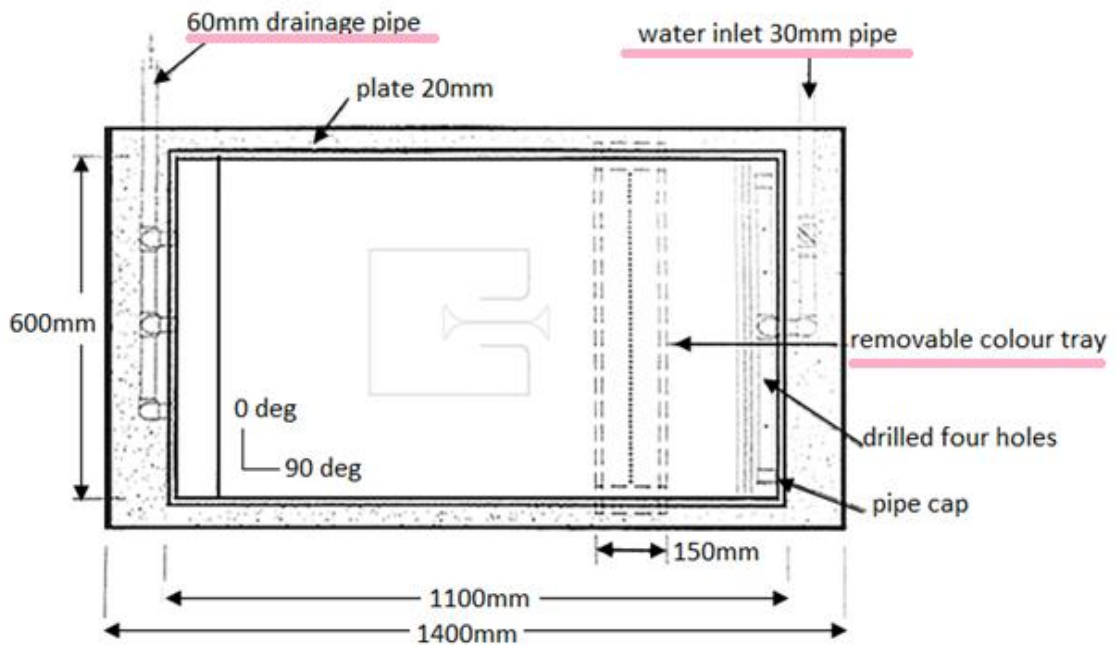


Figure 8- 1 Physical dimension and plan view of the water table for ventilation

test.

### 8.1.2 Reynolds number

Reynolds number defined for “a number of different situations where a fluid is in relative motion to a surface” (Reis et al., 2011).

$$Re = \frac{\rho v L}{\mu} = \frac{v L}{\nu} \quad (8-1)$$

Where,

$V$  is the mean velocity of the object relative to the fluid (m/s)

$L$  is a characteristic linear dimension, (travelled length of the fluid or hydraulic diameter) (m)

$\mu$  is the dynamic viscosity of the fluid (kg/ms)

$\nu$  is the kinematic viscosity (m<sup>2</sup>/s)

$\rho$  is the density of the fluid (kg/m<sup>3</sup>)

Therefore, Reynolds number of air calculated as:

$$Re = \frac{\rho V L}{\mu} = \frac{V L}{\nu} = \frac{1.293 \text{ kg/m}^3 \times 1 \text{ m/s} \times 0.05 \text{ m}}{1.33 \times 10^{-5} \text{ kg/ms}} = 4860$$

Therefore, the velocity of water flow in the water flow experiment,  $V=0.57\text{m/s}$ .

## **8.2 FLOW VISUALIZATION**

Flow visualization by direct injection technique conducted to verify the numerical results visually. A counter flow ventilated window model (made of sandwich plastic sheets). Several experiments selected to develop the methodology potential. The models of conventional window, conventional wing wall, and ventilated window with wing wall plus rounded-inlet ventilated duct at different incident angles of inflow have tested in the flow visualization studies.

Several trials with a scale of 1: 20 placed in the water tank. A similarity between the external wind flow for the building at Hong Kong and that for the ventilated window building model calculated based on Reynolds number (Nitawichit et al., 2008). In this experiment, the velocity of ink injection moved at the same speed as water.

### **8.2.1 Conventional window**

The first set of the trial performed for wind direction at 45 °, and in a single ventilated room for conventional window. The flow visualization presented in

Figure 8-2. The geometry of conventional window showed in (a) which placed at 45 °to the water tank. (b) Showed the changes of flow patterns

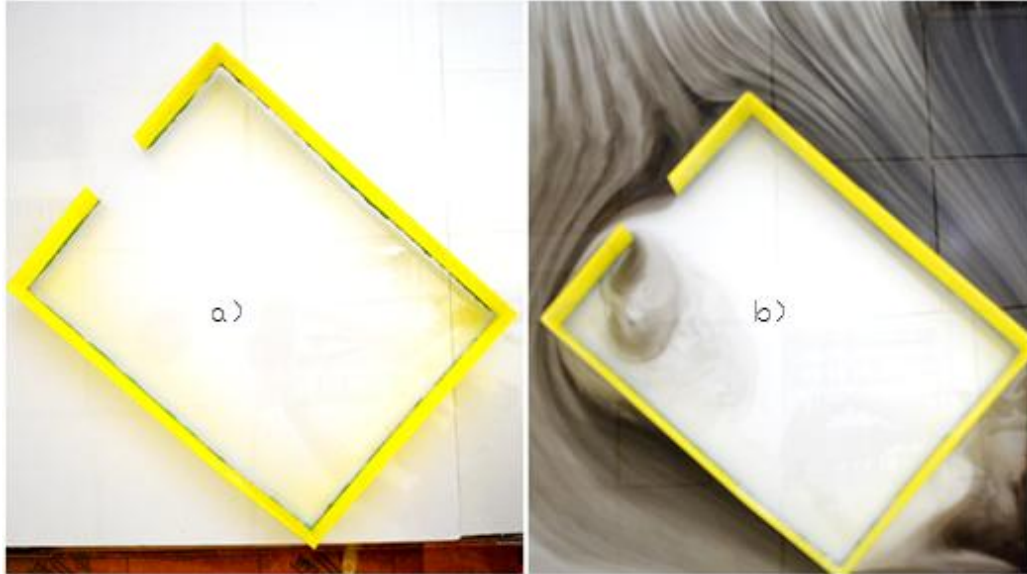


Figure 8- 2 Flow visualization for conventional window.

The inflow and outflow patterns were insignificant as shown in Figure 8-2. Only a small amount of ink injections concentrated inside the left-side of the opening once the mockup placed at 45 °to the wind direction. This simulation presented the flow patterns of conventional window in a single ventilated window. All the flows smoothly passed beside the model, but little ventilation can go through the room.

### 8.2.2 Conventional wing wall

The second set of the trial performed again for wind direction at  $45^\circ$ , and in a single ventilated room for conventional wing wall. The flow visualization presented in Figure 8-3. The geometry of conventional wing wall showed in (a) which placed at  $45^\circ$  to the water tank. (b) Showed the changes of flow patterns. Inflow and outflow became significant this time comparing with the conventional window. There are changes in the outflow path throughout the room. One can observe almost no airflow in the room model for the open window; however, after putting a wing wall in the room model the improvement of airflow is obvious. The flow in this case could cover most of the room space and most of the airflow concentrated at the central room model.

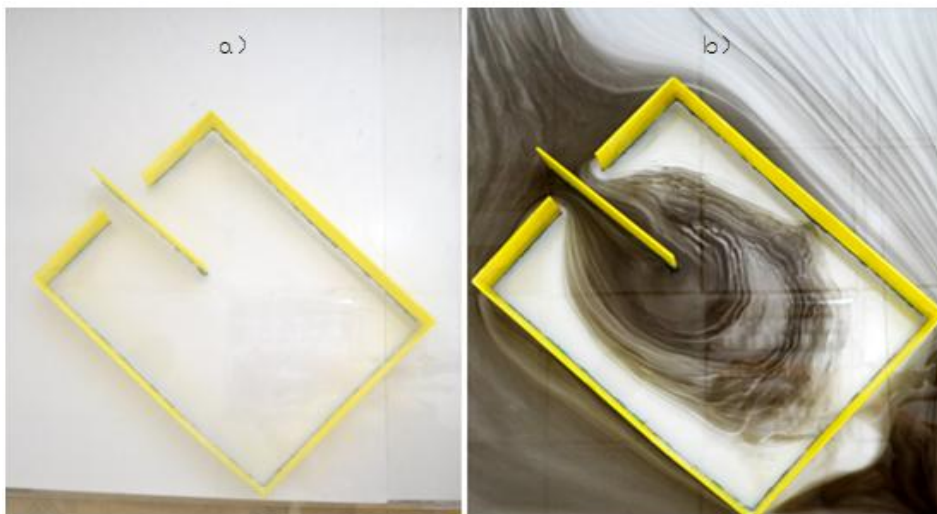


Figure 8- 3 Conventional wing wall.



### 8.2.3 Rounded-inlet wing wall at 0°, 45° and 90°

As mentioned above, the inflow and outflow of wing wall were more significant comparing with the conventional window. There are changes in the outflow path throughout the room. Modifications of the effectiveness of conventional wing wall carried out in the design. Rounded-inlet wing wall (implied a rounded inlet at each side of the traditional wing wall) tested to verify the effectiveness of ventilation performance and see whether there was any improvement comparing with conventional wing wall. Thus, the next trials in this research performed for wind direction from 0°, 45° and 90°, and in a single ventilated room for rounded-inlet wing wall.

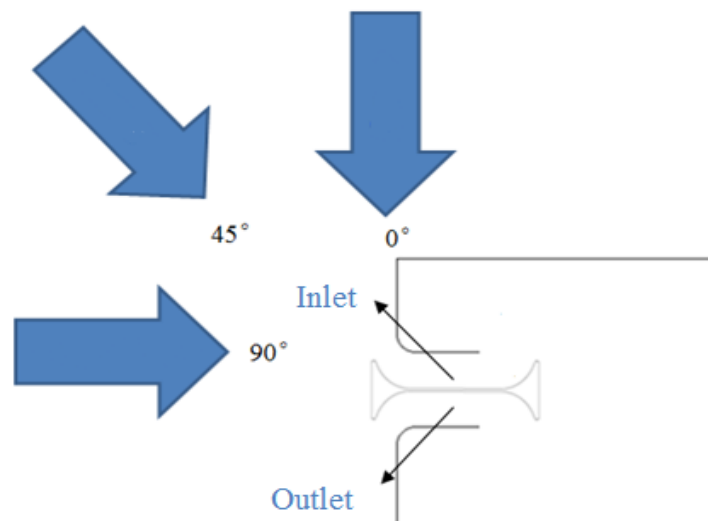


Figure 8- 4 Physical configuration of rounded-inlet wing wall.

Figure 8-5 presented the experiment observations; a) geometry of the ventilated window with rounded-inlet wing wall; b) at 0 °; c) at 45 ° and d) at 90 °.



a)



b)



c)



d)

Figure 8- 5 Flow patterns of rounded-inlet wing wall.

The result for tracing method for angles of incidence of  $0^\circ$ ,  $45^\circ$  and  $90^\circ$  showed in Figure 8-5. The results indicated in any cases of the experiments, part of the flow entered directed into the room model. At any incident angle of the perceiving wind, the airflow can be observed in the room model.

At  $0^\circ$ , the streams flowed downwards as the same direction of the colored water flow in the water tank. Water flow looked steadily entered into the inlet side of the rounded wing wall; however, the outflow of the streams was not detectable.

There is invisible appearance of any airflow, but powerful circulation can be observed inside the model room.

At  $45^\circ$ , it presented a discreet air movement in the model room. The movement in and out is clearly presented. The angle it makes is about like a circulation with the stream directions in the water table. There is a form of visible inflow and outflow at each side of the rounded-inlet wing wall. Small turbulences can also detect in this flow visualization.

At  $90^\circ$ , there are changes in the inflow path throughout the space. Because of the length of the wing wall, part of the stream can run into the model and the other

part of the stream flow off to the other side of the water table as the direction of the water flow. In this test, it does not show any significant change in the outflow inside the room model.

### **8.3 SUMMARY**

Flow visualization is an essential tool to understand the nature of the flow. It provides realistic information that can help determine flow characteristics. The study showed the first evaluations of various analogical airflow simulations performed with scaled model, using the technique of direct ink injection of detergent into the water, with an apparatus called the water table, developed in the laboratory.

The failure of conventional windows has confirmed in the previous studies. From the flow visualization observed in the study, the rounded-inlet wing wall played a better role in enhancing the natural ventilation performance and the presentation of volume of air flow is much better than the ventilation performed by conventional window.

Secondly, wing wall performed meritorious ventilation performance in a single-ventilated room, which is also a valuable benchmark in using natural ventilation in residential buildings in Hong Kong due to its limited space. Many of residences in Hong Kong only support single ventilation.

The studies have clearly shown the advantages: it allows for an instantaneous and dynamic visualization of the airflow outside and inside the room model, as well as a direct and clear explanation of the inlet and outlet opening. The photographic record of the experiments made with a digital camera makes the airflow analyses a remarkably intuitive and effective mask. One can conclude that although the proposed technique is an analogical model and allows only for bi-dimensional airflow visualization, the water table appears to be a tremendously effective tool for supporting the airflow patterns of natural ventilation of ventilated window with wing wall design. For sure, flow visualization is not the only way to understand the flow, but it can help in highlighting the usefulness of the flow visualization techniques.

# **CHAPTER 9**

## **DISCUSSION**

### **9.1 INTRODUCTION**

Numerous studies have shown the effectiveness of noise control in enclosed rooms and other environments for cancelling engine noise and low frequency noise in general. However, there is no research on how both acoustic comfort and ventilation can be achieved. This research will determine whether there is any connection between noise reduction and ventilation and to develop new design which can make a balance between acoustic energy and ventilation.

### **9.2 SUMMARY OF MAJOR FINDINGS**

Wind-driven natural ventilation is an effective way to preserve the comfortable and healthy indoor environment. The conventional wing wall design can perform extraordinarily well in single-sided ventilated room. This assumption has been proven both by previous literature reviews and experimental measurements and

simulations. One key finding of this research is that the single-sided ventilation incorporated with wing walls could benefit from the dual flow ventilation and substantially improve the interior air circulation compared with that without wing walls (Figure 9-1 and Figure 9-2). Indoor ventilation can be achieved at each different angle in the tests of ventilation performance of conventional wing wall.

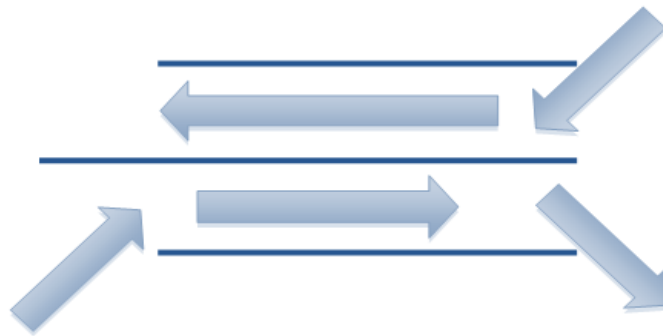


Figure 9- 1 Top views of a dual-flow ventilated window with wing wall.

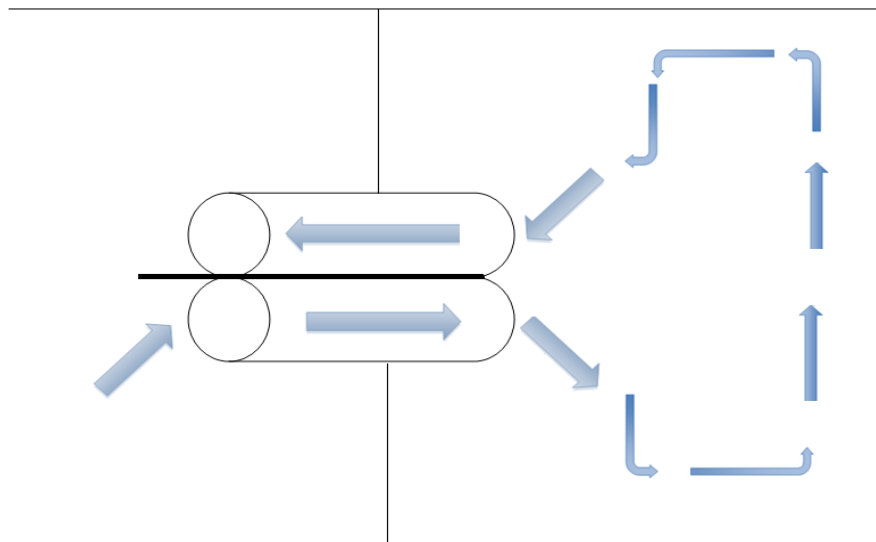


Figure 9- 2 Flow directions of dual-flow ventilated window with wing wall in a single-ventilated room.

In the acoustics aspect, membrane absorbers have the most significant Transmission loss is also significant at a lower frequency level in both of the small-scale and full-scale acoustical experimental measurements in the research when the membrane absorber combined with MQWRs. The duct is simple to be fabricated, and the durability is much higher than that of the conventional fibrous acoustic material. The measured values of the attenuation are in reasonable agreement with the theory. Ventilated window with MQWRs design would not prevent any wind coming through the opening in the experiments.

Further improvements of the design had implemented by changing made the inlet of the wing wall into a rounded inlet rather than straight-inlet rectangular duct (Figure 9-3).

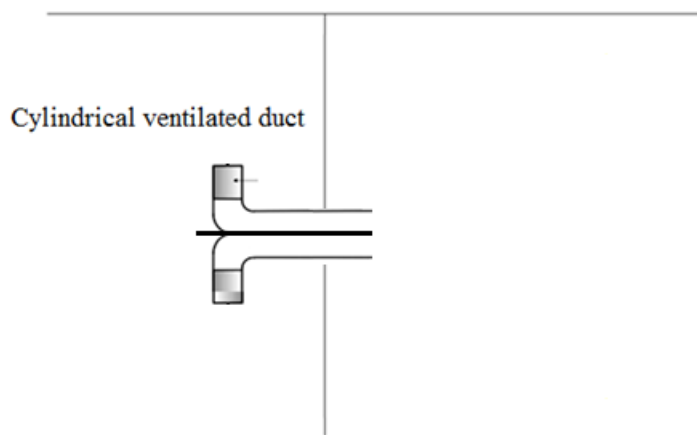


Figure 9- 3 Rounded-inlet cylindrical ducts with wing wall design.

The application of CFD for identifying the movement patterns of a total of four



groups of cases carried out in the research contained: 1) conventional window; 2) conventional wing wall and the revised case; 3) conventional wing wall with two barriers and the revised case; and 4) rounded-inlet wing wall. Among the case studies, rounded-inlet wing wall at prevailing wind at  $45^\circ$  has the best ventilation performance after considering all the factors, and this has a valid agreement with the Givoni's examination results. The performance of wing wall is dependent on wind directions, wind speeds and its size. The rounded-inlet wing wall can perform well in single-sided ventilation, in the model experiments. Wing wall with two barriers can also obtain a superior ventilation performance. It requires a higher prevailing wind than the revised rounded-inlet wing wall design. Flow visualization in this research again verified the air flow patterns obtained from CFD simulations; hence the rounded-inlet wing wall played a better role in enhancing the natural ventilation performance and the coverage of space of air flow is much better than the ventilation performed by conventional window from the simulation results. One of the significance of this research may well be a manifestation of the potential use of the CFD techniques or flow visualization techniques, rather than a generalization of the wing wall experimental or numerical performances.

### **9.3 IMPLICATION OF THE DESIGN**

Conventional window is difficult to fulfill all the functions of noise reduction, lighting and natural ventilation. Figure 9-4 the collisions of noise control with ventilation and lighting function in an openable window. Traditional openable window cannot fulfill all the functions of noise reduction, lighting and natural ventilation.

Large opening ensures ventilation, but it always incurs high noise level due to heavy traffic. There is a conflict between sound and airflow; silencer then needs to be installed in order to improve its sound attenuation performance. In summer time, curtains or double façade are essential in detecting direct sunlight and the direct heating going through the lighting window.

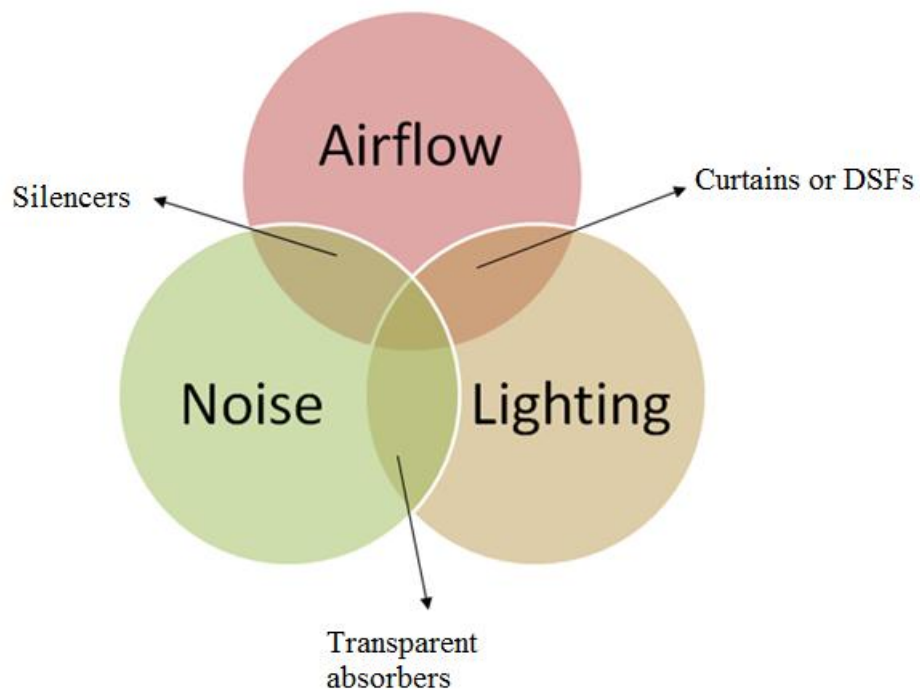


Figure 9- 4 Overlapping functions of a conventional window.

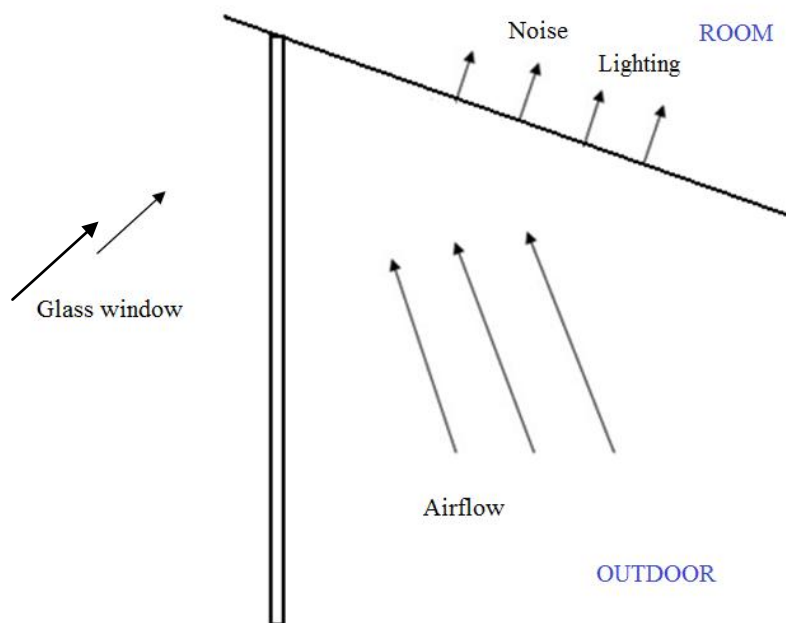


Figure 9- 5 Conventional windows at daytime (top view).

Figure 9-5 shows that the airflow comes into the room at daytime, sound and lighting come in directly at the same time. Figure 9-6 shows noises can still come into the room through conventional window when we use curtains at night time or daylight shading mode; however airflow blocks by curtains in this situation.

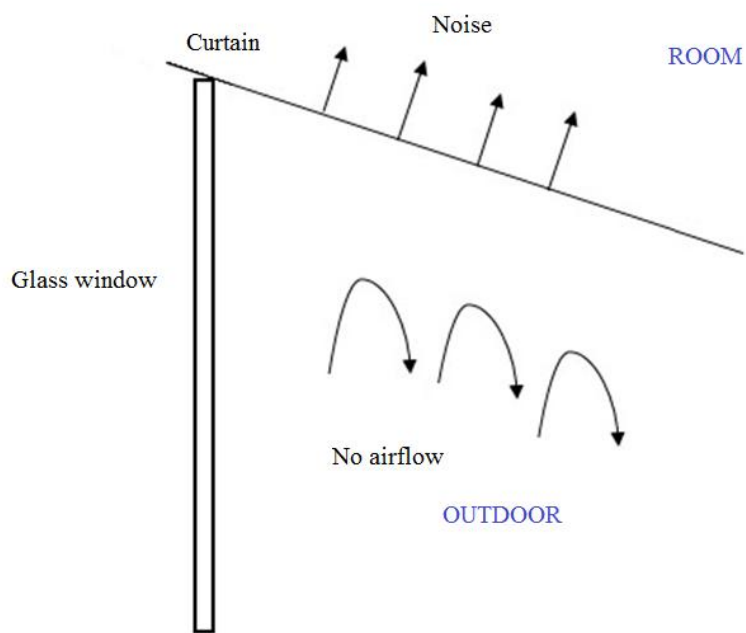


Figure 9- 6 Conventional windows at night time/ sun shading mode (top view).

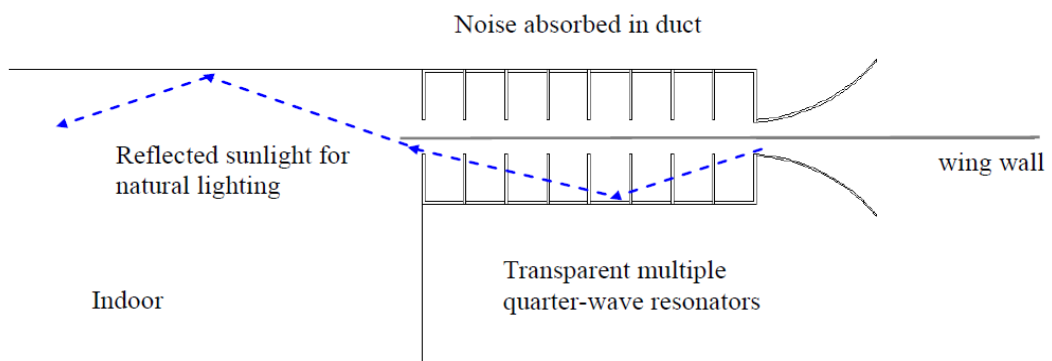


Figure 9- 7 Functions of ventilated window design at sun shading mode.

Functions of ventilated window design at sun shading mode showed in Figure 9-7.

A combination of ventilated window with wing wall is the original concept contrasting with separated conventional window or wing wall. Figure 9-8 and Figure 9-9 explain the functions and views of the wing wall design, respectively.

Multiple ducts and the silencer will to some extent help to reduce the lighting.

While the wing wall and the silencer would enhance the airflow performance and sound attenuation. Lighting function could be maximized since there is no conventional frame. Heat loss could be prevented in winter season and ventilation could be improved in hot seasons at the same time.

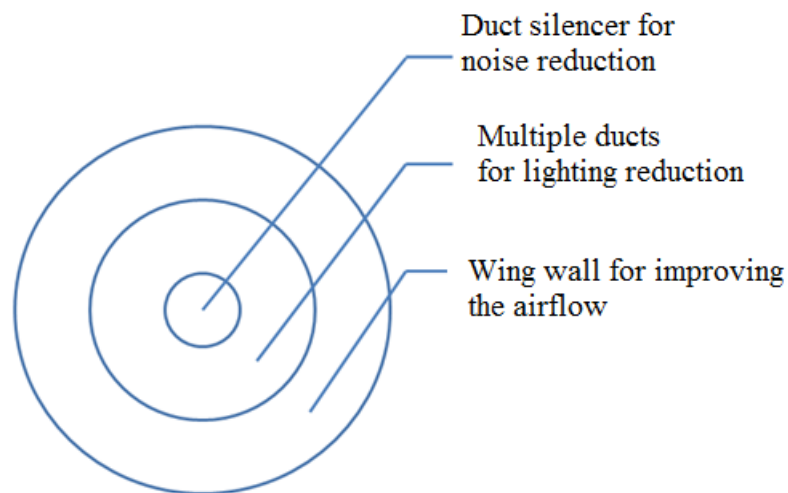


Figure 9- 8 Functions of the wing wall design.

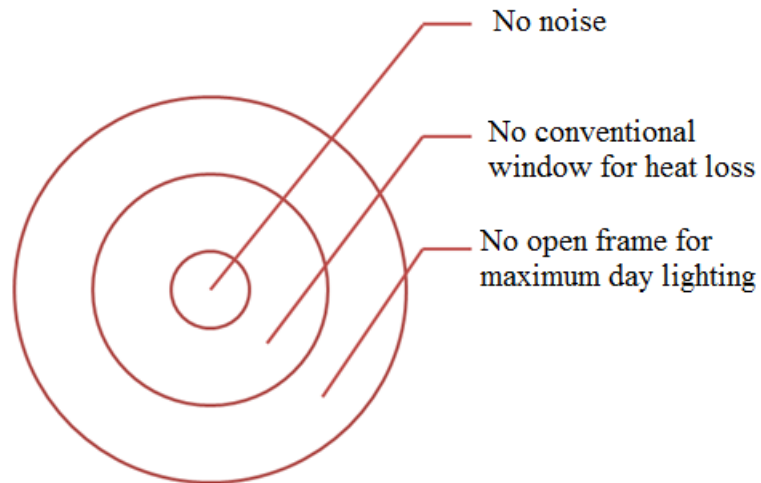


Figure 9- 9 View of the wing wall design.

When the airflow comes through the wing wall, the multiple ducts absorb noise and lighting immediately, whereas the closed lighting window can fulfill the requirement of lighting but also can stay away from noise and heat during daytime. Figure 9-10 shows the functions of ventilated window with wing wall design at daytime. Figure 9-11 shows the functions of ventilated windows with wing wall design at night time or sun shading mode. Curtains stop lighting or heating, but the ventilation flows into the room while noise attenuation performance can be achieved in multiple ducts.

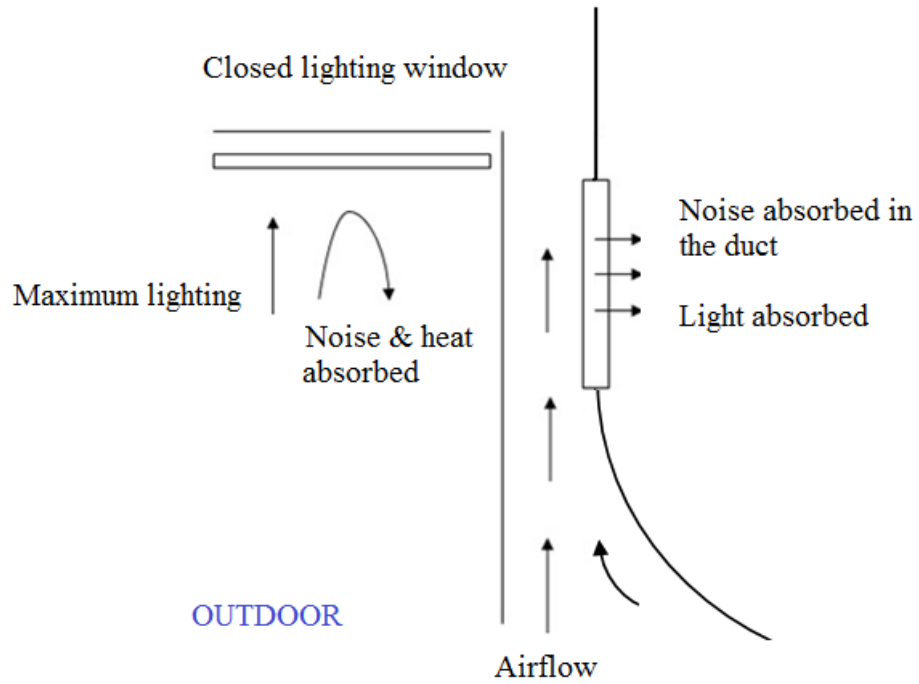


Figure 9- 10 Functions of ventilated window with wing wall design at daytime.

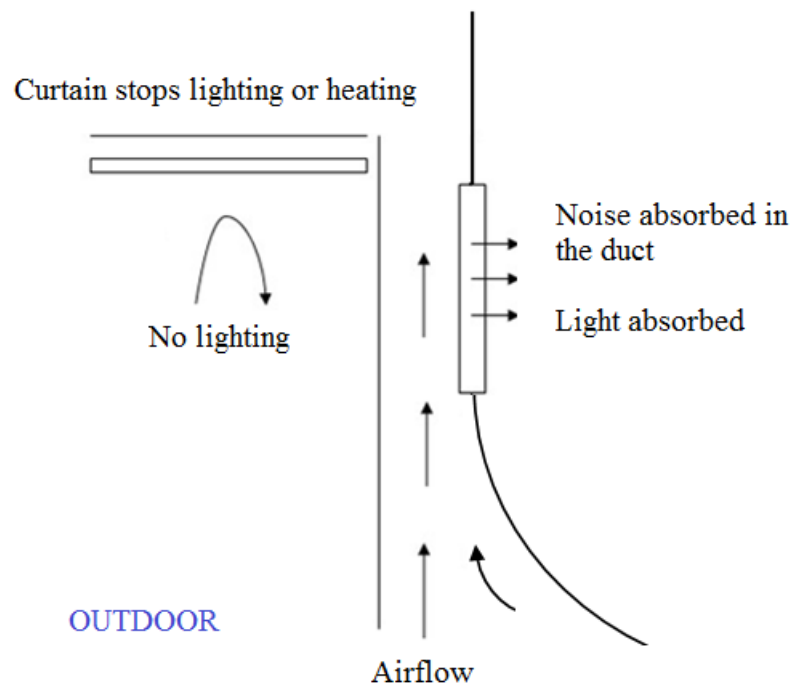


Figure 9- 11 Functions of ventilated window with wing wall design at night time or sun shading mode.

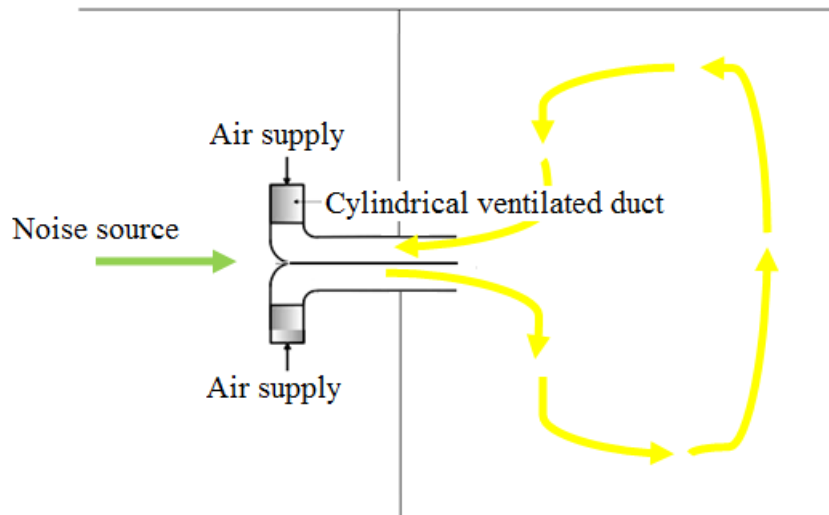


Figure 9- 12 Functions of rounded-inlet cylindrical duct.

Rounded-inlet ventilated duct (Figure 9-12) has satisfactory performance in noise attenuation at any incident angle of the noise source. Even without combining with any acoustic absorptive materials, the ventilated duct can still perform much better than the conventional window in noise reduction. From the measurements of the transmission loss inside the duct, the length and the exposed area of the duct are also crucial in acoustics performance. The duct is similar to a standard acoustic expansion chamber with extended inlet and outlet expansion chamber. The value of such a design is that part of the chamber between the extended pipe and the sidewall acts as a side branch resonator and thus improving the transmission loss.



# CHAPTER 10

## CONCLUSION

### 10.1 INNOVATION OF THE DESIGN

The innovation of the design is the rounded-inlet cylindrical duct; which does not use any absorption materials but can achieve satisfied performance in noise attenuation and in ventilation as discussed in the above chapter.

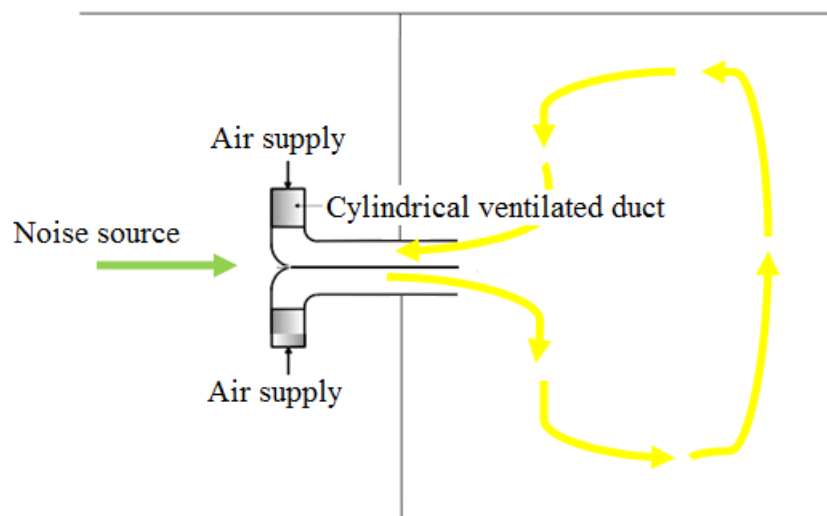


Figure 10- 13 Functions of rounded-inlet cylindrical duct.

The ideal configuration of the rounded-inlet duct is when it faces  $90^\circ$  to the noise source and  $0^\circ$  to the air supply as shown in Figure 10-1. The overall noise reduction can achieve 24dB without using any absorption materials and 70% of

free air flow could pass through the duct opening compared to zero for single sided duct.

Sound attenuation due to muffler effect happens when there is the impedance changes caused by sharp changes in cross-sectional area and the acoustic resonance set up inside the chamber. Sound wave passes through the inlet tube then undergoes sudden expansion then contracts again when leaving through the outlet tube. The greater the ratio of expansion or contraction chamber to the inlet or outlet tube is, the higher will be the sound reduction.

By tuning the extensions to the pass bands of an expansion chamber it is possible to produce a combination of the broadband attenuation domes of an expansion chamber with the resonant peaks of the extended tube resonator. Efficiency decays at standing wave but can significantly reduce noise at other frequencies. Besides the reactive muffler effect there is also quarter-wave resonance at each side of the duct inside as indicated in the boxes (Figure 10-2).

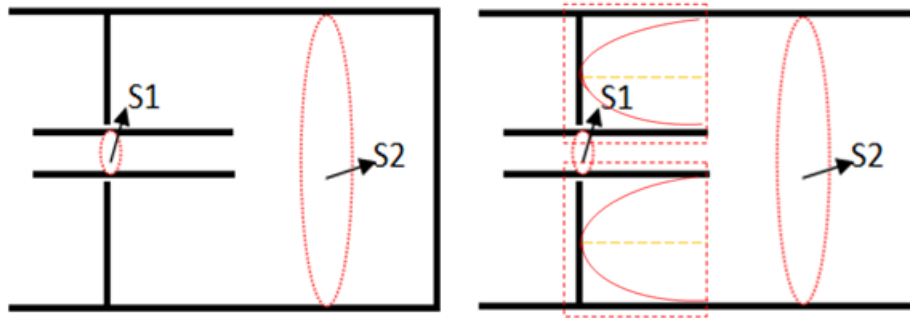


Figure 10- 14 Expansion chamber with extended inlet and outlet.

## 10.2 CONCLUSION

Conventional windows need to be fully closed when the noise level is high outside and no natural wind can enter the indoor space. The ventilated window with wing wall design can provide better human thermal comfort comparing with conventional windows.

Many of residences in Hong Kong only support single sided ventilation. Single-sided ventilation incorporated with wing walls is better than the existing conventional window. Especially during summer time, the production of natural ventilation to control indoor fresh air and to cool buildings can be further enhanced.

Use of multiple-wave resonators to replace the traditional absorption materials can improve the durability, to avoid small particle emissions and toxic gas due to fire. The noise attenuation performance of such a design is obvious and is similar as the performance of membrane absorber. At the same time, it would not block the airflow.

Rounded-inlet cylindrical ventilated duct has satisfactory performance in noise attenuation even without combining with any acoustic absorptive materials comparing with dual-flow ventilated mode (with/without a wing wall). The duct between source and receivers' room is similar to a standard acoustic expansion chamber with extended inlet and outlet expansion chamber. Maximum attenuation occurs when the section length is equal to a quarter wavelengths, which also defines the frequency of maximum attenuation. The value of such a design is that part of the chamber between the extended pipe and the sidewall (rounded-inlet of the duct) acts as a side branch resonator and thus improving the transmission loss.

In this research, both CFD and flow visualization techniques have been carried out to examine the flow patterns of air in different types of design. The CFD

models only apply to examine and evaluate the movement patterns and vector movements. Flow visualization is inexpensive and less time-consuming comparing to the CFD simulations. It also gives people a complete view of the water flow patterns in order to understand the air ventilation flow path of the model. The operation is relatively easy unless the water flow rate has to be carefully controlled. This work also suggests CFD and water table experimental measurements are useful tools for the study of the performance of green features in buildings in the future.

The key findings to improve noise reduction and ventilation performance are as followed:

There are some limitations to this research that regulate the generalization of the results. The wind velocity measurements in small-scale and full-scale experiments had tested only in front of the inlet and outlet opening, but not in the room. The test is not free of errors. The air movements keep changing at all the time due to the unsteady characteristics of wind. Data we collect in this study is the average velocities collected during 60 seconds for each measurement.

Measurements by anemometer cannot determine the airflow patterns and cannot be used as accurate data for calculations and predictions.

CFD simulations in this research only used to determine the general airflow patterns and pressure distributions. As the computational simulation required additional time and expertise to understand and utilize, we did not consider all the input factors during the study process such as boundary conditions, height of the building, and bioclimatic condition.

Presentations of the flow visualization simulation results in this study could be improved in the future studies. The models we used in this simulation are considerable simple, upright design with more accurate dimensions should be cautious. Some of the figures did not look satisfied as the ink injections may vary at each distinct operation.

# Appendix I

## PolyU Homantin Hall Noise and Ventilation Measurement Report

### 1. INTRODUCTION

A site visit was carried out on 4<sup>th</sup> September 2012 to the new PolyU Homantin Hall. Air flow measurement and noise measurement were conducted during the site visit. This report presents the results of the noise and ventilation measurement of the new double glaze window in the new PolyU Homantin Hall.

#### **New Design Single sided glazed ventilated window**

The single sided glazed ventilated window in student rooms consists of two panes of glass that aimed at provide soundproofing while maintaining good ventilation as shown in Figure 1.



Figure 1: Photos of the new design single sided glazed ventilated window.

## **2. MEASUREMENT DETAILS**

The new hall is located in Homantin where is nearby the Chatham Road and Fat Kwong Street. Chatham Road is one of the busier roads in Hong Kong with the annual average daily traffic over 110,000 cars. Therefore, traffic noise is one of the major concerns. Site measurement was conducted to measure the noise reduction and natural ventilation performance of the single sided glazed ventilated window.

### **Noise Measurement**

Two Svan 948 noise level meters were set separately to measurement the noise level outside the window and inside the room. The noise level meters were set to auto mode and the measurement range was set from 20 Hz to 20000 Hz with measurement interval of 10 second.

### **Air Flow Measurement**

Air flow speed was measured near the window in bedroom with situation of door closed and door opened.



### 3. RESULTS

The noise reduction and air flow result is shown in the following Table 3 and Figure 4. The noise attenuation of the new design single sided glazed ventilated window is between 10.4 dB(A) to 16.9 dB(A), while conventional window have 10.4 dB(A) noise reduction.

According to the result, the natural ventilation performance of the window was poor when the rooms' door is close and the wind speed was up to 4.4m/s when the door was opened, details are shown in Table 4.

Measurement ID	Floor level	Major noise source	Window type	Noise Level		Noise Reduction, dB(A)
				Outside window	Inside window	
NSR1	23/F	Traffic and construction noise	Double glazed window	79.1	66.3	12.8
NSR2	23/F	Traffic noise	Double glazed window	72.1	55.2	16.9
NSR3	14/F	Traffic noise	Conventional window	74.3	63.9	10.4
NSR4	14/F	Traffic and construction noise	Double glazed window	78.4	66.1	12.3
NSR5	4/F	Traffic noise	Double glazed window	67.9	54.9	13
NSR6	23/F	Traffic and construction noise	Double glazed window	69.4	58.3	11.1
NSR7	23/F	Traffic noise	Double glazed window	70.8	60.4	10.4

Table 1: Noise Measurement Result

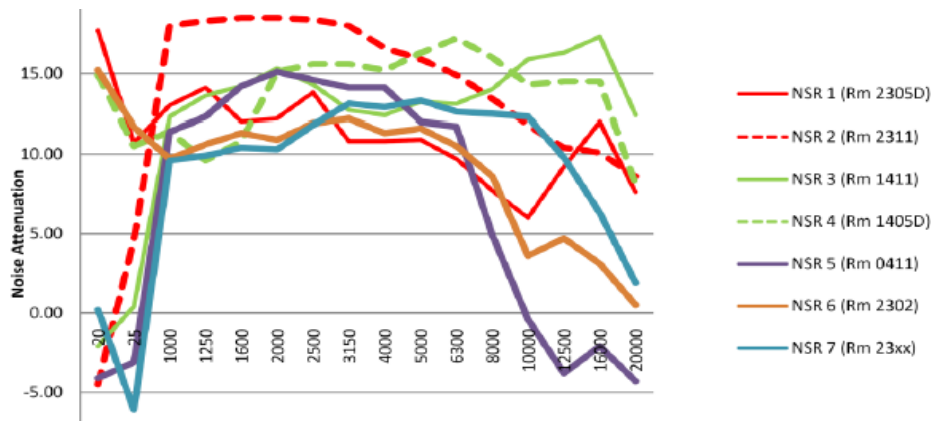


Figure 2: Noise attenuation of the single sided glazed ventilated window

Measurement ID	Floor level	Window type	Wind speed, m/s	
			With door closed	With door opened
NSR1	23/F	Double glazed window	0.4 to 0.7	0.5 to 1.5
NSR2	23/F	Double glazed window	0 to 0.5	1.1 to 4.4
NSR3	14/F	Conventional window	No wind	0.4 to 0.9
NSR4	14/F	Double glazed window	No wind	1.1 to 1.2
NSR5	4/F	Double glazed window	0 to 0.4	1.1 to 3.0
NSR6	23/F	Double glazed window	0 to 0.6	0.5 to 1.7
NSR7	23/F	Double glazed window	0.4 to 0.7	1.2 to 2.5

Table 2: Air Flow Measurement Result.

#### 4. CONCLUSIONS

The acoustic reduction performances of the single sided glazed ventilated window in PolyU Homantin Hall is between 10.4 dB(A) to 16.9 dB(A), and have poor natural ventilation performance. It seems that the new design single sided

glazed ventilated window does not improve the noise reduction and the natural ventilation significantly.

## APPENDIX II

### 1. FLEXIBLE ABSORBER

#### Formula of the resonant frequency

The resonant frequency  $f_{(m,n)}$  of a rectangular plate whose dimensions are  $a \times l$  (m) of the top and bottom of the plastic duct with simply supported edge can be expressed as

$$f_{(m,n)} = \frac{1}{2\pi} \left[ \left( \frac{m}{a} \right)^2 + \left( \frac{n}{l} \right)^2 \right] \sqrt{\frac{\pi^4}{m_s} \left( \frac{Eh_t^3}{12(1-\sigma^2)} \right)} \text{ (Hz)} \quad (\text{A-1})$$

Where  $m, n$  are arbitrary positive integers,  $E$  (kN/m<sup>2</sup>) is Young's modulus of the plate,  $h_t$  (m) is the plate thickness and  $\sigma$  is Poisson's ratio,  $m_s$  (kg/m<sup>2</sup>) is the mass per unit area of the plate. The formula can be used to design the panel absorber for a specified resonance frequency. It can be seen that the resonance frequency increases with smaller dimensions  $a, l$  and thicker panels  $h_t$ .

#### Formula of joint acceptance

It should be noted that acoustic impedance  $Z$  is not constant along the plate due to the non-uniform displacement of the plate. Since the pressure is not distributed

uniformly over the plate, the joint acceptance function should be considered when calculating the average acoustic impedance of a panel. The joint acceptance function  $J_r$  is a factor which describes the proportion of this force which a particular mode of distortion can accept and convert into the corresponding generalized force.

Suppose a field of plane harmonic waves impinges upon a plate. Consider only the case when the sound wave travels in the direction of the length of the plate without any component of velocity across the width of the plate (Figure A-1).

The wave-fronts make an intercept of  $\lambda_l$  on the plate.

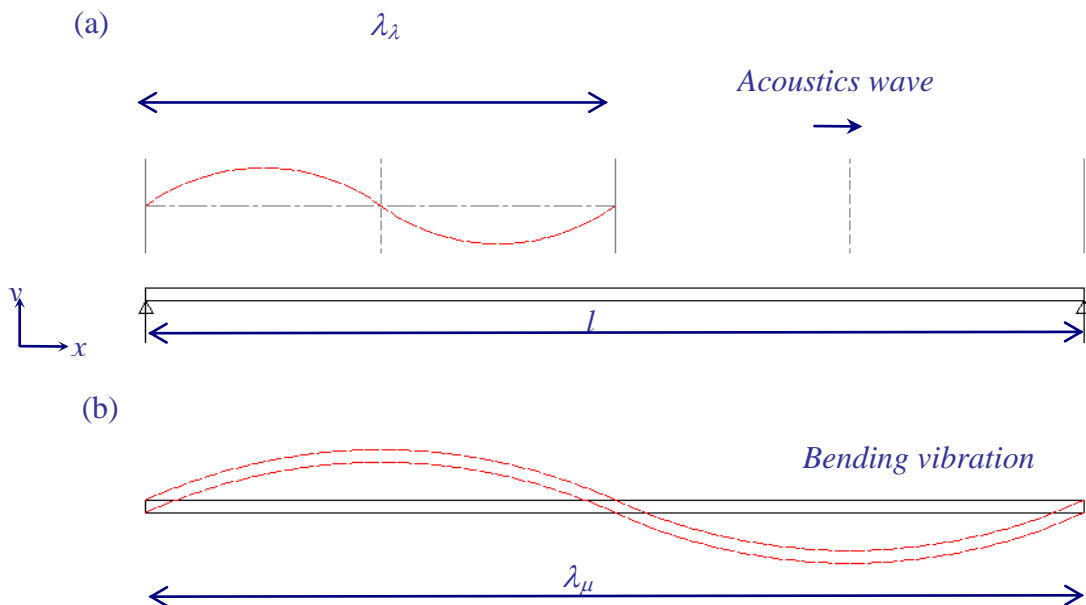


Figure A-1 (a) Diagram illustrating a sound field impinging on the plate. (b)

Bending vibration of plate

The instantaneous pressure at any point along the plate is

$$p(x,t) = p_o \cos\left(\omega t - \frac{2\pi x}{\lambda_l}\right),$$

The displacement of plate in y-direction is given by  $W = \sin \frac{r\pi x}{l} \sin \frac{\pi y}{a}$

Let  $r$  be the number of mode and  $a$  (m) be the width of the plate, the generalized

force is given by:

$$\begin{aligned} L_r(t) &= \int_0^b \int_0^l p_o \cos\left(\omega t - \frac{2\pi x}{\lambda_l}\right) \sin \frac{r\pi x}{l} \sin \frac{\pi y}{a} dx dy \\ &= p_o \frac{2a}{\pi} \int_0^l \cos\left(\omega t - \frac{2\pi x}{\lambda_l}\right) \sin \frac{r\pi x}{l} dx \end{aligned} \quad (\text{A-2})$$

Evaluating the integral, and replacing  $l/r$  by  $\lambda_m/2$  (the half wavelength of the mode of vibration) we find:

$$L_r(t) = p_o lb \frac{4}{\pi^2} \left\{ \frac{\cos\left(\frac{\pi}{2} r \lambda_m / \lambda_l\right)}{r \left| \frac{\lambda_m}{\lambda_l} \right|^2 - 1} \right\} \cos(\omega t + \varepsilon) \quad (\text{A-3})$$

is a constant, the joint acceptance function is:

$$J_r = \frac{4}{\pi^2} \left\{ \frac{\cos\left(\frac{\pi}{2} r \lambda_m / \lambda_l\right)}{r \left| \left(\frac{\lambda_m}{\lambda_l}\right)^2 - 1 \right|} \right\} \quad (\text{A-4})$$

Therefore,  $L_r(t) = p_o S_p J_r \cos(\omega t + \varepsilon)$

$S_p = al$  is the surface area of plate ( $\text{m}^2$ ).

### Formula of Transmission Loss due to flexible absorber

For vibrating plate with single degree of freedom, acoustic impedance  $Z$  can be expressed as

$$Z = R + Xj$$

$$Z = \frac{\text{Pressure}}{\text{Velocity}} = \frac{C}{S_p J_r} + \frac{K - M\omega^2}{S_p \omega J_r} j \quad (\text{A-5})$$

By Equation (A-5), we have

$$R = \frac{C}{S_p J_r}, X = \frac{K - M\omega^2}{S_p \omega J_r} \quad (\text{A-6})$$

Where  $M$  is the modal mass (kg),  $K$  is the modal stiffness (N/m),  $C$  is modal damping constant (N/m/s) and  $S_p$  is the surface area of plate ( $\text{m}^2$ ).

$$\alpha = \frac{4R_0 R}{(R_0 + R)^2 + X^2} \quad (\text{A-7})$$

Where  $\alpha$  is the absorption coefficient and  $J_r$  is the joint acceptance function.

$$R_0 = \rho_0 c \text{ where } R_0 \text{ is the acoustic impedance for air at } 20^\circ\text{C}$$

$$\text{Absorption area, } A = 2\alpha S_p$$

Area of duct,  $S = ah$ , where  $h$  is the thickness of tube.

$$\text{NR} = 10 \log \left( \frac{2\alpha l}{h} \right)$$

In the measurement, the receiving side in tube is constructed with anechoic termination; therefore, the result of noise reduction is equals to the value of transmission loss.

## 2. MULTIPLE QUARTER-WAVE RESONATORS

### Formula of the resonant frequency

A tube closed at one end and open at the other can form a quarter-wave resonator.

The rigid end of the tube confines air within the resonator cavity. Under certain conditions this body of air can be brought to a state of resonant. The fundamental resonant can be formed is a quarter wave in a cavity. The displacement of air in cavity is shown in Figure A-2, the minimum displacement is at the closed end of cavity and maximum displacement is at the open end of cavity. It is clear that  $d = (2n-1) \lambda / 4$ , where  $n = 0,1,2,3\dots$ . The resonant frequencies ( $f_n$ ) can be calculated from

$$f_n = c (2n-1) / 4d \quad (A-8)$$

where  $c$  is speed of sound. The acoustic energy can be dissipated due to quarter-wave resonant in the cavity.

The installation of duct on the opening of building, an enlargement of the duct cross-section can be formed. Thus the muffler effect is can be perform in the experimental test in two rooms rather than in the tube. The resonant frequencies ( $f_n$ ) can be calculated from

$$f_n = c (2n-1) / 4l \quad \text{where } n = 0,1,2,3 \quad (A-9)$$



The acoustic energy can be dissipated due to muffler effect from room to room.

### Formula of Transmission Loss due to quarter-wave resonant

The transmission loss due to the effect of quarter-wave resonator can be defined as the following equation:

$$TL = 10 \log \left( 1 + \frac{S_{sb}^2}{4S^2} \left( \frac{1}{r^2 + \cot^2 kd} \right) \right) \quad (\text{A-10})$$

The dependence of the transmission loss on  $kd$  (where  $kd=2fd/c$ ) is shown for different values of area ratio  $S_{sb}/S$ .  $r$  is the nondimensional acoustic resistance parameter = 0.1. The maximum transmission loss can be achieved near the resonant frequencies.

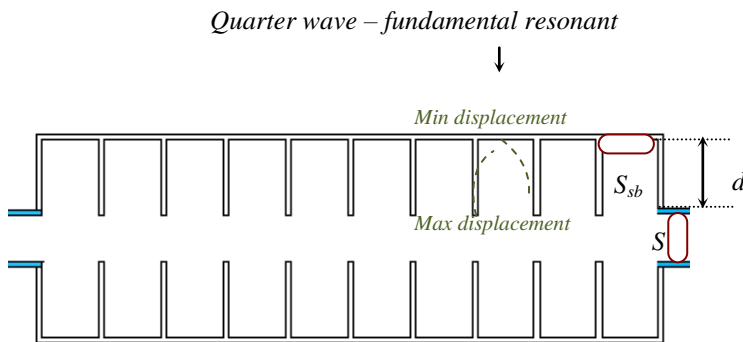


Figure A-2 Dimensions express of a quarter-wave resonator

## LIST OF BIBLIOGRAPHY

Asfour, O. S. & Gadi, M. B. (2008). Using CFD to investigate ventilation characteristics of vaults as wind-inducing devices in buildings. *Applied Energy*, 85 1126-1140.

Awbi, H. (2003). *Ventilation of buildings. 2<sup>nd</sup> edition*. London: Spon Press.

Buratti, C. (2006). Indoor noise reduction index with an open window. *Applied Acoustics*, 67 383-401.

Burnett, A. W., Mullins, H. T. & Patterson, W. P. (2004). Relationship between atmospheric circulation and winter precipitation  $\delta^{18}\text{O}$  in central New York State, *Geophysical research letters*, 31.

Byrne, K., Skeen, M. & Kessissoglou, N. (2006). Measurement of the sound transmission loss of a small expansion chamber muffler to consider the effects of mean flow and wall compliance. *Proceedings of ACOUSTICS 2006. 20<sup>th</sup>-22<sup>nd</sup> November 2006, Christchurch, New Zealand*.

Chaitanya, P. & Munjal, M. L. (2011). Effect of wall thickness on the end corrections of the extended inlet and outlet of a double-tuned expansion chamber.

*Applied Acoustics*, 72 65-70.

Chan, A. L., Chow, T. T., Fong, K. F. & Lin, Z. (2009). Investigation on energy performance of double skin façade in Hong Kong. *Energy and Buildings*, 41 1135-1142.

Chan, W. W. & Lam, J. C. (2001). Environmental costing of electricity consumption in Hong Kong hotel industry. *In Asia Pacific Journal of Tourism Research*, 6 (1), 1-11.

Chen, Q. Y. & Glicksman, L. R. (2003). *System performance evaluation and design guidelines for displacement ventilation*. : American Society of Heating, Refrigerating, and Air-Conditioning Engineers, Incorporated, 2003.

Chen, Q., Lee, K., Mazumdar, S., Poussou, S., Wang, L., Wang, M. & Zhang, Z. (2010). Ventilation performance prediction for buildings: Model Assessment. *Building and Environment*, 45 (2), 295-303.

Chow, W. K. (2004). A short note on fire safety for new architectural features.

*International Journal on Architectural Science*, 5 (1), 1-4.

Chu, C. R. & Wang, Y. W. (2010). The loss factors of building openings for wind-driven ventilation. *Building and Environment*, 45(10), 2273-2279.

Craggs, A. (1976). A finite element method for damped acoustic systems: an application to evaluate the performance of reactive mufflers. *Journal of Sound and Vibration*, 48(3), 377-392.

Etheridge, D. & Sandberg, M. (1996). *Building ventilation: theory and measurement*. Wiley.

Field, C. D. & Fricke, F. R. (1998). Theory and applications of quarter-wave resonators: A prelude to their use for attenuating noise entering buildings through ventilation opening. *Applied Acoustics*, 53(1-3), 117-132.

Field, C., Fricke, F., Hill, F & Lawrence, R. (Eds.) (1996) *A multiple quarter-wave resonator system for the attenuation of noise entering buildings through ventilation opening*, Proceedings InterNoise 96, 1769-1772

Field, C. D. (2008). Acoustic design criteria for naturally ventilated buildings. *The journal of the Acoustical Society of America*, 123 (5), 2814.

Frommhold, W., Fuchs, H. V. & Sheng, S. (1994). Acoustic performance of membrane absorbers. *Journal of sound and vibration*, 170 621-636.

Gao, C. & Lee, W. L. (2011). Evaluating the influence of openings configuration on natural ventilation performance of residential units in Hong Kong. *Building and Environment*, 46 961-969.

Givoni, B. (1976). Chapter 15 Design factors affecting ventilation. In B. Givoni *Man, Climate and Architecture* (p.296). London: Applied Science Publisher.

Givoni, B. (1976). *Man Climate and Architecture*. London: Applied Science Publisher.

Gosselin, J. R. & Chen, Q. Y. (2008). A dual airflow window for indoor air quality improvement and energy conservation in building. *American Society of Heating, Refrigerating and Air-Conditioning Engineers*, 14 (3), 359-372.

Gratia, E. & Herde, A. D. (2003). Design of low energy office buildings. *Energy and Buildings*, 35 473-491.

Gratia, E. & Herde, A. D. (2004). Natural ventilation in a double-skin façade. *Energy and Buildings*, 36 137-146.

Haase, M. & Amato, A. (2006). Ventilated façade design for hot and humid climate, Proceedings of the Fifteenth Symposium on Improving Building Systems in Hot and Humid Climates. Orlando, FL, July 24-26.

Heiselberg, P. (Ed.) (2002), *Principles of hybrid ventilation*, IEA Annex 35

Hosaam, E. D. & Woloszyn, P. (2005). The acoustical influence of balcony depth and parapet form: experiments and simulations. *Applied Acoustics*, 66 533-551.

Huang, L. X. (1999). A theoretical Study of Duct Noise Control by Flexible Panels. *Journal of the Acoustical Society of America*, 106 (4), 1801-1809.

Huang, S. P., Lui, R. H. & Lai, R. P. (2012). A study on performance of ventilated soundproof windows with fans. *The Journal of the Acoustical Society of America*, 131 (4), 3320.

ISO 7235: 2003 Acoustics (2003). *Laboratory measurement procedures for ducted silencers and air-terminal units – Insertion loss, flow noise and total pressure loss*.

Kalogrious, S. A. (2009). Chapter 6 Space cooling and heating. In *Solar energy engineering: processes and systems* (p. 346). : Academic Press.

Kang, J. & Brocklesby, M.W. (2005). Feasibility of applying micro-perforated absorbers in acoustic window systems. *Applied Acoustics*, 66(6) 669-689.

Kang, J. & Li, Z. (2007). Numerical simulation of an acoustic window system using finite element method. *Acustica/acta acustica- European Journal of Acoustics*, 93(1) 152-163.

K-epsilon model, Retrieved April 22, 2014 from Website:

[http://www.cfd-online.com/Wiki/K-epsilon\\_models](http://www.cfd-online.com/Wiki/K-epsilon_models)

Kindangen, J., Krauss, G. & Depecker, P. (1997). Effects of roof shapes on wind-induced air motion inside buildings. *Building and Environment*, 32(1), 1-11.

King, V. (Photographer). (2012). *Extended double skin façade creates “wing wall effect” in Post Tower* [Photograph], Retrieved May 26, 2013 from website:

<http://www.archdaily.com/231521/flashback-post-tower-murphyjahn/>

Komatsu, Y., Sagara, K., Yamanaka, T., Kotani, H., Higuchi, M., Lim, E. & Waatanabe, H. (2008). Study on airflow around building roof for design of natural ventilation by chimney-Part2. Wind Velocity Distribution above Building Roof-Osaka University *AIVC 29<sup>th</sup> Conference: Advanced building ventilation*



*and environmental technology for addressing climate change issues*, Kyoto, Japan.

Kutz, M. (2005). Chapter 35 Noise measurement and control. In G. M. Diehl *Mechanical Engineers' Handbook: Materials and Mechanical Design 3rd Edition* (pp. 1230-1252). New York: Wiley

Lee, J. W. & Kim, Y. Y. (2009). Topology optimization of muffler internal partitions for improving acoustical attenuation performance. *International Journal for Numerical Methods in Engineering*, 80(4), 455-477

Lee, I. B., Sase, S. & Sung, S. H. (2007). Evaluation of CFD accuracy for the ventilation study of a naturally ventilated broiler house. *Japan Agricultural Research Quarterly*, 41 (1), 53-64.

Levermore, G. J., Jones, A. M. & Wright, A. J. (2000). Simulation of a Naturally Ventilated Building at Different Locations. *ASHRAE Transactions*, 106 (Part 2).

Mak, C. M., Cheng, C. & Niu, J. L. (2005) The application of computational fluid dynamics to the assessment of green features in buildings: Part 1: Wing Wall. *Architectural Science Review*.

Mak, C. M., Niu, J. L. Lee, C. T. & Chan, K. F. (2007). A numerical simulation of wing walls using computational fluid dynamics. *Energy and Building*, 39 995-1002.

Matthias, H., Wong, F. & Amato, A. (2007). Double-skin façade for Hong Kong. *Surveying and Built Environment*, 18 (2), 17-32.

McWilliams, J. (2002). *Review of airflow measurement techniques*. Energy Performance of Building Group Environmental Energy Technologies Division Lawrence Berkeley National Laboratory: Berkeley.

Menter, F. R. (1994). Two equation eddy-viscosity turbulence models for engineering application. *AIAA Journal*, 32 (8) 1598-1605.

Modera, M. P. & Persily, A. K. (1995). A Study of Ventilation Measurement in an Office Building. In W. S. Dols, A. K. Persily *Airflow Performance of Building Envelopes, Components, and Systems ASTM STP 1255* (pp. 23-46). :Astm International.

Munjal, M. L. (1987). *Acoustics of ducts and mufflers with application to exhaust and ventilation system design*. New York: Wiley.

Naish, D. A, Tan, A. C. & Fur, D. F. (2012). Estimating health related costs and savings from balcony acoustic design for road traffic noise. *Applied Acoustics*, 73 (5), 497-507.

Naish, D. A, Tan, A. C. & Nur, D. F. (2013). Speech interference and transmission on residential balconies with road traffic noise. *Journal of Acoustics Society America*, 133 (1), 210-226.

Nitatwichit, C., Khunatorn, Y. & Tippayawong, N. (2008). Computational analysis and visualization of wind driven naturally ventilated flows around a

school building. *Maejo International Journal of Science and Technology*, 2 (01), 240-254.

Paepe, M., Pieters, J., Merci, B., Cornelis, W., Gabriels, D. & Demeyer, P. (2009) *Computational Modelling and Scale Model Validation of Airflow Patterns in Naturally Ventilated Barns*, Guidelines for the measurement of airflow and mercury in cell room ventilation 3<sup>rd</sup> edition.

Pereira, F. O. R. & Toledo, A. M. *Analogical visualization of natural ventilation in buildings due to wind action*, Plea 2004- the 21th Conference on Passive and Low energy Architecture.

Reis, P. N. B; Iacob, D. & Minea, A. A. (2011). Heat transfer in composite materials. *Metalurgia*, 63(6), 5.

Salis, M. H., Oldham, F. J. & Sharples, S. (2002). Noise control strategies for naturally ventilated buildings. *Building and Environment*, 137 471-484.

Shield, T. J., Silcock, G. W. H. & Flood, M. F. (2001). Performance of a single glazing assembly exposed to enclosure corner fires of increasing severity. *Fire and Materials*, 25 123-152.

Tan, G. & Glicksman, L. R. (2005). Application of integrating multi-zone mockup with CFD simulation to natural ventilation prediction. *Energy and Buildings*, 37 1049-1057.

Tang, S. K. (2005). Noise screening effects of balconies on a building façade. *Journal of the Acoustical Society of America*, 118 (1), 213-221.

Tavoularis, S. (2005). *Measurement in Fluid Mechanics*. Cambridge: Cambridge University Press.

Tsou, J. Y. (2001). Strategy on applying computational fluid dynamic for building performance evaluation. *Automation in Construction*, 10 327-335.

Tye, T. (Photographer). (2006). *UMNO Tower by Ken Yeang 1 Photo* [Photograph], Retrieved May 26, 2013 from:

<http://www.penang-traveltips.com/menara-umno.htm>

Wakeling, J. & Ellington, C. (1997). Dragonfly flight: gliding flight and steady-state aerodynamic forces. *The Journal of Experimental Biology*, 543-556.

Wang, C. Q., Han, J. & Huang, L. X. (2006). Optimization of a clamped plate silencer. *Journal of the Acoustical Society of America*, 119 2628-2638.

Walker, A. (2010). *Natural ventilation*. Retrieved May 28, 2013 from National Institute of Building Sciences, Website:

[http://www.wbdg.org/resources/naturalventilation.php?r=resist\\_hazards](http://www.wbdg.org/resources/naturalventilation.php?r=resist_hazards)

Wilson, A. R. (2011). *Sustainable building design in architectural services department*. Retrieved June 29, 2013 from Architectural Services Department,

Website: [http://www.science.gov.hk/paper/ArchSD\\_AWilson.pdf](http://www.science.gov.hk/paper/ArchSD_AWilson.pdf)

Wong, H. K., Yung, C. N. & Tang, S. K. (2012). On site performance of ventilation windows for public housing development. *The Journal of the Acoustical Society of America*, 13 (4), 3509.

Wood, A. & Salib, R. (2012). Menara UMNO, Penang, 1998. *In Natural ventilation in high-rise office building* (pp. 51-56). : Taylor & Francis.

Wood, A. & Salib, R. (2012). Post Tower, Bonn, 2002. *In Natural ventilation in high-rise office building* (pp. 74-83). : Taylor & Francis.

Mahmood, M. (2011). Flow visualization in wind tunnels. In L. C. Lerner & U. Boldes (Eds.), *Wind tunnels and experimental fluid dynamics research* (pp. 99-114). : Croatia: INTECT.

Yin, W., Zhang, G. Q., Yang, W. & Wang, X. (2010). Natural ventilation potential mockup considering solution multiplicity, window opening percentage, air velocity and humidity in China. *Building and Environment*, 45 338-344

Zhao, Y. & Jones, J. R. (2007). Decision support for natural ventilation of nonresidential buildings. *Journal of Architectural Engineering*, 13 95-104.

